pmod wrc

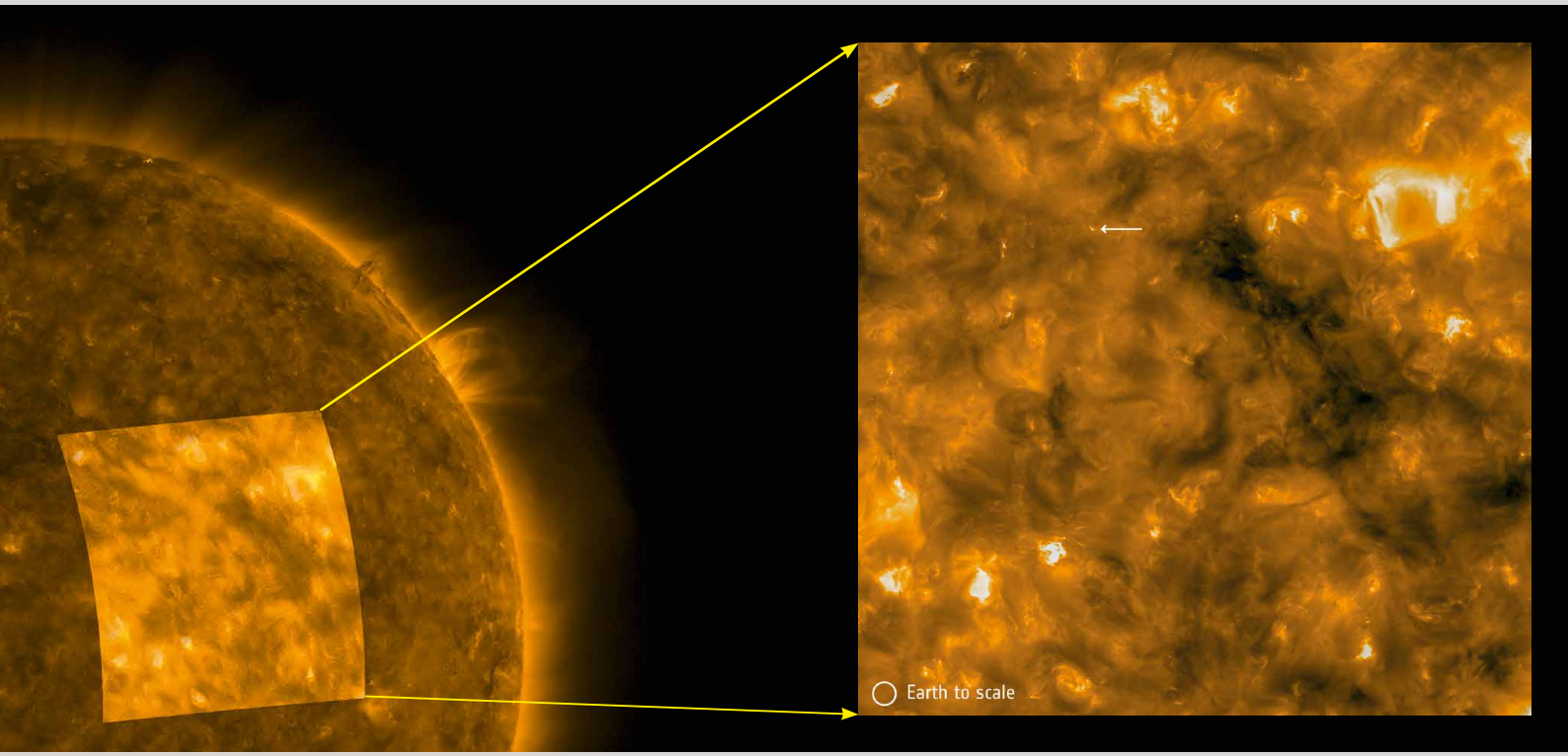

Annual Report
Jahresbericht 2020

Physikalisch-Meteorologisches Observatorium Davos und Weltstrahlungszentrum PMOD/WRC

Mission

Unsere 6 Kernaktivitäten sind auf Seite 3 aufgelistet.

Auftragerteilung

Das Physikalisch-Meteorologische Observatorium Davos (PMOD) beschäftigt sich seit seiner Gründung im Jahr 1907 mit Fragen des Einflusses der Sonnenstrahlung auf das Erdklima. Das Observatorium schloss sich 1926 dem Schweizerischen Forschungsinstitut für Hochgebirgsklima und Medizin Davos an und ist seither eine Abteilung dieser Stiftung. Auf Ersuchen der Weltmeteorologischen Organisation (WMO) beschloss der Bundesrat im Jahr 1970 die Finanzierung eines Kalibrierzentrums für Strahlungsmessung als Beitrag der Schweiz zum Weltwetterwacht-Programm der WMO. Nach diesem Beschluss wurde das PMOD beauftragt, das Weltstrahlungszentrum (World Radiation Center, WRC) zu errichten und zu betreiben.

Kerntätigkeiten

Das Weltstrahlungszentrum unterhält das Primärnormal für solare Bestrahlungsstärke bestehend aus einer Gruppe von hochpräzisen Absolut-Radiometern. Auf weitere Anfragen der WMO wurden 2004 das Kalibrierzentrum für Messinstrumente der atmosphärischen Langwellenstrahlung eingerichtet und 2008 das Kalibrierzentrum für spektrale Strahlungsmessungen zur Bestimmung der atmosphärischen Trübung. Seit 2013 wird auch das Europäische UV Kalibrierzentrum durch das Weltstrahlungszentrum betrieben.

Das Weltstrahlungszentrum besteht heute aus vier Sektionen: Solare Radiometrie (WRC-SRS), Infrarot Radiometrie (WRC-IRS), Atmosphärische Trübungsmessungen (WRC-WORCC), UV Kalibrierzentrum (WRC-WCC-UV)

PMOD/WRC ist vollständig in die Europäische Vereinigung nationaler Metrologie Institute (EURAMET) und Bureau International des Poids et Mesures (BIPM) eingebettet. PMOD / WRC ist ein assoziiertes Mitglied von EURAMET und wurde von METAS am BIPM im Rahmen der Vereinbarung über die gegenseitige Anerkennung als designiertes Institut für die Einheit Sonneneinstrahlung registriert.

Das PMOD/WRC entwickelt und baut Radiometer, die zu den weltweit genauesten ihrer Art gehören und sowohl am Boden als auch im Weltraum eingesetzt werden. Diese Instrumente werden auch zum Kauf angeboten und kommen seit langem bei Meteorologischen Diensten weltweit zum Einsatz. Ein globales Netzwerk von Stationen zur Überwachung der atmosphärischen Trübung ist mit vom Institut entwickelten Präzisionsfilterradiometern ausgerüstet.

Im Weltraum und mittels Bodenmessungen gewonnene Daten werden in Forschungsprojekten zum Klimawandel und der Sonnenphysik analysiert. Diese Forschungstätigkeit ist in nationale, insbesondere mit der ETH Zürich, und internationale Zusammenarbeit eingebunden.

Mission

Our 6 core activities are listed on Page 6.

Mission Assignment

Since its establishment in 1907, the Physikalisch-Meteorologisches Observatorium Davos (PMOD) has been studying the influence of solar radiation on the Earth's climate. In 1926, the Observatory joined the Swiss Research Institute for High Altitude Climate and Medicine Davos and has since become part of this foundation. At the request of the World Meteorological Organization (WMO), the Federal Council decided in 1970 to finance a calibration center for radiation measurement as Switzerland's contribution to the World Weather Monitoring Program of the WMO. Following this decision, the PMOD was commissioned to establish and operate the World Radiation Center (WRC).

Core Activities

The World Radiation Center maintains the primary standard for solar irradiance consisting of a group of high-precision absolute radiometers. In response to further inquiries from the WMO, a calibration center for atmospheric longwave radiation measuring instruments was established in 2004, and in 2008 the calibration center for spectral radiance measurements to determine atmospheric turbidity. Since 2013, the European UV calibration center has also been operated by the World Radiation Center.

The World Radiation Center today consists of four sections: Solar Radiometry (WRC-SRS), Infrared Radiometry (WRC-IRS), Atmospheric Turbidity (WRC-WORCC), UV Radiometry (WRC-WCC-UV)

PMOD/WRC is fully embedded in the European Association of National Metrology Institutes (EURAMET) and the framework of the Bureau International des Poids et Mesures (BIPM). PMOD/WRC is an associated member of EURAMET and has been registered as a designated institute for the unit, solar irradiance, by METAS at BIPM in the frame of the Mutual Recognition Arrangement.

The PMOD/WRC develops and builds radiometers that are among the most accurate of their kind in the world and are used both on the ground and in space. These instruments are also available for purchase and have long been used by Meteorological Services worldwide. In addition, a global network of atmospheric turbidity monitoring stations is equipped with precision filter radiometers developed by PMOD/WRC.

Data collected in space and by means of ground measurements are analysed in research projects on climate change and solar physics. This research activity is integrated into national (in particular with ETH Zurich) and international projects.

Front Cover: The Sun on 30 May 2020. Image left: The solar disc imaged (171 Å) by the Solar Dynamics Observatory (SDO) with a superimposed image (174 Å) from the Extreme Ultraviolet Imager (EUI) onboard Solar Orbiter. Visualisation using JHelioviewer (Müller et al., 2017; doi.org/10.1051/0004-6361/ 201730893). Image right: High resolution EUI image (174 Å) showing the Earth to scale and 'campfires' (white arrow). Image credits: ESA/Solar Orbiter/EUI and SDO/NASA.

Das PMOD/WRC ist eine Abteilung der Stiftung Schweizerisches Forschungsinstitut f. Hochgebirgsklima und Medizin in Davos, Schweiz.

The PMOD/WRC is a department of the Swiss Research Institute for High Altitude Climate and Medicine (SFI) in Davos/Switzerland.

Physikalisch-Meteorologisches Observatorium
Davos/ World Radiation Center (PMOD/WRC)
Dorfstrasse 33,
7260 Davos Dorf
Schweiz

Tel. +41 (0)81 417 51 11
www.pmodwrc.ch

pmod wrc

Annual Report
Jahresbericht 2020

Table of Contents

Einleitung

Louise Harra

Das Jahr 2020 war in vielerlei Hinsicht ein denkwürdiges Jahr. Es stand ganz im Zeichen der Covid-19-Pandemie, aber die Arbeit am Physikalisch-Meteorologischen Observatorium Davos und am World Radiation Center (PMOD/WRC) ging bestens weiter. Die Mitarbeiter sorgten dafür, dass die wichtige instrumentelle Arbeit weitergehen konnte, und zwar auf eine Covid-sichere Weise.

Das erste große Vorhaben für PMOD/WRC war der Start des ESA Solar Orbiter am 9. Februar 2020 von Cape Canaveral. Im Vorfeld vor dem Start führte das PMOD/WRC eine Reihe von Informationsveranstaltungen durch, die in einem Tag der offenen Tür mit einer Live-Schaltung nach Florida und lokalem Bier zur Feier des Starts gipfelten, gefolgt von einem Beitrag des Schweizer Fernsehens in der Sendung *Schweiz Aktuell*. PMOD/WRC war am Bau von zwei Instrumenten an Bord beteiligt - dem Spektrometer (SPICE) und dem Extreme UV Imager (EUI). Der Start war erfolgreich, alle zehn Geräte wurden in den folgenden Monaten trotz der Pandemie und der Einschränkungen durch das Home Office erfolgreich zugeschaltet.

Im Zuge der Einschränkungen durch die Pandemie ging die Arbeit im PMOD/WRC weiter, wobei die bedeutendste Unterbrechung die Verschiebung des Internationalen Pyrheliometervergleichs war, der normalerweise alle 5 Jahre stattfindet. Dieser wurde auf Herbst 2021 verschoben.

Die Zusammenarbeit mit der ETH-Zürich, Institut für Teilchenphysik und Astrophysik (IPA) wird mit der Einbindung in Lehre und Projektstudenten und der Zusammenarbeit in der Technik fortgesetzt.

Die sechs Kernbereiche, die PMOD/WRC übernommen hat, sind:

- World Radiation Center: dient als internationales Kalibrierungszentrum für meteorologische Strahlungsinstrumente und entwickelt Strahlungsinstrumente für den Einsatz am Boden und im Weltraum.
- Weltraumprojekte: Entwicklung von Instrumenten zur Bildgebung und Strahlungsmessung der Sonne.
- Technologie: Grundlage für das Design und die Entwicklung der Instrumente für Boden und Weltraum.
- Klimawissenschaft: Erforschung des Einflusses der Sonnenstrahlung auf das Klima der Erde.
- Sonnenwissenschaft: Erforschung der Ursachen der Sonnenaktivität.
- Lehrtätigkeit: Durchführung von Lehrveranstaltungen auf verschiedenen Ebenen an der ETH-Zürich.

Aufgrund der Pandemie haben wir einen halbjährlichen virtuellen PMOD/WRC-Wissenschaftstag ins Leben gerufen, an dem die Mitarbeiter ihre Arbeit ihren Kollegen präsentieren. Dieser verlief sehr erfolgreich, und es war für uns erfreulich, neue Ergebnisse aus den einzelnen Disziplinen zu erfahren.

Im Jahr 2020 gab es viele wichtige Erfolge. Hier sind ein paar Highlights:

- Die Weltraummission Solar Orbiter wurde erfolgreich gestartet, und alle Instrumente wurden eingeschaltet. *Siehe Seite 23*.

- Die Beteiligung an verschiedenen Kursen an der ETH-Zürich D-PHYS begann, und neue Studentenprojekte wurden gestartet.

- Das Swiss Space Office (SSO) hat unsere Beteiligung an der Solar-C-Mission der japanischen Raumfahrtbehörde (JAXA) befürwortet - zum Bau eines Solar Spectral Irradiance Monitor (SoSPIM). *Siehe Seite 17*.

- Die Entwicklungsarbeiten für den Lagrange Extreme UV Coronal Imager (LUCI) auf der ESA Lagrange Mission wurden fortgesetzt. *Siehe Seite 17*.

- Die NASA-Mission Solaris gehörte zu den wenigen Kandidaten, die im Rahmen einer Phase-A-Studie zur weiteren Betrachtung ausgewählt wurden - wir sind an der S-EUVI (EUV-Imager) beteiligt. *Siehe Seite 18*.

- Aufgrund der zu erwartenden Zunahme von Mitarbeitern und Studenten haben wir neue Büroräume für das PMOD/WRC im Innovation Center Davos (ICD, dem ehemaligen SIAF-Gebäude) angemietet.

- Die SOHO-Weltraummission mit dem PMOD/WRC-Instrument VIRGO an Bord arbeitet seit 25 Jahren erfolgreich, wobei ein neuer Code für maschinelles Lernen entwickelt wurde, um eine langfristige Degeneration zu korrigieren. *Siehe Seite 19*.

- Das neu entwickelte Atmosphäre-Ozean-Chemie-Klimamodell SOCOLv4 hat die Bedeutung des Montreal-Protokolls sowohl für die Ozonschicht als auch für die Nachhaltigkeit des Klimas gezeigt. *Siehe Seite 29*.

- Der Gartenbereich am PMOD/WRC wurde erweitert, um Platz für neue Instrumente zu schaffen.

- Unsere Bodeninstrumente haben im Jahr 2020 bedeutende Ereignisse beobachtet, darunter hohe Strahlungsintensität in den Niederlanden, Brände in Kalifornien und Sandstürme in der Sahara.

- Das Upgrade des Global Atmosphere Watch Precision Filter Radiometer (GAW-PFR) Netzwerks ist in vollem Gange. *Siehe Seite 43*.

- Eine erfolgreiche Mondkampagne zur Messung der optischen Tiefe von Aerosolen wurde in Lindenberg, Deutscher Wetterdienst, Deutschland, durchgeführt. *Siehe Seite 46*.

- Durch die Zusammenarbeit mit der Physikalisch-Technischen Bundesanstalt (PTB) wurde ein wichtiger Meilenstein zum Nachweis der Rückführbarkeit von langwelligen Bestrahlungsstärkemessungen (WISG/IRIS) auf das SI erreicht. *Siehe Seite 44*.

- Die Vorentwicklungsphase für die ESA Mission für rückführbare Radiometrie (Traceable Radiometry Underpinning Terrestrial- and Helio- Studies, TRUTHS) hat begonnen. *Siehe Seite 18*.

- Das Digitale Absolute Radiometer (DARA) wurde erfolgreich auf der Fengyun-3E (FY-3E) Joint Total Solar Irradiance Absolute Radiometer (JTSIM) Plattform in China integriert und getestet. *Siehe Seite 16*.

- Verbesserungen am kryogenen Radiometer (CSAR und MITRA) haben begonnen, um den neuen primären Standard für bodengestützte Messungen der Sonneneinstrahlung zu etablieren und die World Standard Group (WSG) zu ersetzen. *Siehe Seite 10.*

Ich möchte diese Gelegenheit nutzen, um allen Mitarbeitern des Instituts für ihre harte Arbeit und ihr Engagement in der Zeit der Pandemie zu danken, sowie dem Kuratorium und der Aufsichtskommission für die kontinuierliche Begleitung und Unterstützung. Meine Kolleginnen und Kollegen an der ETH haben die Arbeit in Zeiten der Pandemie, einschließlich des Unterrichts, ruhig organisiert, so dass alles zeitgerecht ablaufen konnte - auch das hat außergewöhnliche Arbeit, Initiative und Planung erfordert.

Eine Collage mit einigen der Erfolge ist rechts abgebildet.

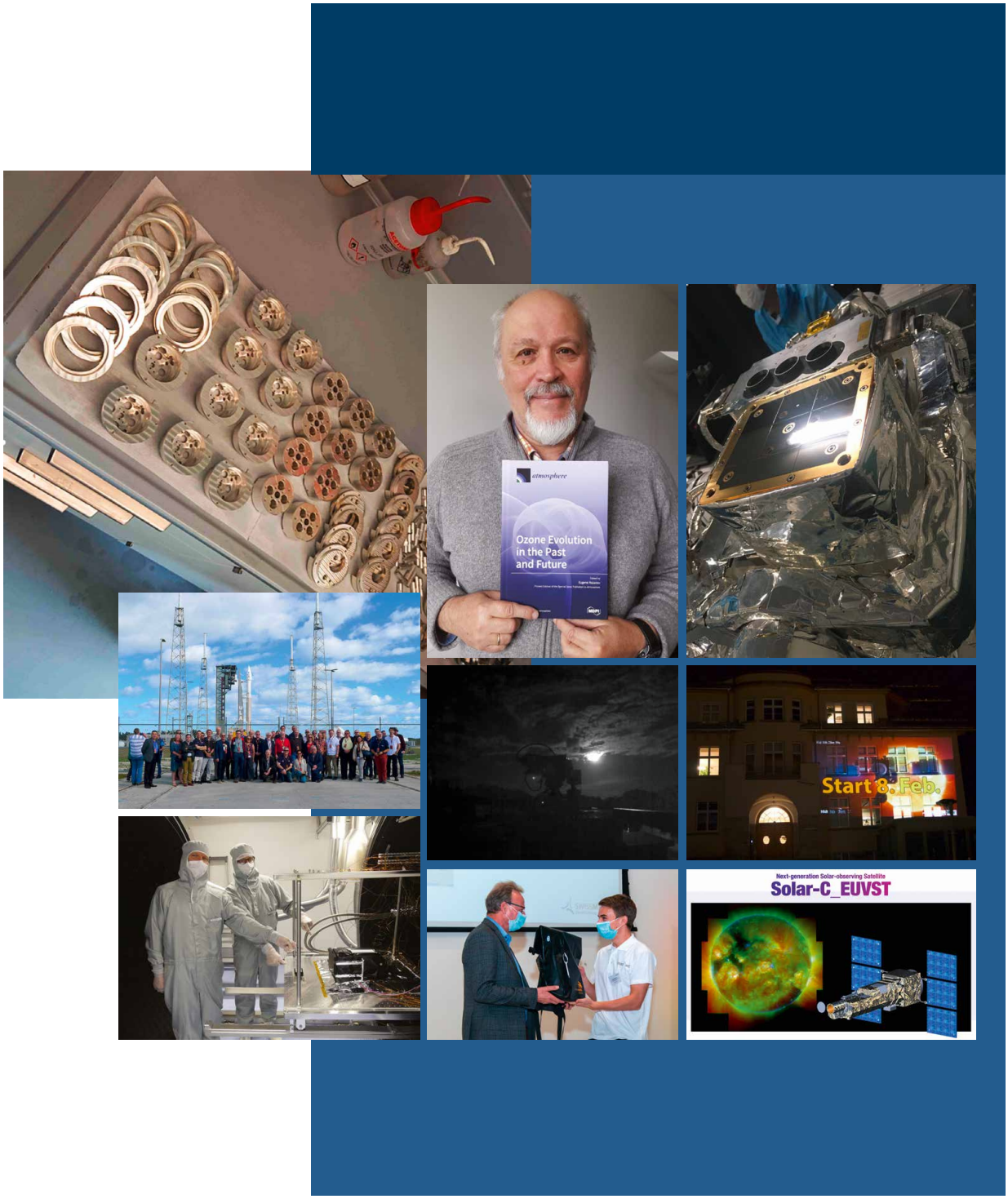

Abbildung 1: Von oben links nach unten rechts: die Entwicklung der neuen PFRs, die Veröffentlichung von Ozone Evolution in the Past and Future, herausgegeben von Eugene Rozanov, JTSIM-DARA auf dem Tracker in China, die PIs und Projektwissenschaftler am Startplatz für Solar Orbiter (Kennedy Space Center, USA), Kampagne um Aerosol optische Dicke mittels Mondlicht zu messen (Deutschland), das beleuchtete PMOD/WRC-Gebäude zur Feier des Starts von Solar Orbiter, Test von Proba-3 DARA, Lehrling Yanick Schoch erhält eine Auszeichnung für den 7. Platz in der Schweiz bei Swiss Skills, eine Impression des Solar-C-Raumschiffs.

Figure 1: From top left to bottom right: the development of the new PFRs, the publication of Ozone Evolution in the Past and Future, edited by Eugene Rozanov, JTSIM-DARA on the tracker in China, the PIs and project scientists at the launch site for Solar Orbiter (Kennedy Space Center, USA), aerosol optical depth measurement campaign using moonlight (Germany), the PMOD/WRC building lit up to celebrate the launch of Solar Orbiter, testing of Proba-3 DARA, apprentice Yanick Schoch receiving an award for achieving 7th place in Switzerland in Swiss Skills, an artist's impression of the Solar-C spacecraft.

Introduction

Louise Harra

The year 2020 was a memorable one in many ways. It was dominated by the pandemic, but work carried on at the Physikalisch-Meteorologisches Observatorium Davos and World Radiation Center (PMOD/WRC) in an excellent way. Staff rallied to ensure that key instrumental work could carry on, and in a Covid-safe way.

The first major event for PMOD/WRC was the launch of the ESA Solar Orbiter on 9 February 2020 from Cape Canaveral. In the period before launch, PMOD/WRC carried out a number of outreach events culminating in an open house event with a live link to Florida and local beer celebrating the launch, followed by a feature on Swiss TV in the *Schweiz Aktuell* programme. PMOD/WRC was involved in the building of two onboard instruments – the spectrometer (SPICE) and the Extreme UV imager (EUI). The launch was successful and all ten instruments were successfully switched on in the following months despite the pandemic and the restrictions of home office.

After pandemic restrictions were imposed, work at PMOD/WRC carried on, with the most significant disruption being the postponement of the International Pyrheliometer Comparison which normally takes place every 5 years. This has been delayed to Autumn 2021.

The collaboration with ETH-Zürich, Institute for Particle Physics and Astrophysics (IPA) continues with involvement in teaching and project students, and collaboration on technology.

The six core areas that PMOD/WRC have undertaken are:

- World Radiation Center: serve as an international calibration center for meteorological radiation instruments and develop radiation instruments for use on the ground and in space.
- Space projects: develop instruments for imaging and radiation measurements of the Sun.
- Technology: underpin the design and development of the instruments for ground and space.
- Climate science: research the influence of natural and anthropogenic activity on Earth's climate.
- Solar Science: research the causes of solar activity.
- Teaching: carry out teaching at different levels at ETH-Zurich.

Due to the pandemic, we started a bi-annual virtual PMOD/WRC science day, when staff would present their work to their colleagues. This was very successful, and it was enjoyable for us to catch up on new results in each discipline.

There have been many key successes during 2020. Here are a few highlights:

- The Solar Orbiter space mission was launched successfully, and all instruments switched on. *See page 23*.
- Involvement in different courses at ETH-Zürich D-PHYS began, and new student projects started.
- The Swiss Space Office (SSO) endorsed our involvement in the Japanese space agency (JAXA) Solar-C mission – to build a Solar Spectral Irradiance Monitor (SoSPIM). *See page 17*.
- Development work for the Lagrange Extreme UV Coronal Imager (LUCI) on the ESA Lagrange mission continued. *See page 17*.
- The NASA Solaris mission was among the few candidates selected for further consideration in a phase A study – we are involved in the S-EUVI (EUV imager). *See page 18*.
- Due to an anticipated increase of staff and students, we have rented new office space for PMOD/WRC at Innovation Center Davos (ICD, the former SIAF building).
- The SOHO space mission and PMOD/WRC VIRGO instrument onboard has been operating successfully for 25 years, with new machine learning code developed to correct for long term degradation. *See page 19*.
- The newly developed atmosphere-ocean-chemistry climate model SOCOLv4 demonstrated the importance of the Montreal protocol for both the ozone layer and climate sustainability. *See page 29*.
- The garden area at PMOD/WRC has been extended to allow for new instruments.
- Our ground-based instruments observed significant events in 2020 including high irradiance in the Netherlands, California fires and Saharan sandstorms.
- The upgrade of the Global Atmosphere Watch Precision Filter Radiometer (GAW-PFR) network is well underway. *See page 43*.
- A successful lunar campaign to measure aerosol optical depth was carried out at Lindenberg, Deutscher Wetterdienst, Germany. *See page 46*.
- A significant milestone was achieved towards demonstrating traceability of longwave irradiance measurements (WISG/IRIS) to SI through collaboration with the National Metrology Institute of Germany (Physikalisch-Technische Bundesanstalt, PTB). *See page 44*.
- The pre-development phase for the ESA Traceable Radiometry Underpinning Terrestrial- and Helio-Studies (TRUTHS) mission has started. *See page 18*.
- The Digital Absolute Radiometer (DARA) was successfully integrated and tested on the Fengyun-3E (FY-3E) Joint Total Solar Irradiance Absolute Radiometer (JTSIM) platform in China. *See page 16*.
- Improvements on the cryogenic radiometer (CSAR and MITRA) have started in order to establish the new primary standard for ground-based solar irradiance measurements and to replace the World Standard Group (WSG). *See page 10.*

I would like to take this opportunity to thank all the staff at the institute for their hard work and dedication throughout the time of the pandemic, and the board of trustees and the supervisory commission for continuing guidance and support. My colleagues at ETH organised pandemic work, including teaching in a calm manner, allowing everything to proceed in a timely fashion – this has also taken exceptional work, initiative and planning.

A collage of some of the successes is shown on page 5.

World Radiation Center / Operational Services

Quality Management System, Calibration Services, Instrument Sales

Ricco Soder, Wolfgang Finsterle, and Julian Gröbner

Calibration and Measurement Capabilities (CMCs)

PMOD/WRC has 8 different CMCs in the Key Comparisons Database (KCDB) of the Bureau International de Poids et Mesure (BIPM). Depending on the instrument's wavelength range, the CMCs belong to different WRC calibration sections. They include:

- Responsivity, solar irradiance pyranometer (1)
- Responsivity, solar irradiance pyrheliometer (1)
- Responsivity, solar irradiance broadband detector (4)
- Responsivity, solar spectral irrad. solar spectroradiometer (2)

Organisation and Human Resources

No changes occurred in personnel regarding functions or responsibilities within the QMS.

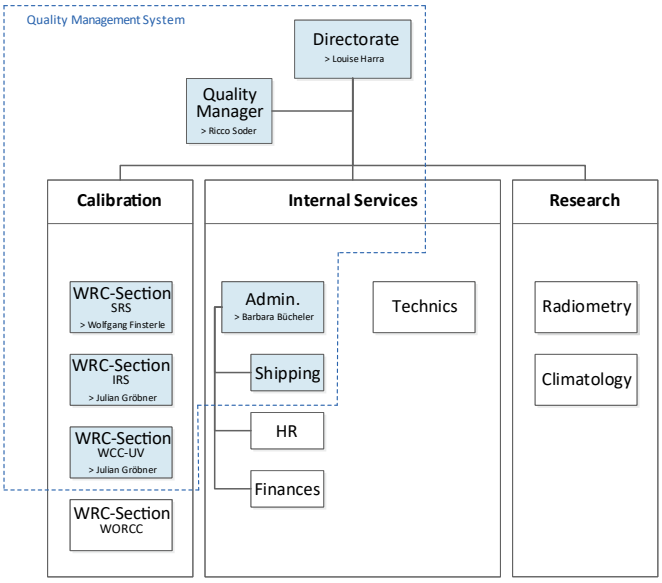

Figure 1. PMOD/WRC Quality Management System (QMS) - organisational chart. The WRC-SRS, WCC-UV, and WRC-IRS sections (in blue), perform calibrations according to EN ISO/IEC standard 17025.

Activities

The pandemic (Covid-19) strongly influenced working life at PMOD/WRC which led to only one participation in interlaboratory comparisons as well as the postponement of IPC 2020.

The deadline for achieving the requirements of the revised ISO standard 17025:2018 was postponed by EURAMET to June 2021. Nevertheless, our QM documentation was adapted and the transition phase was almost completed in 2020. Furthermore, QM-related documentation of all WRC sections has been updated continuously throughout the year. Two of our WRC sections and the Administration Department were assessed by internal audits. The outcome was very positive and will support the continuous improvement process of QM at PMOD/WRC. Training of staff was performed in accordance with a section-specific training schedule.

Calibration Services

In 2020, a total of 168 instruments were calibrated within the different World Radiation Center (WRC) calibration sections (Figure 2). The decrease of almost 20% compared to 2019 is Covid-related and mainly affected the Solar Radiation Section (SRS) and the World Calibration Center for UV (WCC-UV).

Solar Radiometry Section (WRC-SRS)

The WRC-SRS section calibrated 30 pyrheliometers and 75 pyranometers. Due to a discrepancy regarding the stated level of uncertainty, only 19 pyrheliometer certificates were issued with the CIPM logo.

While there was a slight decrease in pyranometer calibrations, the number of pyrheliometer calibrations increased by more than 30% compared to 2019. This is most probably due to the postponed 13th International Pyrheliometer Comparisons.

Infrared Radiometry Section (WRC-IRS)

The WRC-IRS section performed 24 pyrgeometer calibrations in 2020. Marc Baker started in December as a new member of the technical personnel in the science department of the WRC -IRS and WRC-WCC-UV sections. In addition, IRIS radiometers were validated during a measurement campaign (Figure 3) with the National Metrology Institute of Germany (Physikalisch-Technische Bundesanstalt; PTB) in September 2020 at PMOD/WRC.

Atmospheric Turbidity Section (WRC-WORCC)

The WRC-WORCC section calibrated 11 Precision Filter Radiometers (PFR) against the WORCC Triad standard. In addition, three Precision Spectroradiometers (PSR) were calibrated against a reference standard, traceable to the PTB. An intercomparison campaign with the PMOD/WRC Lunar-PFR (Figure 4) was held in Aug.–Sep. 2020 at Lindenberg, German Meteorological Service (Deutscher Wetterdienst; DWD), Germany.

World Calibration Center for UV Section (WRC-WCC-UV)

The section WCC-UV calibrated 21 UVB broadband radiometers and issued 78 certificates. The certificates typically cover different units. Furthermore, this section performed two lamp/diode calibrations, while two spectrometers were calibrated against the QASUME travelling reference.

These calibrations resulted in two certificates which were issued without the CIPM logo.

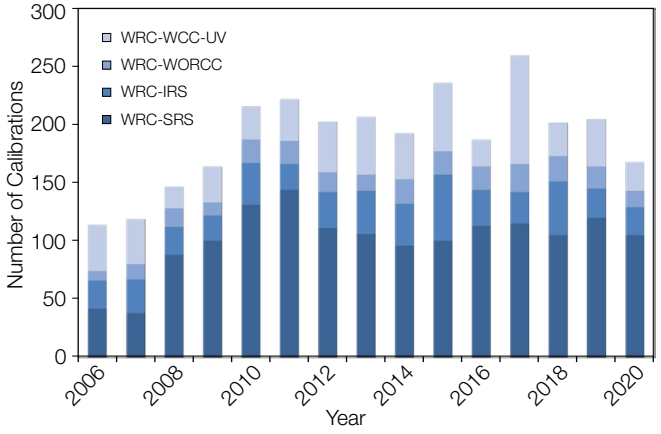

Figure 2. The number of instrument calibrations conducted at PMOD/WRC during the 2006–2020 period. Note: One instrument can result in more than one calibration certificate.

Figure 3. Vlew of an IRIS radiometer during a measurement campaign with the National Metrology Institute of Germany (PTB).

Figure 4. The Lunar-PFR during an intercomparison campaign at Lindenberg, German Meteorological Service (DWD), Germany.

Instrument Sales

In 2020, PMOD/WRC sold no instruments for several reasons, although one accessory was sold (diffuser system). The first reason was due to the outsourcing of the sale and production of PMO6-cc absolute radiometers to Davos Instruments (https://www.davos-instruments.ch/) during the last several years. A new generation of absolute radiometers has been developed, the PMO8, along with a new control unit. PMOD/WRC will continue to be responsible for the calibration of absolute radiometers against the World Standard Group. As a result, absolute radiometers will no longer appear in the sales statistics of Figure 5.

The second main reason for the lack of instrument sales was the global Covid-19 pandemic along with the postponement of the 13th International Pyrheliometer Comparison (IPC-XIII) to September 2021. This also meant postponement of the 5th Filter Radiometer Comparison (FRC-V) and the 3rd International Pyrgeometer Comparison (IPgC-III).

We are therefore cautiously optimistic that instrument sales will return to normal levels when IPC-XIII, FRC-V and IPgC-III take place. In addition, the new generation of Precision Filter Radiometers (see: page 21) will be available in 2021, which have already been pre-ordered by several customers.

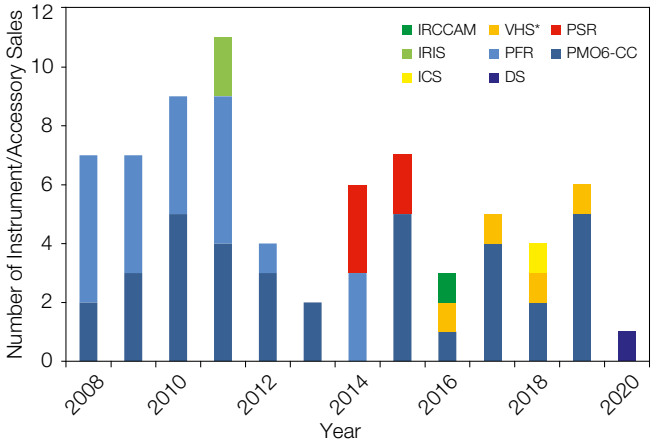

Figure 5. Number of PMOD/WRC instrument sales from 2008 up to and including 2020: i) IRCCAM = Infrared Cloud Camera, ii) VHS = Ventilated Heating Systems, iii) PSR = Precision Spectroradiometer, iv) IRIS = Infrared Integrating Sphere Radiometer, v) PFR = Precision Filter Radiometer, vi) PMO6-CC = absolute cavity pyrheliometer, vii) ICS = Irradiance Calibration System, and viii) DS = Diffuser System for UV spectroradiometers.

**Note: VHS sales/year shown as a single unit for ease of interpretation. Actual VHS units sold: 2016 = 7; 2017 = 2; 2018 = 36; 2019 = 5.*

Solar Radiometry Section (WRC-SRS)

Wolfgang Finsterle

The Solar Radiometry Section (SRS) of the WRC maintains and operates the World Standard Group (WSG) of Pyrheliometers which represents the World Radiometric Reference (WRR) for ground-based total solar irradiance measurements. The SRS operates the ISO 17025 certified calibration laboratory for solar radiometers (pyrheliometers and pyranometers). During the 2020 calibration season, 105 calibration certificates were issued. Due to the pandemic situation, the 13th International Pyrheliometer Comparison IPC-XIII was postponed to 2021.

In 2020, the SRS/WRC calibrated 105 radiometers: these consisted of 75 pyranometers, 19 pyrheliometers with a thermopile sensor and 11 absolute cavity radiometers. The WSG was operated on 66 days. The Cryogenic Solar Absolute Radiometer and Monitor for Integrated Transmittance (CSAR/MITRA) underwent successful functional tests towards their re-commissioning in 2021.

In preparation for IPC-XIII, which was originally supposed to be held in September/October 2020, the SRS has invested in a replacement of the data acquisition computer. The old computer is more than 10 years old and will be kept as a back-up solution in case of a technical failure of the new system.

In October 2020, Natalia Engler joined the SRS as an instrument scientist for CSAR/MITRA, supported by Louise Harra's ETH start-up grant. Her goal is to re-define the WRR based on CSAR/MITRA measurements. The first milestone is to get CSAR/MITRA ready for IPC-XIII in September/October 2021. Based on the solar measurements acquired in 2015/16, it was decided to re-design MITRA for triple-sensor operation (from the current dual-cavity design) to allow for compensation of ambient temperature changes. A new type of flat receiver with a carbon-nanotube black coating will be used instead of the old conical cavity with conventional black paint.

These receivers have been developed together with the spin-off company, Davos Instruments AG. The CSAR vacuum tank will be equipped with an additional vacuum gate which allows swapping of the CSAR and MITRA windows without breaking the vacuum. Both modifications are expected to significantly boost the absolute accuracy and stability of the CSAR/MITRA measurements. In parallel with the hardware improvements, the CSAR and MITRA control software were merged to allow the synchronous operation of both components.

Table 1. The WRR factors for the WSG pyrheliometers. These are the factors to multiply the readings with in order to represent the WRR.

WSG	IPC-XII
PMO2	0.998189
PMO5	0.999395
CROM2L	1.003118
MK67814	1.001702
HF18748	0.998258

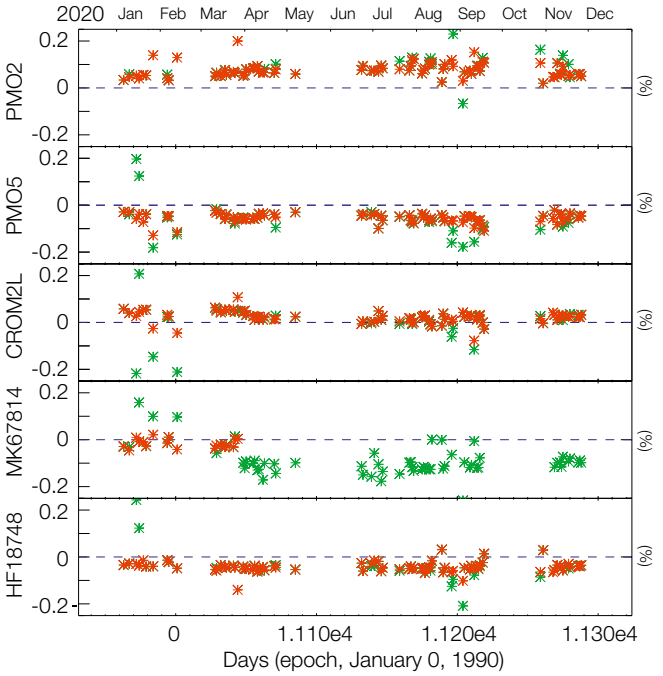

Figure 1. World Standard Group (WSG) measurements during 2020. Plotted here are the ratios of each WSG pyrheliometer with respect to the average of the group, i.e. the WRR. Red symbols indicate valid data points, while the green data points were not used to calculate the WRR. MK67814 experienced a problem in April, causing it to read low. The remaining four operational WSG pyrheliometers show no unusual behaviour with respect to the group average. The relative offsets of each WSG pyrheliometer represent the reciprocal WRR factors, as determined during IPC-XII (Finsterle, 2016).

Due to the travel restrictions imposed by the Covid-19 pandemic, it was not possible for the SRS to participate in any inter-laboratory comparisons during 2020. The stability assessment of the WRR was therefore based on the regular internal comparison of the WSG pyrheliometers and by monitoring of the calibration results of recurring external (customer) pyrheliometers. No indication of a drift was found with these methods.

References: Finsterle W.: 2016, IPC-XII Final Report, WMO IOM Report No. 124.

Infrared Radiometry Section (WRC-IRS)

Julian Gröbner, Christian Thomann, and Stephan Nyeki

The Infrared Radiometry Section of the WRC maintains and operates the World Infrared Standard Group of pyrgeometers (WISG) which represents the world-wide reference for atmospheric longwave irradiance measurements.

The WISG serves as an atmospheric longwave irradiance reference for the calibration of pyrgeometers operated by institutes around the world. The WISG has been in continuous operation since 2004, and consists of four pyrgeometers which are installed on the PMOD/WRC roof platform. The measurements of the individual WISG pyrgeometers with respect to their average are shown in Figure 1 for the period 2004 to the end of 2020. As can be seen in the figure, the WISG long-term stability is very good, with measurements of the four pyrgeometers within ±1 Wm^{-2} over the whole time period.

Simultaneous measurements carried out with the IRIS radiometers and ACP 96 provided on loan by NREL were performed on 68 clear sky nights between 7 January and 19 December alongside the WISG. In total, IRIS radiometers measured on 222 clear sky nights since January 2016. The differences between the WISG and IRIS radiometers over this time period are shown in Figure 2 for values of precipitable water vapour larger than 8 mm. Under drier atmospheric conditions, found primarily in winter in Davos, the differences between the WISG and IRIS show a pronounced dependence with water vapour as discussed in Gröbner et al. (2014).

As can be seen in Figure 2, the average difference between the WISG and IRIS radiometers is -3.75 ±1.2 Wm^{-2}, which is about 1 Wm^{-2} higher than that observed by Gröbner et al. (2014), but still well within the observed variability of the measurements.

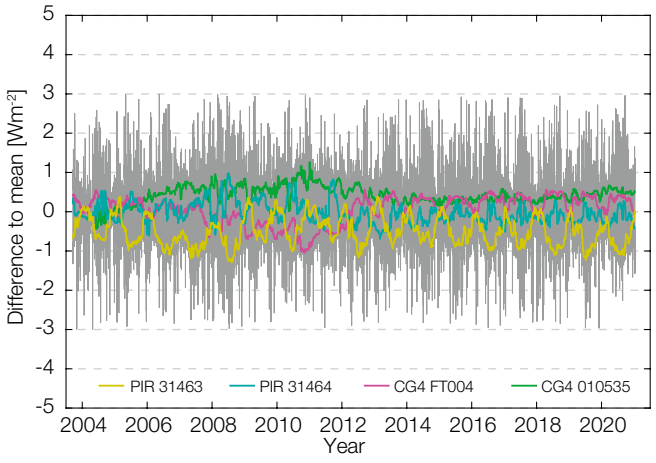

Figure 1. Night-time atmospheric longwave measurements of the WISG pyrgeometers relative to their average. The coloured lines represent a 30-day running mean of each WISG pyrgeometer, while the grey-shaded area represents daily averages.

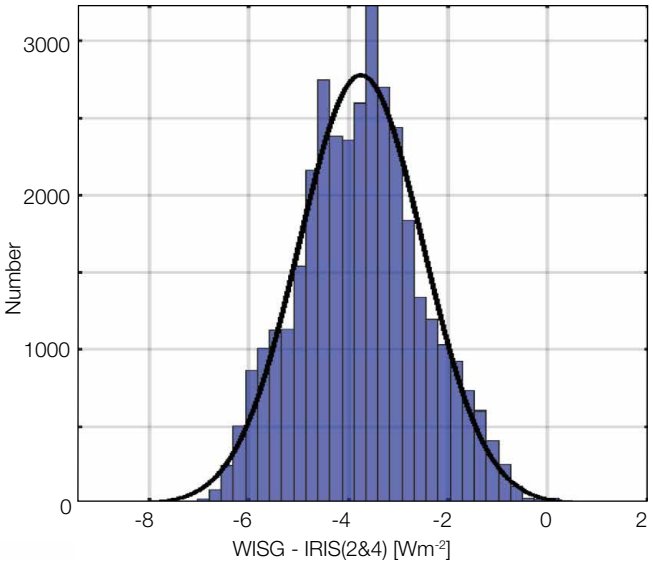

Figure 2. Difference in atmospheric longwave radiation between the WISG and IRIS radiometers 2 & 4 for the 2016–2020 period.

The traceability of the WISG to SI is realised by comparison to the IRIS radiometers which are used as transfer standards to link the WISG with the PMOD/WRC reference blackbody, BB2007. The calibration of IRIS with BB2007 was validated in the EMPIR METEOC-3 project during a measurement campaign held in September 2020 at PMOD/WRC with the participation of the PTB. During this campaign, PTB operated a radiation thermometer and a hemispherical blackbody to provide traceability of longwave irradiance to the primary ammoniac blackbody reference at PTB in Berlin, Germany. The measurements from this comparison are discussed in more detail in the science section of this annual report (see: "Comparison of the PMOD blackbody with the PTB radiation temperature scale" on page 44).

These activities form a core part of the tasks defined by the Expert Team on Radiation References (WMO, 2020), with the aim of formalising the WISG traceability chain to SI and developing guidelines on an eventual modification of the terrestrial reference scale represented by the WISG.

References:

Gröbner J., Reda I., Wacker S., Nyeki S., Behrens K., Gorman J.: 2014, A new absolute reference for atmospheric longwave irradiance measurements with traceability to SI units, J. Geophys. Res. Atmos., 119, doi:10.1002/2014JD021630

WMO: 2020, Expert Team on Radiation References, https://community.wmo.int/governance/commission-membership/commission-observation-infrastructures-and-information-systems-infcom/commission-infrastructure-officers/infcom-management-group/standing-committee-measurements-instrumentation-and-traceability-sc-mint/expert-team-0

Atmospheric Turbidity Section (WRC-WORCC)

Stelios Kazadzis, Natalia Kouremeti, and Julian Gröbner

The Atmospheric Turbidity Section of the WRC maintains a standard group of three Precision Filter Radiometers (PFR) that serve as a reference for Aerosol Optical Depth (AOD) measurements within WMO. WORCC also operates the Global Atmospheric Watch PFR (GAW-PFR) network for AOD and collaborates with other global aerosol networks.

The World Optical depth Research and Calibration Center (WORCC) calibration hierarchy uses a reference (so-called Triad) based on the average of three well-maintained Precision Filter Radiometers (PFRs) that are located at Davos, Switzerland. In addition, instruments operating at high mountain stations such as Mauna Loa (USA) and Izaña (Canary Islands, Spain) perform Langley calibrations and are sent (one instrument every six months) to WORCC in order to check the Triad stability with an independent instrument.

Analysis of these scheduled comparisons showed differences less than 1% in all cases. In addition, the average differences of each of the Triad PFRs compared with the Triad average was less than 0.005 (Aerosol Optical Depth; AOD) in more than 99% of the cases (1-minute measurements since 2005). This number is well below the WMO limits. No changes have been introduced to the Triad data set. Annual quality assured data from five GAW-PFR stations were updated and submitted to the World Data Center for Aerosols (WDCA). In 2020, four instruments from the GAW-PFR network and 10 other instruments, all part of the extended GAW-PFR network, were calibrated against the reference Triad at Davos.

Within the QA4EO project (sponsored by ESA), a PFR travelling standard was installed at the AERONET European calibration site to provide continuous traceability of AOD measurements to the PFR Triad. The objective is to test, as a pilot study, the possibility of linking the WORCC and ACTRIS/AERONET calibration scales (see: "Traceability of AERONET-EUROPE to the GAW-PFR WMO Reference for Aerosol Optical Depth" on page 43).

The Lunar-PFR participated in two comparison campaigns: 1) the Arctic Night Aerosol Characterization Campaign (ANACC) which aims to close the gap in the annual cycle of the Arctic AOD climatology, held at Ny-Ålesund, Svalbard, from 1 Feb. – 15 Mar. 2020, and 2) SCILLA: Summer Campaign for Intercomparison of Lunar measurements of Lindenberg's Aerosol. Held from 25 Aug. – 10 Sep. 2020, at Deutscher Wetterdienst, Metorological Observatory Lindenberg – Richard Assmann Observatory ("DWD/MOL-RAO"), where the performance of lunar photometers was examined under different atmospheric conditions.

WORCC has continued the collaboration with AERONET Europe and SKYNET Europe and Asia. Results of Skynet traceability to WORCC have been included in the overview publication by Nakajima et al. (2020). See also Figure 1. The 5th Filter Radiometer Comparison (FRC-V) originally scheduled for October 2020 has been postponed for one year due to Covid-19 travel restrictions.

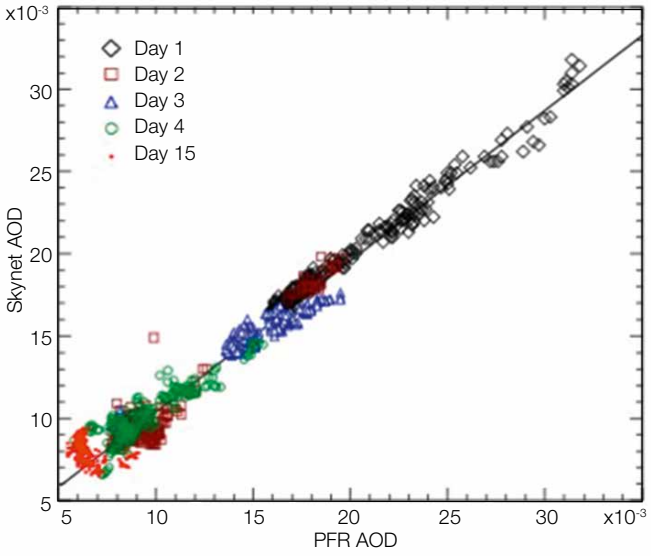

Figure 1. Comparison of AOD values at 870 nm obtained by the sky radiometer and PMOD/WRC PFR. Credit: Nakajima et al. (2020).

In 2020, the production of a new PFR series continued with small delays due to the Covid-19 pandemic. The new PFR series has been constructed with full compatibility to the existing data acquisition systems, and with improvements based on current technology and 21 years of experience since the first PFR series in 1998. The prototype instrument has been operational since Dec. 2019, and several of the new instruments will also be taking part in FRC-V in Sep.–Oct. 2021 (see: "The Next Generation Precision Filter Radiometer Series 2019" on page 21).

PFR AOD data from Cabauw (The Netherlands) have been used in order to investigate their effect on the record high solar irradiance in Western Europe during the Spring of 2020. Based on analyses of ground-based and satellite observations, as well as experiments with a radiative transfer model, it was estimated that a 1.3% (2.3 $W m^{-2}$) increase in surface irradiance with respect to the 2010–2019 mean occurred due to: i) low median AOD, ii) a 17.6% (30.7 $W m^{-2}$) increase due to several exceptionally dry days, and iii) a very low cloud fraction overall (van Heerwaarden, 2021).

A PhD student, A. Karanikolas, was registered as a student at ETH Zurich, D-PHYS, in the field of "aerosol optical properties, measurements and modelling".

References: Nakajima T., et al.: 2020, An overview of and issues with sky radiometer technology and SKYNET, AMT, 13, 4195-4218, ISSN 1867-8548

van Heerwaarden C.C., et al.: 2021, Record high solar irradiance in Western Europe during first COVID-19 lockdown largely due to unusual weather, Commun. Earth Environ. 2, 37, doi.org/10.1038/s43247-021-00110-0

World Calibration Centre for UV (WRC-WCC-UV)

Julian Gröbner, Gregor Hülsen, and Luca Egli

The objective of the World Calibration Center for UV (WCC-UV) of the WMO Global Atmosphere Watch (GAW) is to assess the data quality of the Global GAW UV network and to harmonise the results from monitoring stations in order to ensure representative and consistent solar UV radiation measurements on a global scale.

Unfortunately, due to the Covid-19 pandemic, no quality assurance site visits with the transportable reference spectroradiometer QASUME were carried out in 2020. However, at Davos, the calibration activities were unaffected. Twenty-one UV broadband radiometers were calibrated as well as two irradiance standards and two spectroradiometer systems.

The main activity in the 19ENV04 MAPP (Metrology for Aerosol Properties) project (EMPIR programme co-funded by participating states and EU Horizon 2020) was the improvement of the angular responsivity measurement setups, located in the WCC-UV laboratory. The single-axis goniometer was replaced by a two-axis system which facilitates pointing measurements of sun photometers and devices measuring direct irradiance (Figure 1).

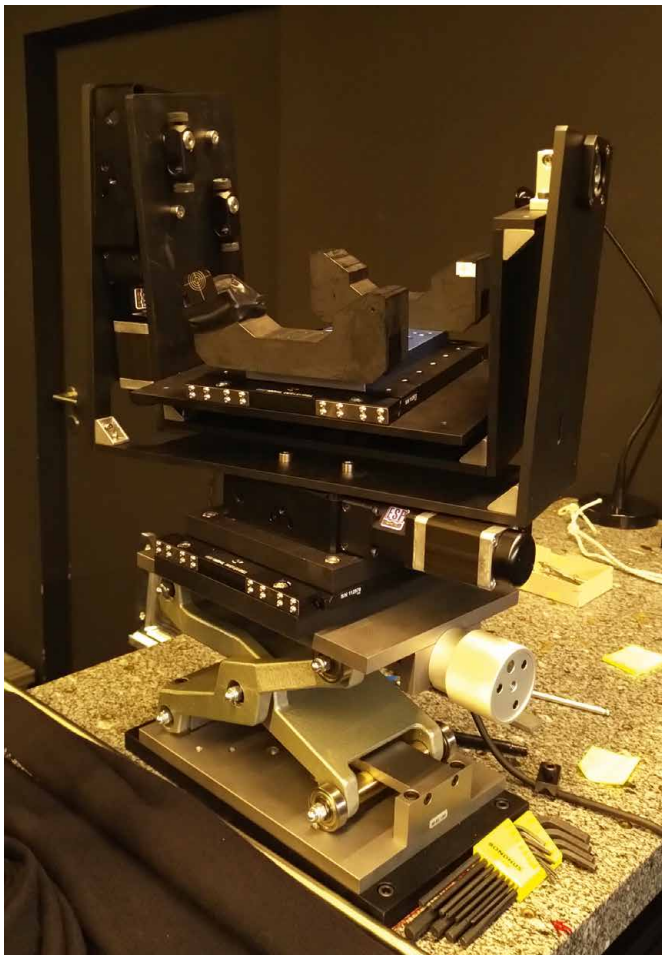

Figure 1. The new Angular Response Function (ARF) pointing measurement setup of the WRC with two Newport goniometers.

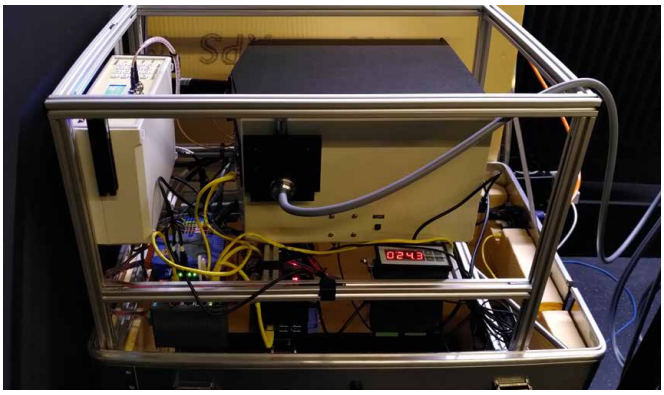

Figure 2. The QasumeIR spectroadiometer system with a Bentham single monochromator inside a temperature-controlled box. The fibre is connected to an integrating sphere acting as an input optic.

In the same project, a new spectroradiometer system was built: QasumeIR (Figure 2) is based on the long experience of the Qasume and QasumeII UV spectroradiometers. The wavelength range of QasumeIR is in the visible and extends into the infrared. The system is intended for direct solar irradiance measurements from 500 nm up to 1.7 µm.

The long-term solar UV measurements at Davos were used as a reference dataset in two studies: The first validated the surface UV radiation product of the TROPOMI satellite, while the second study calculated highly spatially resolved maps of UV index over Europe (Lakkala et al., 2020, Kosmopoulos et al., 2021).

As part of the restructuring of the WMO, a new Expert Team on Atmospheric Composition Measurement Quality (ET-ACMQ) was established. At a recent meeting of members from the scientific community, presentations were given about how different calibration laboratories were providing traceability to SI. A status report of WCC-UV activities was given at this first meeting, organised in September 2020. Similarly, a meeting of the WMO Scientific Advisory Group on Ozone and UV took place online in October. The ozone and UV activities at PMOD/WRC were discussed during this meeting.

References:

Lakkala K., et al.: 2020, Validation of the TROPOspheric Monitoring Instrument (TROPOMI) surface UV radiation product, Atmos. Meas. Tech., 13, 6999-7024, doi.org/10.5194/amt-13-6999-2020

Kosmopoulos P., et al.: 2021, Real-time UV-Index retrieval in Europe using Earth Observation based techniques and validation against ground-based measurements, Atmos. Meas. Tech. Discuss. [preprint], doi.org/10.5194/amt-2020-506, in review.

Section Ozone: Total Ozone Column and Umkehr Measurements

Julian Gröbner, Herbert Schill, Franz Zeilinger, and Luca Egli

Operational Total Ozone Column and Umkehr measurements are performed at PMOD/WRC with two Dobson and three Brewer spectrophotometers to monitor the stratospheric ozone layer, hence extending the world's longest continuous total ozone time-series at Arosa and Davos, Switzerland.

The stratospheric ozone measurements in Arosa and Davos continued with direct sun (total ozone) measurements performed with two Dobsons (D051 and D101) and three Brewers (B072 and B156 from Meteoswiss and B163 from PMOD/WRC), while observations at Arosa also continued with one Dobson (D062) and one Brewer (B040) (see Figures 1 and 2). Dobson D051 is mainly dedicated to Umkehr measurements, and therefore only occasionally used for direct sun observations to compare with D101 and D062. Table 1 gives some annual statistics for the Dobson as well as the Brewer direct sun measurements taken at both sites.

At the end of May 2020, the technician Franz Zeilinger took over the full supervisional responsibility of operational ozone measurements at PMOD/WRC from MeteoSwiss. During this year, he homogenised the hardware parts of the Dobson systems in order to have redundancy in case of breakdowns (see also Figure 3).

With the goal to measure in-situ ground ozone, which could be used to correct the total ozone column at Davos with respect to the Arosa site, two MonitorLab systems were installed in October 2020 at the PMOD/WRC next to the Dobson container and on the SLF research field near the Weissfluhjoch station, Davos.

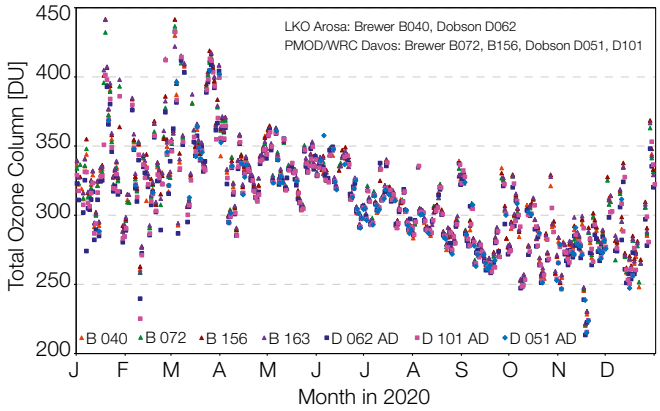

Figure 1. Daily total ozone values in 2020 from direct sun measurements with Brewer and Dobson spectrophotometers at LKO, Arosa (Brewer B040 and Dobson D062) and PMOD/WRC, Davos (Brewers B072, B156, B163 and Dobsons D051, D101).

Figure 3. The effort during winter to continue ozone measurements.

Table 1. Number of yearly direct sun measurements in 2019 and 2020 from Dobsons and Brewers at LKO, Arosa, and PMOD/WRC, Davos: Number of days with measurements, number of all measurements, number of unflagged (i.e. reliable) measurements and the percentage of the latter of the total number.

Direct sun measurements at Arosa and Davos in 2019 and 2020						
Dobson	at	year	days	all	unflagged	percent
D062	Arosa	2019	348	44855	24781	55%
		2020	362	49734	31004	62%
D101	Davos	2019	354	48229	28618	59%
		2020	361	49229	32919	67%
D051	Davos	2019	91	11720	7267	62%
		2020	113	14492	9541	66%
Brewer	at	year	days	all	unflagged	percent
B040	Arosa	2019	346	28779	17198	60%
		2020	345	23863	14684	62%
B072	Davos	2019	340	28323	16473	58%
		2020	324	23896	13241	55%
B156	Davos	2019	348	31389	15579	50%
		2020	336	24988	12918	52%
B163	Davos	2019	297	4949	4857	98%
		2020	362	5998	4659	78%

In July, the data quality control of Dobson D018 and Brewer 071 at the GAW-station in Nairobi (Kenya), became part of the QC/QA duties of Herbert Schill. This task is financially and technically supported by MeteoSwiss. See: “Total ozone column measurements and data quality control of Nairobi data” on page 39.

Substantial efforts were made to reduce the seasonal and overall differences between Dobson and Brewer direct sun measurements by using more appropriate absorption spectra: see “Consistency of total ozone column measurements between the Brewer and Dobson spectroradiometers of the LKO Arosa and PMOD/WRC Davos” on page 41.

References: Gröbner J., Schill H., Egli L., Stübi R.: 2021, Consistency of total column ozone measurements between the Brewer and Dobson spectroradiometers of the LKO Arosa and PMOD/ WRC Davos, Atmos. Meas. Tech. Discuss. [preprint], doi.org/10.5194/amt-2020-497, in review.

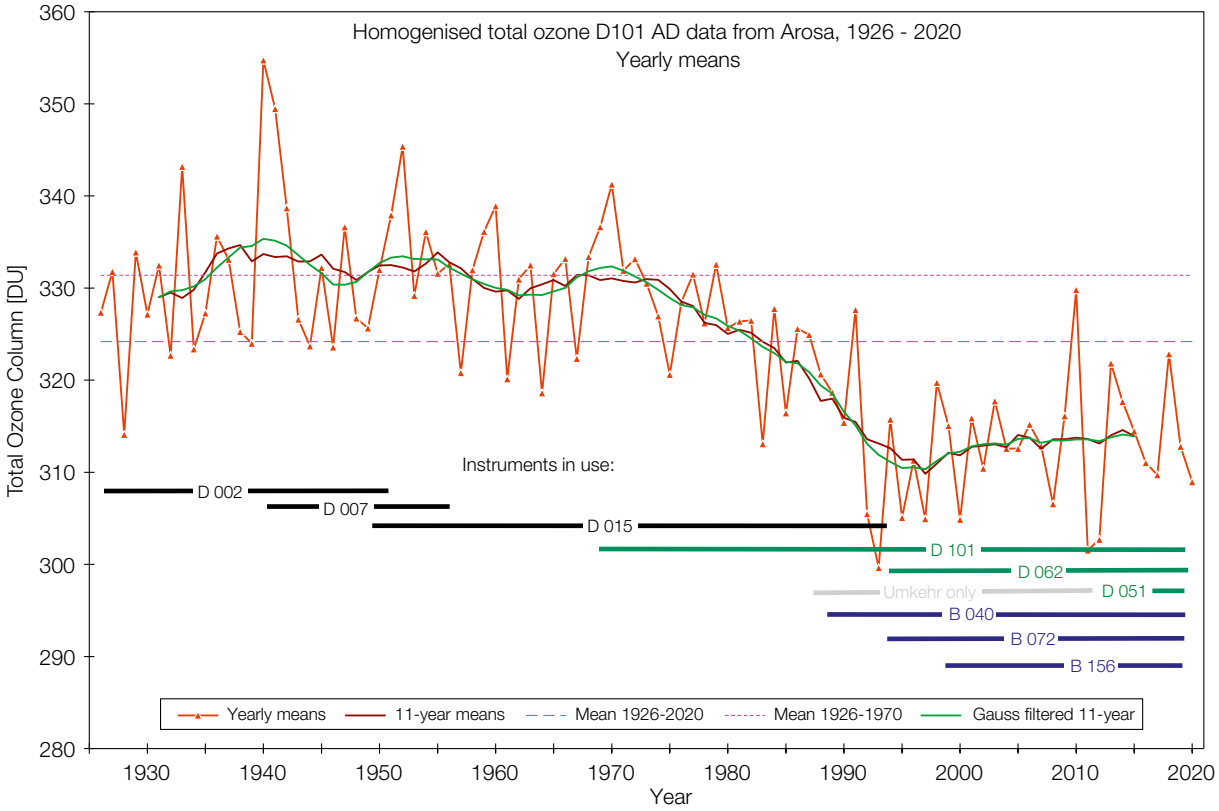

Figure 2. Yearly (red), 11-year (burgundy and Gaussian-filtered 11-year (light green) averages of homogenised total ozone column at Arosa. Timelines for the different instruments in operation at LKO, Arosa and PMOD/WRC, Davos are shown in the lower half.

Instrument Development

Space Missions in the Build Phase

Andrea Alberti, Valeria Büchel, Wolfgang Finsterle, Matthias Gander, Margit Haberreiter, Louise Harra, Manfred Gyo, Silvio Koller, Patrik Langer, Daniel Pfiffner, Werner Schmutz, Marcel Spescha, Daniel Tye and Liviu Zambila

PMOD/WRC is involved in six missions at different stages of development. There are Digital Absolute Radiometer (DARA) instruments on two different space missions that will be launched in 2021 – 2023. One is for the Chinese mission FY-3E, to be launched in 2021/2022, and one for the ESA-Proba-3 mission scheduled for 2023. These are designed to measure the Total Solar Irradiance (TSI). Development is underway for the ESA (Traceable Radiometry Underpinning Terrestrial- and Helio-Studies) TRUTHS mission and Lagrange space weather mission, both due to be launched in 2027. In addition, our involvement is approved for a solar spectral irradiance monitor for the Japan Aerospace Exploration Agency (JAXA) Solar-C mission, which is due to be launched in 2026. We are involved in the NASA solar polar mission, Solaris, during the phase A study.

JTSIM-DARA / FY3-E

FY-3E is an Earth observation satellite by the Chinese Meteorological Administration (CMA). The satellite also carries the Joint Total Solar Irradiance Monitor (JTSIM; Figure 1) experiment that consists of two solar radiometers, one from China and DARA from PMOD/WRC. The year 2020 was used for spacecraft-level integration and testing in China. After the successful calibration campaign in December 2019, the JTSIM-DARA stayed in China where it was integrated on the JTSIM solar tracker and later on, the FY-3E spacecraft. During these tests an electrical connector failed on JTSIM-DARA that had to be replaced by Chinese engineers under video supervision by PMOD/WRC. The JTSIM experiment will provide new measurements of TSI, which is an important Essential Climate Variable (ECV). The launch of FY-3E is planned as of June 2021.

DARA / Proba-3

The Digital Absolute Radiometer (DARA), is a payload onboard the ESA Proba-3 formation flying mission. DARA is a 3-channel radiometer designed for the long-term stable and highly accurate measurement of TSI which is fully traceable to SI. The tasks done during the past year concerned assembly and testing of both DARA flight models, the Engineering Qualification Model/Flight Spare (EQM/FS), and the Flight Model (FM). In May 2020, the EQM/FS was sent to QinetiQ Space N.V. in Belgium for electrical and software interface tests to the spacecraft. Both instruments are now completed, almost fully tested, and calibrated at the component-level. At the beginning of 2020, the Optical Surface Reflectors (Figure 2) were placed on the front shields.

The thermal cycle test was performed on the DARA EQM/FS at PMOD/WRC to qualify the instrument for thermal vacuum application in a representative environment. The thermal balance test was conducted at the University of Bern towards the end of 2020 to verify the thermal model and analysis (Figure 3), which were performed during earlier engineering phases. To verify the complete thermal hardware, an engineering version of the instrument Multi-Layer Insulation was applied, delivered by the Italian company Aviotec.

The FM calibration campaign using sunlight began and involved a comparison with the World Radiation Reference at PMOD/WRC. Operation and pipeline software have mostly been completed, and are in use for calibration data acquisition. Ongoing tasks include: finalising the instrument, all environmental acceptance tests with the FM, and operation documents. The last major step foreseen is an end-to-end absolute calibration against the TSI Radiometer Facility at the Laboratory for Atmospheric and Space

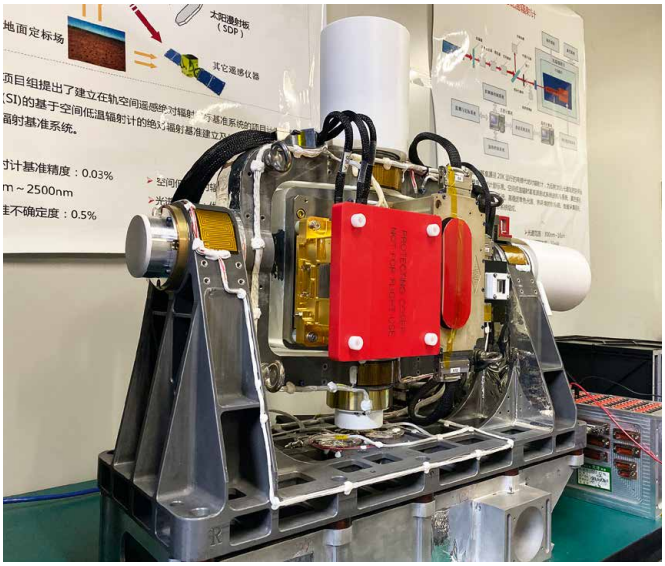

Figure 1. JTSIM-DARA (with red protective cover) was integrated in Spring 2020 on the JTSIM solar tracker alongside the Chinese SIAR instrument. After successful environmental tests, the JTSIM solar tracker was integrated on the FY-3E satellite for testing at the spacecraft-level.

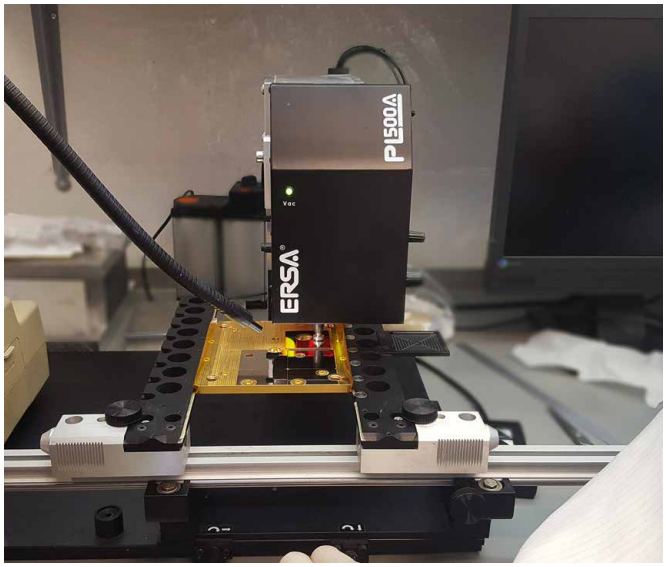

Figure 2. Adjustment of the Optical Surface Reflectors on an X-Y table, under a PMOD/WRC clean bench hood.

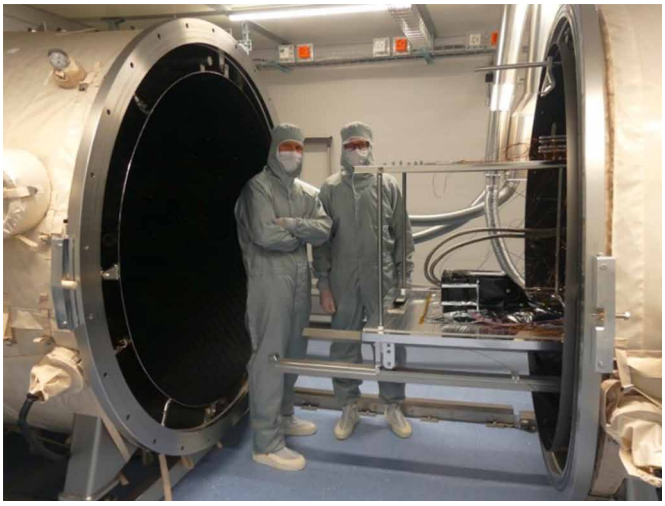

Figure 3. Thermal balance test in the vacuum chamber used previously for the Characterising Exoplanet Satellite (CHEOPS) mission at the University of Bern.

Physics (LASP; Boulder, USA) and then the DARA instruments are ready for launch – presently scheduled for 2023.

SoSpIM / Solar-C

Solar-C is the next Japanese solar physics mission to be developed with significant contributions from US and European countries. The mission carries an Extreme UV (EUV) imaging spectrometer with a slit-jaw imaging system called EUVST (EUV High-Throughput Spectroscopic Telescope) as the mission payload, to take a fundamental step towards answering how the plasma universe is created and evolves, and how the Sun influences the Earth. In April 2020, ISAS (Institute of Space and Astronautical Science) of JAXA (Japan Aerospace Exploration Agency) made the final down-selection as the fourth in the series of the competitively chosen M-class mission to be launched with an Epsilon launch vehicle in the mid-2020s.

A second instrument, led by PMOD/WRC, provides spectral irradiance capability through a Solar Spectral Irradiance Monitor (SoSpIM). This provides both scientific and calibration capabilities. SoSpIM and EUVST will work hand-in-hand. EUVST will provide consistent spectral observations from the chromosphere to the corona, tracking the energy flow on small spatial scales. SoSpIM will provide 'Sun-as-a-star' measuring in two wavelength bands that overlap EUVST. This provides measurements of all solar flares visible from Earth, not just those within the EUVST field-of-view. The SoSpIM instrument provides the connectivity between the flare processes captured in detail on the Sun by EUVST and the impact of those irradiance changes in different layers of the Earth's atmosphere.

LUCI / Lagrange

The Lagrange EUV Coronal Imager (LUCI; West et al., 2020) is one of the payloads onboard ESA's upcoming Space Weather mission, Lagrange. The LUCI consortium is led by Centre Spatial de Liège (CSL; Belgium) and further includes the Royal Observatory of Belgium (ROB; Belgium) and PMOD/WRC.

LUCI will take images of the Sun and the extended corona with a field-of-view of up to 2.5 solar radii in the direction of Earth. The viewpoint at the Lagrange Point L5 will allow active regions on the solar disc to be monitored before they can be seen from Earth. This will give forecasters some lead-time for the warning of potentially severe space weather events.

In 2020, the key activity of the LUCI project was Phase I of the pre-development (PD) covering the design of the mechanical structure and the Front-End Electronics (FEE). Figure 4 shows the latest mechanical design of the instrument as of the end of PD Phase I. The most notable change from the earlier design iteration is a considerably larger radiator (see the plate at the top of the instrument) along with a new mounting design. With the structural analysis, it was verified that the instrument is mechanically stable and is expected to survive severe loads during launch. The verification of the thermal behaviour, also part of this PD, was carried out by CSL.

Regarding the electronics, the design of the analogue board was completed, and the breadboard of the analogue electronics assembled and commissioned.

Finally, functional tests (see Figure 5) of all individual electronic components as well as the fully assembled system were successfully performed. Parallel to PD, the so-called Bridging and Spanner Phase were pursued during which additional PA tasks were addressed. At the end of PD Phase I, both the FEE and TM sub-systems underwent an in-depth design review.

Figure 4. Status of the mechanical structure at the end of pre-development Phase I of the Lagrange LUCI instrument.

CSAR / TRUTHS

The Traceable Radiometry Underpinning Terrestrial- and Helio-Studies (TRUTHS) is a climate mission led by the UK Space Agency (UKSA), which will be delivered by the European Space Agency (ESA) to enable in-flight calibration of Earth observation (EO) satellites. PMOD/WRC will contribute the radiometer controller (hardware and software) as well as other hardware parts to the Cryogenic Solar Absolute Radiometer (CSAR) on TRUTHS.

The start of the pre-development was set in October 2020, although contract negotiations are still ongoing to date and therefore the work on the actual project has not yet started. During the pre-development phase, PMOD/WRC hopes to develop a prototype of the radiometer controller to demonstrate the space readiness of the technology.

In 2020, PMOD/WRC also contributed to the User Requirement Document study (URD) and to the Mission Accompanying Consolidation Study (MCAS).

Solaris Mission

Solaris is a solar polar mission of discovery to address fundamental questions about the Sun and Heliosphere that can only be answered from a high latitude (polar) vantage point. Solaris will be the first mission to obtain sustained coverage of the solar interior and atmosphere from high latitudes, uniquely and comprehensively investigating the global Sun and Heliosphere. It will use a Jupiter fly-by, and achieve an inclination of 55° above the ecliptic, and have a 3-month pass about the solar poles.

Solaris will provide direct imaging of the solar poles with the EUV Imager (S-EUVI), whose design is built on the Solar Orbiter EUI and Lagrange LUCI instruments. NASA selected five proposals for concept study, two of which will go forward. PMOD/WRC along with Fachhochschule Nordwestschweiz (FHNW; CH), Royal Observatory of Belgium (ROB; Belgium) and Inst. D'Astrophysique Spatiale (IAS; France) are the S-EUVI instrument team.

References: West M.J., Kintziger C., Haberreiter M., Gyo M., Berghmans D., Gissot S., Büchel V., Golub L., Shestov S., Davies J.A.: 2020, LUCI onboard Lagrange, the next generation of EUV space weather monitoring, J. Space Weather Space Clim., 10, 49, doi.org/10.1051/swsc/2020052

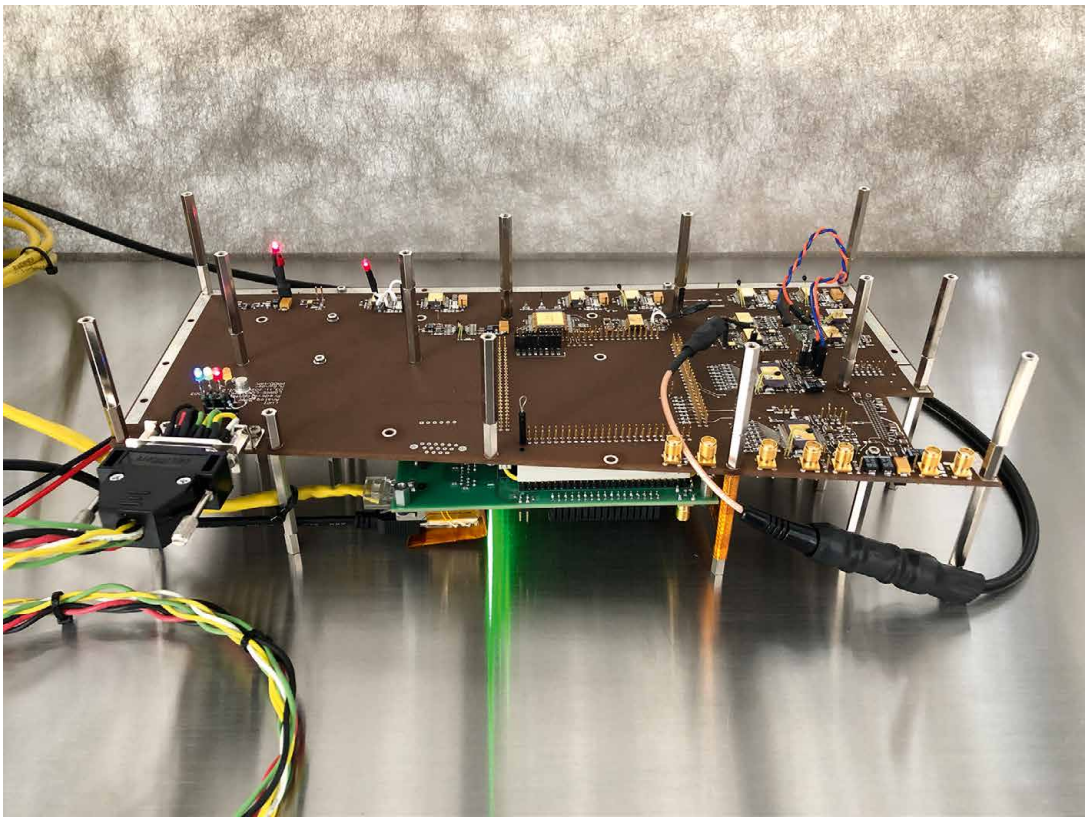

Figure 5. Setup for first functional tests of the assembled LUCI analogue board.

Space Missions in the Operations Phase

Wolfgang Finsterle, Margit Haberreiter, Louise Harra, Silvio Koller, Jean-Philippe Montillet, Daniel Pfiffner, and Elena Podladchikova

PMOD/WRC is involved in the operations of instruments onboard six operational spacecraft. The ESA SOHO mission was launched back in 1995, and the PMOD/WRC instrument, Variability of solar IRradiance and Gravity Oscillations (VIRGO) is still operational. The ESA Proba-2 mission, launched in 2001, hosts the LYRA instrument with PMOD/WRC involvement, measuring the solar spectral irradiance. The Compact Lightweight Absolute Radiometer (CLARA), launched in 2017, is a payload onboard the Norwegian NorSat-1 micro-satellite and is a new generation of radiometer to measure the total solar irradiance. Finally, our latest involvement is in the ESA/NASA Solar Orbiter mission, launched in 2020. We are involved in both the imager and spectrometer.

We have operational, calibration and scientific responsibilities on all of the instruments PMOD/WRC have been involved in developing. These include irradiance measurements (VIRGO, LYRA and CLARA), and more recently imaging and spectroscopic measurements. We have been funded through Karbacher Fonds to support these efforts since the end of 2019.

VIRGO / SOHO

Various space missions have measured the total solar irradiance (TSI) since 1978. Among them, the Variability of Irradiance and Gravity Oscillations (VIRGO) on the mission Solar and Heliospheric Observatory (SOHO), which started in 1996 and is still operational. Like most TSI experiments (e.g., Figure 1), they employ a dual-channel approach with different exposure rates to track and correct the inevitable degradation of their radiometers. Until now, the process of degradation correction has been mostly a manual process based on assumed knowledge of the sensor hardware.

In the last two years, together with students from the ETH Dept. of Computer Science, PMOD/WRC has developed a new data-driven process to assess and correct instrument degradation using a machine-learning and data fusion algorithm, that does not require deep knowledge of the sensor hardware. The algorithm

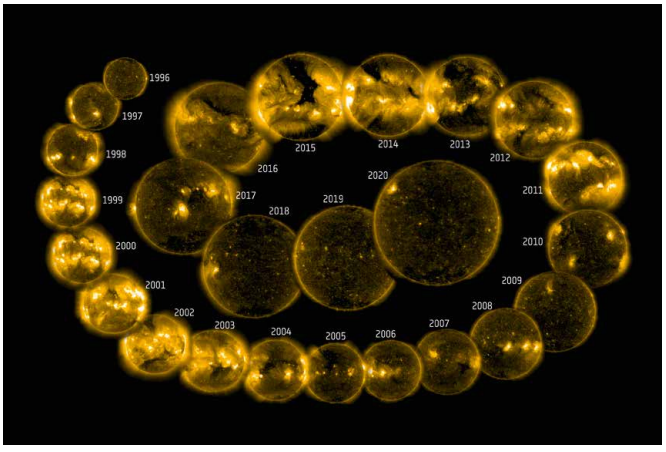

Figure 1. Solar irradiance variability through solar cycles 23 and 24. Image credit: SOHO, ESA & NASA.

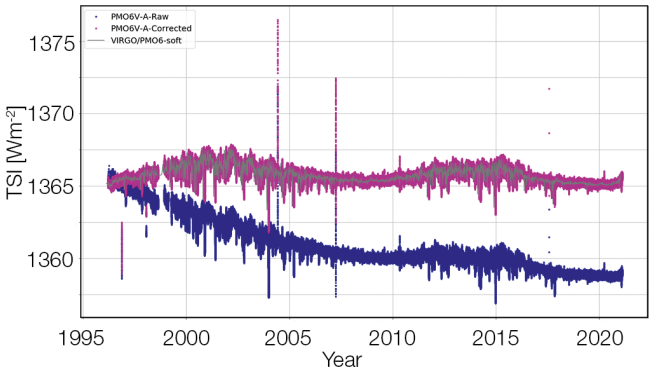

Figure 2. SOHO/VIRGO channel A, before (raw; blue) and after (corrected; purple) the degradation-correction, together with the fusion (grey) of the degradation-corrected observations on both channels (A and B). Shown here are the VIRGO TSI data on their pre-launch calibrated scale, i.e. traceable to the WRR. Later, Fehlmann et al. (Metrologia, 49, 2012) found a 0.34% scale offset between the WRR and SI (WRR reading higher). Note that this offset correction is not part of our degradation correction algorithm. For climate research or solar energy applications the offset should be subtracted.

is applied to the VIRGO TSI records to produce a new version of the VIRGO TSI time-series and to extend the previously published data set which had been maintained by the late Claus Fröhlich. The VIRGO TSI time-series has been receiving a lot of attention from the community. Our new version will be made available to the community on www.pmodwrc.ch. It nicely reproduces Claus Fröhlich's version during the time when they overlap as well as naturally extending it. The data fusion part of the algorithm (see Figure 2) can also be used to combine data from different instruments and missions into a composite time-series. Based on the fusion of the degradation-corrected VIRGO/PMO6 and VIRGO/DIARAD time-series, we find no significant change (i.e -0.17±0.29 W/m^2) between the TSI levels during the two most recent solar minima in 2008/09 and 2019/20. This work was published in Scientific Reports (Finsterle et al., 2021) in order to release an update of the post-processed data set to the TSI scientific community.

Future work will focus on refining the underlying assumptions of the machine-learning algorithm, including: i) additional TSI experiments in order to feed them into the "community composite" approach of a 40-year time-series starting with the early experiments in the late 1970's, and ii) to validate the result by comparing it to a composite based on our data fusion approach.

CLARA / NorSat-1

CLARA onboard NorSat-1 was launched on 14 July 2017, and is the most recent operational TSI radiometer built at PMOD/WRC. Its primary science goal is to measure the TSI and contribute to the long-term record of TSI measurements from space. After the failure of a reaction wheel on the NorSat-1 platform on 13 May 2018, a new platform operation scheme was implemented and CLARA became operational again in November 2019. As the solar pointing capabilities of NorSat-1 have been limited since then, we

have developed a new scheme, allowing us to flag data with poor solar pointing by using the onboard Precision Sun Sensor (PSS).

In addition, we have further applied a quality check on the heater cycle of the instrument. We have investigated in detail the performance of the so-called nominal error and control signal. These two parameters indicate how stable the control loop of the cavity heater is. The quality of these two signals is crucial for TSI measurements, as they are directly used to determine the solar power. A quality check of both parameters allowed us to further improve these measurements. Figure 3 shows the individual processing steps to achieve the final CLARA TSI time-series (black stars). A paper on the data analysis and comparison to other available TSI data is currently in preparation (Haberreiter et al., in preparation).

Besides measuring TSI, CLARA also determines Earth's Longwave Outgoing Radiation (LOR) when the satellite is in eclipse. Similar data filtering as for TSI is also applied to LOR measurements. The terrestrial measurements are a new scientific avenue for PMOD/WRC's absolute radiometers. Specifically, they serve as an in-flight demonstration for the determination of the Earth's radiation budget and hence also the Earth's Energy Imbalance (EEI) from space.

Solar Orbiter

PMOD/WRC is involved in two instruments on Solar Orbiter. The first is the Extreme Ultraviolet Imager (EUI), consisting of three telescopes, optimised to image the solar atmosphere in Lyman-α (121.6 nm, temperature ~30000 K) and Extreme UV (EUV; 17.4 nm and 30.4 nm, temperatures ~1 MK and 0.08 MK, respectively). The second is the Spectral Imaging of the Coronal Environment (SPICE). This instrument is an EUV imaging spectrograph designed to remotely characterise plasma properties of the solar corona. In 2020, the instruments were commissioned successfully, and the mission is now in cruise phase. During this phase, the remote sensing telescopes are mostly switched off but have five check-out windows. Data from these periods are being used to understand the calibration and behaviour of the instruments. The first perihelion (0.55 A.U.) was in June 2020, which gave a spatial resolution of 400 km. When we reach operational phase at a perihelion of 0.3 A.U., this will improve by a factor of nearly two. The first light data was released from the mission in Summer 2020 (see Figure 4). All the instrument papers have now been published, as well as the planning, which was complex. Planning involves Solar Orbiter specific operations, and coordination with other facilities such as space satellites (Parker Solar Probe, Hinode, IRIS) and ground-based telescopes. This coordination opens up new areas of research including 3-D spectroscopy.

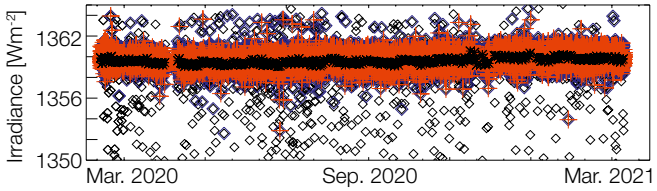

Figure 3. CLARA TSI measurements before any filtering (black diamonds), after the pointing filtering (blue diamonds), after the quality check of the heater signal (red crosses) and the final daily data (black stars).

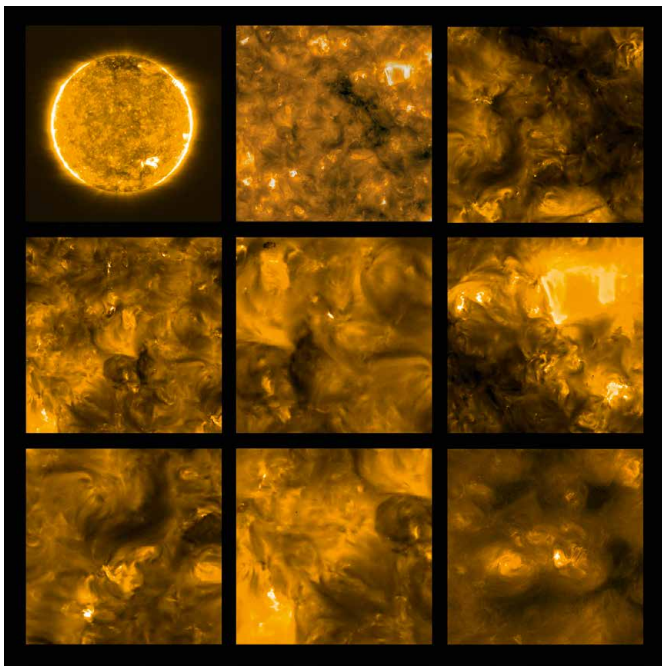

Figure 4. First images from the EUI instrument on Solar Orbiter. The top left is a full Sun image, and the other panels are high resolution images with arrows highlighting the bright features called 'campfires'. Image credit: SOHO, ESA & NASA.

At PMOD/WRC, we have developed a software tool for combining spectrometers in Earth orbit with Solar Orbiter when it is off the Sun-Earth line. A paper describing this was submitted to the Solar Orbiter special edition in Astronomy & Astrophysics (Podladchikova et al., 2021). The software is available for the international community, and data has been released to the public and can be accessed through the Solar Orbiter archive at the European Space Operations Centre (ESOC, Darmstadt, Germany; soar.esac. esa.int/soar). The instruments are being calibrated. The PMOD/WRC group has developed an advanced algorithm which leads to the derivation of high-quality data, obtained in the harsh radiative environment. The algorithm was tested by the consortium and found to be efficient, and has been applied to raw data in order to produce a calibrated version. Development of the algorithm is ongoing.

References: Finsterle W., Montillet J.P., Schmutz W., Šikonja R., Kolar L., Treven L.: 2021, The total solar irradiance during the recent solar minimum period measured by SOHO/VIRGO, Sci Rep. 2021 Apr 9; 11(1):7835. doi: 10.1038/s41598-021-87108-y

Haberreiter M., Finsterle W., Montillet J.-P., et al.: 2021, CLARA First Light measurements and in-flight performance, to be submitted to A&A.

Podladchikova O., Harra L.K., Barczynski K., et al.: 2021, Stereoscopic measurements of coronal doppler velocities, A&A, submitted.

The Next Generation Precision Filter Radiometer Series 2019

Lloyd Beeler, Patrik Langer, Pascal Schlatter, Natalia Kouremeti, Stelios Kazadzis, and Julian Gröbner

The Precision Filter Radiometer (PFR) was designed in the early 1990's to be a reference instrument for autonomous long-term aerosol optical depth (AOD) monitoring at four narrow spectral bands centred at specific wavelengths recommended by the WMO. The next PFR generation is being developed to secure the continuous operation of the Global Atmosphere Watch PFR (GAW-PFR) network and its ancillary stations for the foreseeable future. The main design features of the PFR are its long-term stability and automated operation under harsh weather conditions.

Due to the fact that spare parts have become difficult to obtain, a next generation of PFRs was developed by PMOD/WRC to secure the continuous operation of the Global Atmosphere Watch PFR (GAW-PFR) network and its ancillary stations for the foreseeable future (Kazadzis et al., 2018).

The main focus of the re-design was to include backward compatibility with existing instrument holders and data acquisition systems. Improved features are an upgraded sensor head and a newly designed temperature stabilisation system. In the PFR-19 design (see Figure 1), great effort went into the modular construction. The main objective was to develop an efficient instrument assembly process as well as a reduction in maintenance and repair interventions. The design of the optical filter holder was standardised and now allows the installation of different optical filter types for up to 12 wavelength channels. In this way, the instrument serves as a base instrument which can be adapted for different wavelengths without hardware adjustments becoming necessary. The rather fragile, cemented set-up of the previous input precision aperture and the corresponding muffler blades structure was replaced by a sturdy, metallic set-up which was bolted together. To keep the optics inside the instrument as clean as possible, low outgassing materials are used, e.g. instead of PVC (polyvinyl chloride) isolated wires, PTFE (polytetrafluoroethylene) counterparts were installed. Similarly, in order to reduce the formation of dust particles from shutter wear, the mechanics of the shutter were improved so that no mechanical stops are necessary.

On the electronics side, the focus was on instrument safety. On that account, input protection circuits, which provide over and under-voltage as well as short-circuit protection, were introduced

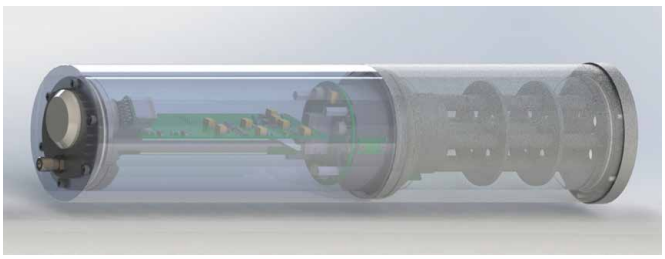

Figure 1. Mechanical design of the PFR-19 showing the electronic board (green) and the front-end muffler.

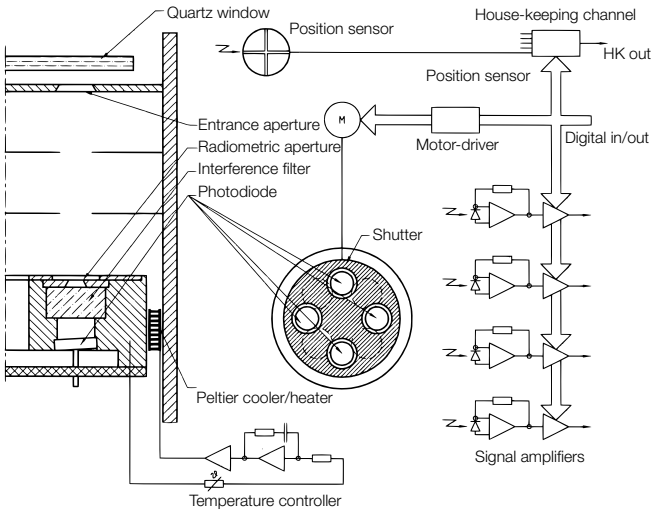

Figure 2. Optical layout on the left and primary diode amplifier stage on the right.

on all in and outgoing connections to the sensor head. Partial power loss is also handled and results in a safe shut down of the sensor head. The second objective was to decrease noise on the diode and housekeeping signals. In order to do so, the power electronics, namely the Peltier system, are no longer supplied via the head printed circuit board (PCB) which accommodates the sensitive, analogue signal amplifiers. Instead, the Peltier system is wired directly to the main (PCB) board which comprises the control circuit. In the external data acquisition electronics box, the 230V AC-DC power supply was replaced with a linear one so that high frequency switching noise and its harmonics do not affect the instrument. The remaining signal noise is further reduced by efficient low pass filters on all signal amplifiers which cut off undesired frequencies higher than 5 Hz. Finally, a gain-switched amplifier was re-introduced into the diode signal path (see Figure 2) which allows gain change to optimise the full-scale measurements, thus enabling a higher signal resolution over a period of a full day (sunrise to sunset).

An initial batch of ten PFR-19 are currently being assembled which will replace defective instruments from the GAW-PFR network. A second batch of ten commercial PFRs will be constructed and assembled during 2021 for interested external PFR users. Subsequent PFR series will be built, depending on commercial orders from the scientific community. A future development will include a high-sensitivity version of the above-described solar PFR for measuring lunar irradiance during night-time AOD measurements.

References: Kazadzis S., Kouremeti N., Nyeki S., Gröbner J., Wehrli C.: 2018, The World Optical Depth Research and Calibration Center (WORCC) quality assurance and quality control of GAW-PFR AOD measurements, Geosci. Instrum. Method. Data Syst., 7, 39–53, doi.org/10.5194/gi-7-39-2018

Scientific Research Activities

Overview

Louise Harra

Projects at PMOD/WRC are related to solar radiation in which we address questions regarding the radiation energy budget in the terrestrial atmosphere, as well as problems in solar physics in order to understand the mechanisms concerning the variability of solar irradiance. Hardware projects at our institute are part of investigations into Sun-Earth interactions which involve measurements of solar irradiance.

The choice of projects to be conducted at the institute is governed by the synergy between the know-how obtained from the Operational Services of the World Radiation Center and other research activities. The same instruments are built for space-based experiments as are utilised for ground-based measurements. In addition, with the involvement in the Solar Orbiter and Lagrange missions, the instrumentation extends to imaging and spectroscopy. The research activities can be grouped into four themes: i) climate modelling, ii) atmospheric physics, iii) development of reference instruments for meteorological radiation measurements, and iv) solar physics.

The majority of research activities are financed through third party funding. During 2020, there were a range of funding sources which included projects supported by the Swiss National Science Foundation, Karbacher Fonds, Innosuisse, European COST action, Meteoswiss, European H2020, ESA, and EURAMET. These funding sources supported three PhD thesis projects, four post-doctoral positions, and two instrument scientists.

Swiss participation in ESA's PRODEX programme (PROgramme de Développement d'EXpériences scientifiques) funds the hardware development of space experiments. The institute's four PRODEX projects paid for the equivalent of five technical department positions.

In the area of climate modelling, research projects study both long and short-term changes in the Earth's atmosphere. The evolution of the ozone layer is being modelled and predicted. The impact of solar protons on the ionosphere has been assessed and particularly strong historical events are analysed. A new area of study is understanding the outgoing radiation at the top of the Earth's atmosphere with the NorSat-1 CLARA mission.

The solar physics focus turns to Solar Orbiter following its launch in February 2020. These topics cover the creation of the slow and fast solar wind.

The institute's infrastructure and most of its overheads are paid for by the operational service of the World Radiation Center. We are proud of the fact that at the PMOD/WRC, the Center's services are based on research that is state-of-the-art in their respective fields. The data from new instruments are being analysed, such as the new spectroradiometer which measures from 500 nm to 1.7 μm and a Lunar Precision Filter Radiometer (PFR). The accuracy of measurements is constantly being improved, which ensures that long-term datasets can be actively used, such as the Arosa/Davos ozone measurements. The long-term operation of the global aerosol optical depth monitoring network, GAW-PFR, has been secured with the development of a new generation of PFRs to replace the fleet of original network instruments constructed more than 20 years ago. The research carried out at PMOD/WRC is intertwined with the instrumentation, both ground and space-based. In addition, a transfer of knowledge on solar radiation is being carried out through the development of a short-term forecast model of solar energy.

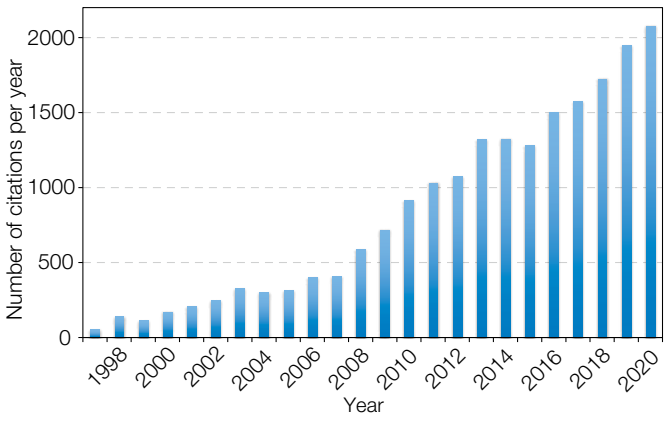

Figure 1. Number of annual citations to articles including an author with a PMOD/WRC affiliation. In March 2021, there were 21,163 citations to 753 articles included in Thomson Reuter's Web of Science. The articles were selected using the search criteria address = (World Rad C*) OR (PMOD* NOT PMOD Technol* OR pmodak) OR (Phys* Met* Obs*).*

Exploring the Sources of the Solar Wind. Probing Regions of Upflow in the Quiet Sun and Coronal Holes

Louise Harra, Conrad Schwanitz, and Elena Podlachikova

One of the key questions in solar physics is how the solar wind is formed and accelerated. The Solar Orbiter mission was launched in February 2020, with a key aim to address this question. The Parker Solar Probe mission has reached less than 35 solar radii to the Sun, revealing the solar wind is extremely dynamic. We have explored possible sources of these persistent fluctuations in the 'quiet' solar wind through two means. The first is through spectroscopic analysis of coronal hole data searching for upflow regions, and the second is through the very first measurements of the quiet Sun using the EUV Imagers on Solar Orbiter. We found new sources of upflow (Schwanitz et al., 2021), and measured the smallest ever dynamic features in the quiet Sun (Berghmans et al., 2021).

One of the major challenges in solar physics is understanding the wide array of sources of the solar wind. We are now in a new era of studying the Sun, with missions getting close in (Parker Solar Probe has already reach less than 35 solar radii), and Solar Orbiter has already reached 0.5 A.U. during cruise phase. Solar Orbiter (Müller et al., 2020) was launched and successfully commissioned during 2020, despite the pandemic. This is the culmination of ~20 years work across the teams involved. PMOD/WRC is involved in two instruments – the EUV imagers (EUI; Rochus et al., 2020) and the Spectral Imaging of the Coronal Environment (SPICE; SPICE consortium, 2020). The remote sensing instruments are not in science mode until the end of 2021, but even during commissioning and cruise phase, the data are revealing new phenomena.

Examples of data obtained from EUI during the commissioning phase are shown in Figure1. This was during the first perihelion, reaching 0.55 A.U., during which time the EUV HRI imager reached an exceptional 2-pixel spatial resolution of 400 km. These small features have areas >0.1 Mm^2, and the larger ones can be seen in the Solar Dynamics Observatory (SDO) data. Their brightenings last for >10 s (restricted by the exposure time of 5 s). They are observed at coronal temperatures with no equivalent brightenings being seen in the cooler Lyman alpha channel (Berghmans et al., 2021). However, the cool channel highlights the magnetic network, formed through convective motions from below, and the brightenlngs lie on the network indicating that magnetic fields are key in understanding the physical processes of these structures. Due to the orbit of Solar Orbiter we also have the opportunity of using stereoscopy to explore the heights of these small structures for the very first time in combination with the Earth orbiting SDO spacecraft. The heights lie 100–5000 km above the photosphere. Once Solar Orbiter is in the science orbit at the end of 2021 reaching 0.3 A.U., the spatial resolution will be twice as high again, and we expect to see even more of these small features.

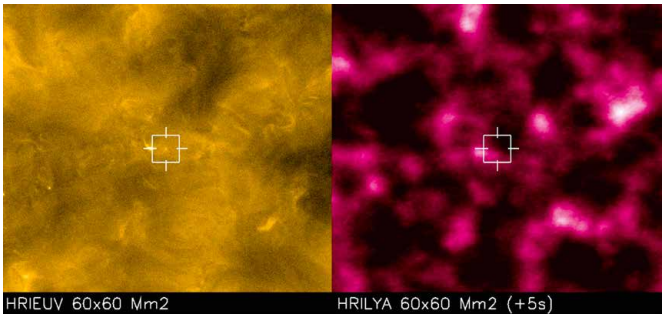

Figure 1. An example of a small EUV brightening seen by EUI in the corona (right image) and it location on the magnetic network seen in Lyman alpha (left), Berghmans et al. (2021).

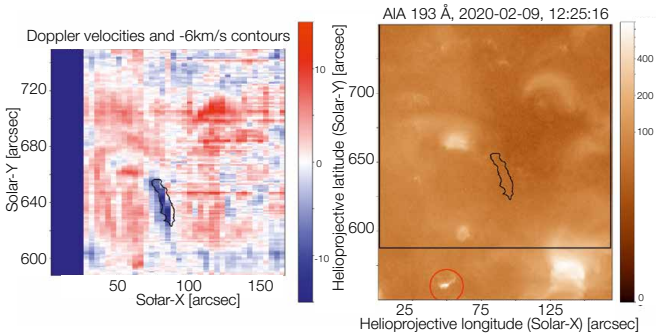

Figure 2. The left hand side shows an upflow region (blue) and the right shows how faint the region is in intensity. The source of the blueshift was found to come from the region highlighted by a red circle in the right hand image.

Using the Hinode spacecraft data, small scale features in coronal holes and the quiet Sun were explored, but this time spectroscopically. This means the bias of only looking at features that increase in intensity is avoided, and the focus is on features that have a measurable upflow which has a chance to make it into the solar wind (see Figure 2). In the analysis, it was found that these small regions of upflow are more regular than normal 'jets' of material seen in intensity. They have several sources – all of which are faint, but most are related to restructuring in some way (Schwanitz et al., 2021). The relationship with the brightenings seen by EUI is not yet known. As of writing, there were no coordinated observations between the instruments, but we look forward to new data in 2021.

References:

Berghmans D., et al.: 2021, EUV quiet Sun brightenings observed by Solar Orbiter/EUI, A&A, submitted.

Müller D., et al.: 2020, The Solar Orbiter mission science overview, A&A, 642, 1, doi:10.1051/0004-6361/202038467

Rochus P., et al.: 2020, The Solar Orbiter EUI instrument: The Extreme Ultraviolet Imager, A&A, 642, A8, DOI doi.org/10.1051/0004-6361/201936663

Schwanitz C., Harra L., et al.: 2021, Probing upflowing regions in the quiet Sun and coronal holes, in prep.

SPICE consortium: 2020, The Solar Orbiter SPICE instrument - An extreme UV imaging spectrometer, A&A, 642, A14, doi: https://doi.org/10.1051/0004-6361/201935574

Exploring the Sources of the Solar Wind. Upflow in Active Regions

Krzysztof Barczynski and Louise Harra

The origin of the slow solar wind is still an open question. The edges of the active regions on the Sun are usually characterised by strong plasma upflow and are considered as a possible source of the slow solar wind. We have investigated the upflow regions using spectroscopic data from Earth-orbiting instruments. From this we determine the behaviour from these regions throughout the solar atmosphere from the low, cool chromosphere to the hot corona. To explain this behaviour, there are three possible mechanisms that can operate simultaneously. In addition, we have explored the response seen by the Parker Solar Probe mission at 35 solar radii in which frequent energetic particle events are seen. Our analysis demonstrated that the active upflows are a potential source of the slow solar wind.

The solar wind generation and propagation mechanisms are complex and not completely understood. The Earth-orbiting missions such as Hinode and Interface Region Imaging Spectrograph (IRIS) allow us to investigate the plasma properties in the outflow regions. Simultaneous spectroscopic and imaging observations of different spacecraft allow the multi-wavelength diagnostics of the plasma properties through the solar atmosphere which key to understanding the physical processes that generated the plasma upflow.

Using simultaneous Hinode and IRIS spacecraft spectroscopic observation, the active region core (the location of dominantly closed loops) and the upflow region (the region of dominantly expanded or open magnetic loops) were investigated in the chromosphere, the transition region, and the solar corona. Figure 1 presents example maps of the active region with an upflow at the active region edge observed in the solar corona. The analysis was provided for six different observations of the same active region. Based on the intensity, Doppler velocity and non-thermal velocity maps it was found that for the upflow region and the active region core, the fluxes are strongly correlated from the chromosphere through the transition region to the corona. The Doppler velocities of the coronal lines are strongly correlated to each other, but

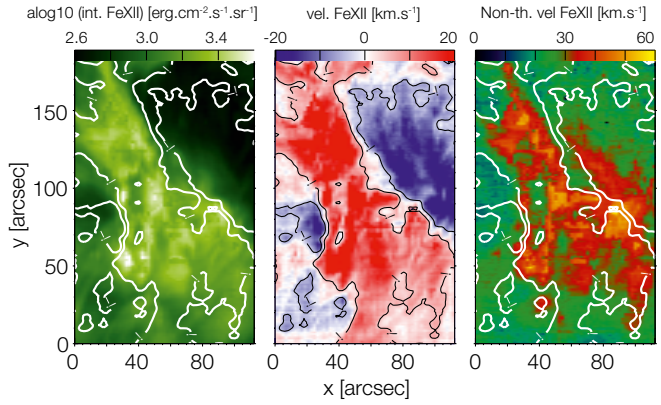

Figure 1. An example of the active region with the upflow at the edge seen in the corona intensity map (right image), Doppler velocity map (middle image) and the non-thermal velocity map (left image). The upflow region is presented inside the contour -5 km/s (blue region the middle panel).

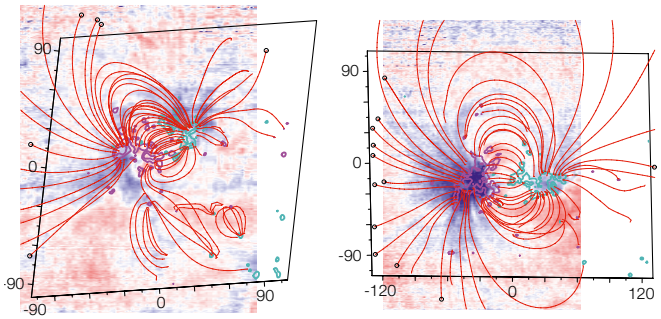

Figure 2. Doppler velocity maps of a small active region emerging (blue is upflow, red is downflow). As it develops, the blue shifted region increases and its behaviour is consistent with the changes in the solar energetic particles observed by PSP.

the transition region and coronal lines show no correlation. In the upflow region, the Doppler velocity and non-thermal velocity are strongly correlated in the solar corona, but there is no such correlation in the active region core. The received results imply that at least three different mechanisms are responsible for the slow solar wind creation: (1) the reconnection between the closed loops and open magnetic field lines in the solar corona, (2) the reconnection between the small-scale chromospheric loops and open magnetic field lines, and (3) plasma escape along open magnetic field lines (Barczynski et al., 2021). The effectiveness of each mechanism in different active regions is not yet known.

The next step is linking sources of the solar wind and energetic particles to data from in-situ instruments. This linkage science is at the centre of the Solar Orbiter science goals. In 2019, Louise Harra formed an ISSI team to combine data from Hinode with data from Parker Solar Probe (PSP). PSP was launched in 2018, and explores the solar wind closer than ever before, revealing much more dynamics and behaviour previously unseen. The first paper from our ISSI team explores the first perihelion (encounter 1) of PSP with the Sun. During PSP's first encounter, frequent and small type III bursts, indicating energetic electrons were observed.

At this stage there was only one small active region on the Sun which had only just emerged. This provided an excellent opportunity to track the impact of a newly emerged active region on the type III bursts. Type III bursts are often associated with energetic particles accelerated in solar flares and on a smaller scale, jets. In this active region there were no flares or jets yet the type III bursts exist. As the active region developed, the upflow regions formed at the edges of the active region. The parameters of this upflow region have been tracked and it is found that this is the most likely source of the persistent type III bursts seen by PSP (see Figure 2).

References: Barczynski K., et al.: 2021, A comparison of the active region properties using simultaneous spectroscopic observations from IRIS and Hinode, A&A, accepted.

Harra L., et al.: 2021, The active region source of a type III radio storm observed by Parker Solar Probe during Encounter 2, A&A, doi.org/10.1051/0004-6361/202039514

Probing Regions of Upflows in Active Regions, II. 3-D Spectroscopy

Elena Podlachikova, Louise Harra, and Krzysztof Barczynski

The Solar Orbiter mission, with an orbit outside the Sun–Earth line, opens up new opportunities for stereoscopic analysis using multi-spacecraft spectrometers. We developed a new method of 3-D spectroscopy, from which we reconstruct the vector velocities in the corona. We applied our methodology to the vector velocity measurements in a solar active region which was observed by the Hinode spacecraft as a test case. 3-D spectroscopy can be applied to two spectrometers with a large angle between them, using future possibilities with SPICE (onboard Solar Orbiter), near-Earth IRIS and EIS (onboard Hinode) (Podladchikova et al., 2021). We are involved in planning the operations for the opportunities at the optimum angle of spacecraft separation.

The presence of persistent high-temperature, high-speed upflows from the edges of active regions (Harra et al., 2008) is a key discovery from the Hinode space mission. Measurements from the Extreme Ultraviolet (EUV) Imaging Spectrometer (EIS) indicate that the upflows reach velocities of 50 to 100 km s^{-1}. It has been suggested that these upflows may lie on open magnetic field lines in the vicinity of solar active regions that connect to the heliosphere and may be a significant source of the low-speed solar wind (Figure 1). Attempts have been made to understand how these flows vary with the location on the solar disc. In order to probe the intrinsic nature of these flows, we develop a 3-D spectroscopy methodology that can be employed to build velocity vectors from a pair of EUV images and from Doppler shift maps taken from different perspectives.

An advantage of having two different views of an active region is that one can determine the projection angles of the loops, and hence the direction of plasma flows along the magnetic loops. We verify our 3-D spectroscopy algorithms with magnetic field 3-D modelling of the active regions. The tools to reconstruct the vector velocity in the solar corona will be released as a suite of 3-D spectroscopy algorithms (Software package DOVES – DOppler VElocities Stereoscopic reconstruction). It includes the algorithm of the spatio-temporal co-alignment between EUV broadband and spectroscopic images shown in Figure 2, and then a suite of de-projection algorithms of the measured Doppler shifts into true velocity vectors.

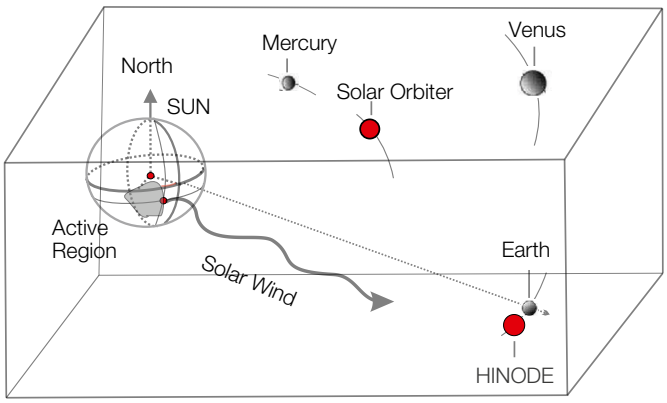

Figure 1. A new concept of a stereoscopic spectrometric facility, consisting of two spacecraft, Hinode and Solar Orbiter.

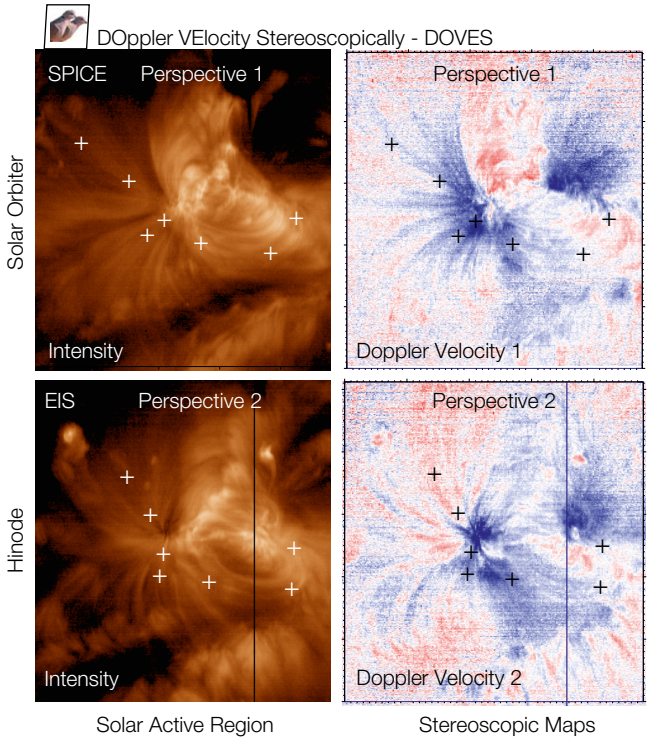

Figure 2. Different angle views of the solar active region. The crosses indicate the projections of the same 3-D point objects onto 2-D images. Vector operations with two Doppler shifts measured in each point allow the true vector velocity to be restored (Figure 1).

A number of new approaches to the triangulation of optically thin objects are established. The latter part of the software is released as open source through the Solar Soft libraries. The full version of the software will be released in 2021.

3-D spectroscopy will significantly facilitate the understanding of the complex flows that take place throughout the solar atmosphere.

References: Harra L.K., et al.: 2008, Outflows at the edges of AR: Contribution to solar wind formation?, ApJ, 2 L147.

Podladchikova O., Harra L.K., Barczynski K., et al.: 2021, Stereoscopic measurements of coronal doppler velocities, A&A, submitted.

Total Solar Irradiance and Terrestrial Longwave Outgoing Radiation (LOR) Measurements with CLARA Onboard NorSat-1

Margit Haberreiter, Wolfgang Finsterle, Jean-Philippe Montillet, Werner Schmutz, Manfred Gyo, and Dany Pfiffner in collaboration with UTIAS-SLF (Canada) and Norwegian Space Agency (Norway)

The Compact Lightweight Absolute RAdiometer (CLARA, Walter et al., 2017; 2018) experiment onboard the Norwegian micro satellite NorSat-1 was launched on 14 July 2017. CLARA's primary science goal is to measure Total Solar Irradiance (TSI) from space and as such to contribute to the long-term record of TSI measurements. After a reaction wheel failure of the platform in May 2018, CLARA measurements were stopped but restarted again in November 2019. Since then, CLARA continues to take TSI as well as Longwave Outgoing Radiation (LOR) measurements of Earth when the satellite is in eclipse.

The Earth Radiation Budget (ERB) is a key driver for the Earth climate system. With CLARA we have the unique opportunity to sequentially measure TSI as well as LOR when the satellite is on the night-side of Earth. These measurements are the first of its kind with a SI-traceable absolute radiometer. Since the restart of CLARA in November 2019, TSI and LOR measurements have been taken almost continuously. After the Level 1 data product of the measurements is produced, taking into account the electrical calibration, the Level 1 to Level 2 transformation is performed.

This step produces TSI in physical units by taking into account all known instrumental and orbital effects. The current version of the CLARA Level 2 data is shown in Figure 1 and compared to the VIRGO (Variability of solar IRradiance and Gravity Oscillations) and TSIS (Total and Spectral solar Irradiance Sensor) data. The comparison shows that since the beginning of 2021, CLARA measurements follow the solar irradiance variability as measured by VIRGO and TSIS. However, from March to November 2020, CLARA gives significantly lower values. A possible reason for this could be a temperature effect which we are currently investigating in detail.

Figure 2 gives examples of the variation of LOR for four orbits on 4 March 2021. The variations are understood to be to some degree due to different emission characteristics of the observed terrestrial scene types, such as land and/or ocean. At the same time, the pointing of the instrument still needs to be quality checked in detail in order to avoid unwanted effects. As part of the International ISSI Team, "Towards the determination of the Earth Energy Imbalance from Space", these CLARA LOR data will be cross-calibrated with other Earth observing instruments that measure the terrestrial outgoing radiation, such as RAVAN, SIMBA and CERES. The international Team consists of members from NASA, LASP and JPL (US), CIOMP (CN), ROB (BE), RMI (BE) and IPM (DE).

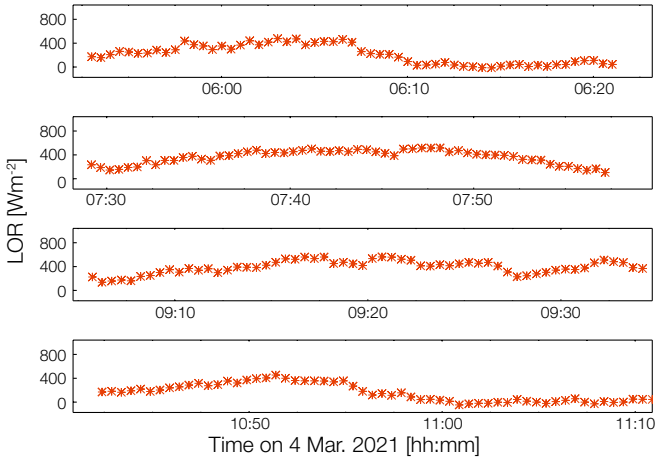

Figure 2. Longwave Outgoing Radiation (LOR) as measured with CLARA on the night-side of Earth during three orbits.

References:

Walter B., Levesque P.-L., Kopp G., Andersen B., Beck I., Finsterle W., Gyo M., Heuerman K., Koller S., et al.: 2017, Meteorologia, 54, 5, 674, doi: 10.1088/1681-7575/aa7a63

Walter B., Andersen B., Beattie A., Finsterle W., Kopp G., Pfiffner D., Schmutz W.: 2018, First TSI results and status report of the CLARA/NorSat-1 solar absolute radiometer, Proc. Int. Astron. Union, 14(A30), 358-360, doi:10.1017/S1743921319004617

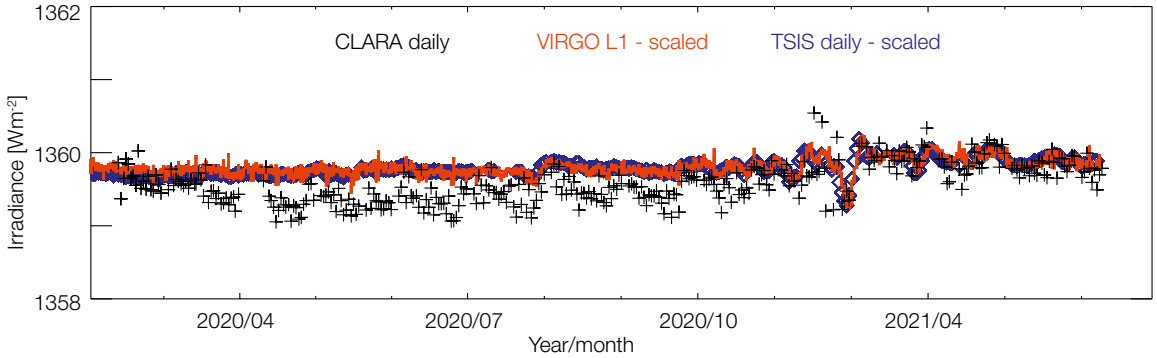

Figure 1. Daily TSI as measured with CLARA compared to VIRGO L1 data and TSIS, both scaled to match the CLARA TSI value.

Validation of the SOCOLv4 Model for the Past Ozone Evolution

Arseniy Karagodin, Timofei Sukhodolov, Tatiana Egorova, and Eugene Rozanov in collaboration with IAC ETH Zurich

The newly developed atmosphere-ocean-aerosol-chemistry-climate model SOCOLv4 has been validated for the satellite era with a focus on the stratospheric ozone trends. To extract the long-term ozone changes, we applied dynamical linear regression analysis. The results show that the new model is in much better agreement with observations than the previous model version, SOCOLv3. However, there are still some model issues, which will be addressed in future upgrades.

SOCOLv4 consists of the Earth System Model MPI-ESM1.2, the chemistry model MEZON, and the sulphate aerosol module AER, which are all interactively coupled with each other. A detailed description of the SOCOLv4 components can be found in Sukhodolov et al. (2021). Figure 1 presents the evolution of the total column ozone from the ensemble runs of SOCOLv4 and its predecessor SOCOLv3, as well as from the observational data sets MSRv2, SBUV, and CMIP6. The results show that the quasi-global total column ozone evolution is much better captured by SOCOLv4 than by SOCOLv3. Although the observed total ozone column seems to continue to recover, recently it was shown that the lower stratospheric trends of the low and mid-latitudes are still negative (Ball et al., 2018). SOCOLv3 was used in that study, but it failed to fully reproduce the observed trends. Further, we analyse the performance of SOCOLv4 in the same respect.

To filter out the sub-decadal variability and validate the modelled long-term ozone trends in detail, we used the dynamical linear regression model (DLM). DLM allows smoothly varying, non-linear background trends to be estimated, without prescribing an explanatory variable for atmospheric chlorine or applying restrictive linear assumptions. In our set-up, DLM uses seven explanatory variables including the Solar F30 index, zonal winds at 30 and 50 hPa as proxies of the quasi-biannual oscillation, stratospheric aerosol optical depth, El-Nino Southern oscillation,

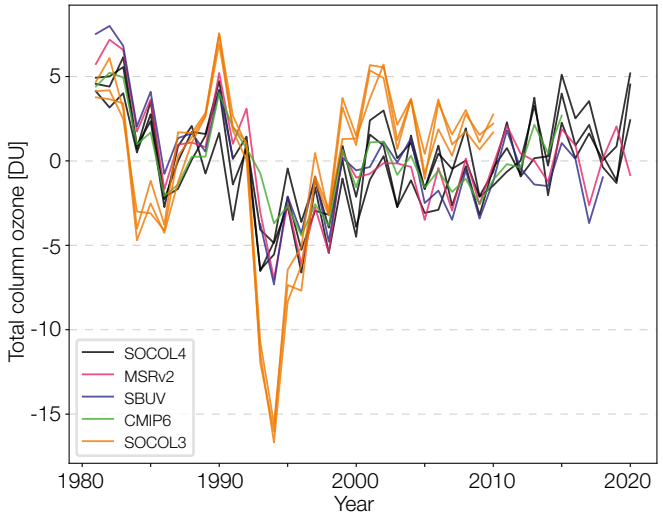

Figure 1. Near global (55°S–55°N) total ozone column evolution normalised by the mean over the whole period simulated with SOCOLv4 (black), MSR2 (pink), SBUV (blue), CMIP6 (light green), and SOCOLv3 (green).

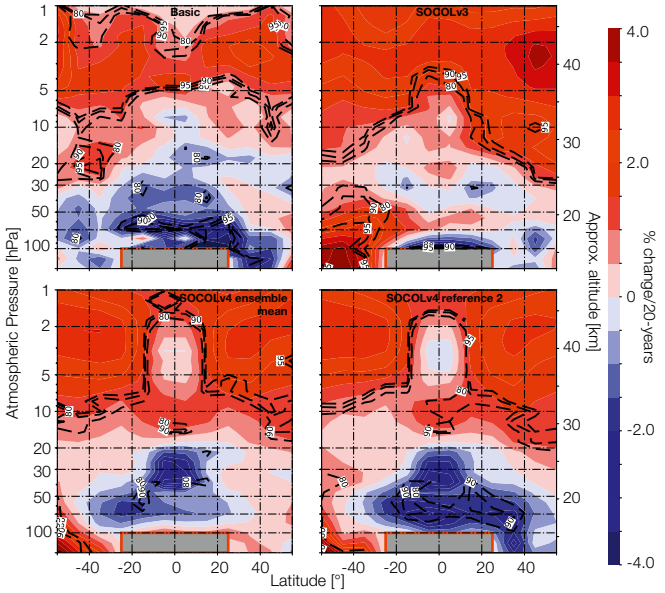

Figure 2. Latitude-pressure ozone changes (%) in the ensemble mean of SOCOLv4, a single run of SOCOLv4, SOCOLv3, and BASIC ozone composite for the ozone recovery phase (1998–2018). The name is indicated in each panel. Dashed contour lines represent statistical significance (%). The grey rectangle hides the tropical troposphere.

and the Arctic and Antarctic oscillation indices. The ozone tendencies for the ozone recovery (1998–2018) phase extracted by DLM analysis are presented in Figure 2.

Compared to SOCOLv3 and the BASIC observational composite, the ensemble mean of SOCOLv4 now better reproduces the tropical lower stratospheric ozone loss by showing the negative trend up to 20 hPa in the tropics. The extra-tropical decline is not visible in the ensemble mean results, but the single SOCOLv4 runs (reference 2 in Figure 2) can reveal trends that are almost identical to those derived from observations. This suggests that the mid-latitude negative trends might be a result of a combination of dynamical factors, which is not always reproduced by the dynamical core of the coupled model due to its stochastic nature. We will continue this analysis and perform additional model sensitivity experiments to identify the reasons for the negative trends.

Overall, SOCOLv4 shows a significant improvement over SOCOLv3. Analysis of other chemical and dynamical parameters of the atmosphere (Sukhodolov et al., 2021) revealed that there are still issues like a biased mixing in the stratosphere and insufficient sink of odd nitrogen, which will be addressed in future model releases.

References:

Ball W. T., et al.: 2018, Evidence for a continuous decline in lower stratospheric ozone offsetting ozone layer recovery, Atmos. Chem. Phys., 18, 1379–1394, doi.org/10.5194/acp-18-1379-2018

Sukhodolov T., et al.: 2021, Atmosphere-Ocean-Aerosol-Chemistry-Climate Model SOCOLv4.0: description and evaluation, Geosci. Model Dev., preprint, doi.org/10.5194/gmd-2021-35

The Role of the Montreal Protocol in Sustainable Recovery of the Ozone Layer and Climate Protection

Tatiana Egorova, Eugene Rozanov, Timofei Sukhodolov, and Arseniy Karagodin-Doyennel in collaboration with IAC ETH Zurich

To understand the past and to project the future behaviour of the ozone layer, the PMOD/WRC Climate Group is working on the SNF project, "POLE". Here we describe the progress during the second year of the project and present an on-going analysis of the simulations performed using the AOACCM SOCOLv4.0 with and without limitations according to the Montreal Protocol and its Amendments (MPA) on the production of halogen containing ozone destroying substances (hODS).

During the second year of the POLE project, we completed a reference run and a run without Montreal Protocol limitations with our new Atmosphere-Ocean-Aerosol-Chemistry-Climate Model (AOACCM), SOCOLv4.0 (Sukhodolov et al., 2021), driven by all recommended forcings for the 1980–2100 period. Figure 1 shows the amount of total column ozone (TCO) which would be left in 2100 if the limitation on the hODS production were not introduced by the Montreal Protocol. The protective ozone layer (the TCO ranges from 200 to 400 DU at present) would be almost completely eliminated making any kind of life impossible without substantial protection.

The obtained results confirm our previously published estimate of MPA benefits (Egorova et al., 2013). Using the new model with interactive ocean, we can now also extend the understanding of the MPA importance for climate change. Figure 2 illustrates the difference in the annual mean surface temperature in the future obtained in our reference and experiment runs. Additional warming caused by the absence of the MPA limitations is very pronounced all over the globe. The effects maximise over land masses reaching 6 K over Siberia and North America. Arctic amplification also causes a large warming of up to 15 K over the Canadian Arctic Archipelago and Chukchi sea with substantial implications for the sea ice concentration. The warming effect is explained by the large increase of the main hODS (CFC-11 and 12) which trap the outgoing longwave radiation leading to global warming.

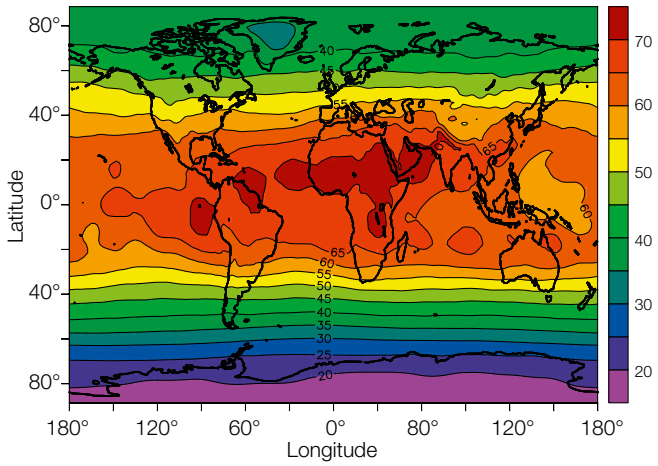

Figure 1. Geographical distribution of the annual mean total column ozone (DU) in 2100 for the case of no Montreal Protocol limitations.

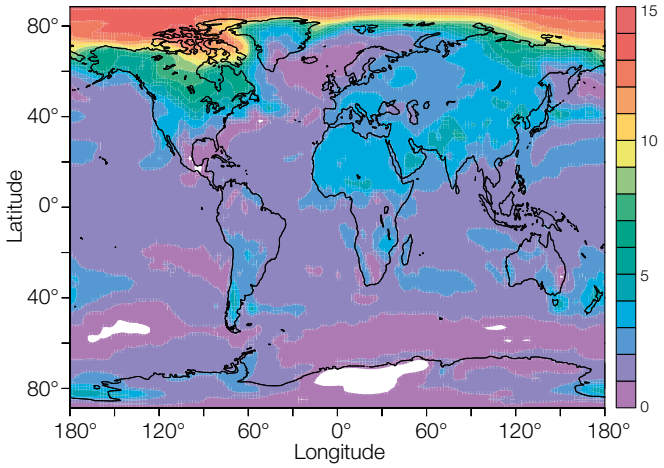

Figure 2. Geographical distribution of annual mean surface air temperature difference between non Montreal Protocol experiment and reference run, integrated over the last 10 years of this century (2090–2100).

The potential impact of many species on the climate system was estimated in the IPCC report (IPCC, 2013) using the Global Warming Potential (GWP) quantity. It was demonstrated that the CFC-11 and CFC-12 climate efficiencies per molecule is up to 10,000 times higher than for CO_2. In the non-MPA case, the emissions of hODS are increasing by 3% per year leading to an almost 50% CFC-11/CFC-12 increase in the future. The additional global warming, in this case shown in Figure 2, is comparable and even exceeds the future warming for the most pronounced increase of greenhouse gases (business as usual scenario) presented in the IPCC (2013) report. In the IPCC RCP-8.5 case, the warming obtained from the multi-model mean is up to 5 K over the northern land masses and up to 12 K in the Arctic area. Our results confirm, once again, that the introduction of the MPA limitations was timely and a dramatically important decision for both the ozone layer and the protection of Earth's climate.

Acknowledgment: The study was funded by the SNSF project, POLE (200020_182239), and supported by CSCS under projects ID S-901 and ID S-1029.

References:

Sukhodolov T., et al.: 2021, Atmosphere-Ocean-Aerosol-Chemistry-Climate Model SOCOLv4.0: description and evaluation, GMDD, doi:10.5194/gmd-2021-35

Egorova T., Rozanov E., Gröbner J., Hauser M., Schmutz W., 2013: Montreal Protocol benefits simulated with CCM SOCOL, Atmos. Chem. Phys., 13, 3811–3823, doi:10.5194/acp-13-3811-2013

IPCC, 2013: Climate Change 2013: The Physical Science Basis. Contribution of Working Group I to the Fifth Assessment Report of the Intergovernmental Panel on Climate Change (Stocker, T.F., D. Qin, G.-K. Plattner, et al., eds.), Cambridge University Press, 1535 pp.

Simulation of the Atmosphere with SOCOLv4.0 for 2022 WMO Ozone Depletion Assessment

Tatiana Egorova, Eugene Rozanov, Timofei Sukhodolov, and Arseniy Karagodin in collaboration with IAC ETH Zurich

The project aims to prepare data about stratospheric ozone evolution to support the 2022 WMO Ozone depletion assessment. For the first phase, data from the hindcast simulation covering the 1960–2018 period were required. We simulated the atmospheric evolution during this period using the recently developed chemistry-climate model SOCOLv4.0 (Sukhodolov et al., 2021). Here we present some of the obtained results.

The model experiment consists of a small ensemble of hindcast simulations performed using specified sea surface temperatures (SST) and sea-ice cover for the 1960 – 2018 period, with a 10-year long spin-up allowing the atmosphere to equilibrate. The main goal of this experiment, coined REF-D1, is to evaluate model performance against satellite observations and meteorological re-analysis. The forcing dataset was mostly based on the observations and largely exploits the fields prepared for the Coupled Model Intercomparison Project phase 6 (CMIP6). A description of the available input parameters can be found at http://goo.gl/r8up31. It was requested to prepare the output data in the netCDF version 4 format following special standards and to submit data to Centre for Environmental Data Analysis in the UK.

One member of the requested small ensemble simulation was carried out in Nov.–Dec. 2020 on the Piz Daint high performance computer system at the Swiss National Supercomputing Centre (CSCS). Figure 1 illustrates the evolution of the global and annual mean total inorganic chlorine (Cl_y) at 60 km, temperature, and ozone mixing ratio at 30 km. The anthropogenically induced Cl_y increase started in 1960 and reached a maximum of 2.5 ppbv in 1996. After the introduction of limitations on ozone depleting substances by the Montreal protocol, the trend became negative and the change in the Cl_y mixing ratio was slightly higher than 2 ppbv in 2018 relative to 1960. The stratosphere is continuously cooling due to the increase in greenhouse gases and lost almost 3 K in 2018.

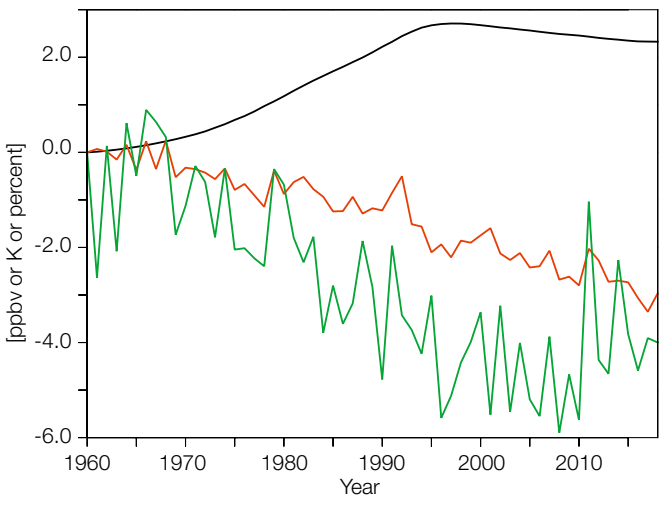

Figure 1. The evolution relative to 1960 of the global and annual mean total inorganic chlorine (Cl_y) at 60 km (ppbv, black line), temperature (K, red line) and ozone mixing ratio (%, green line) at 30 km.

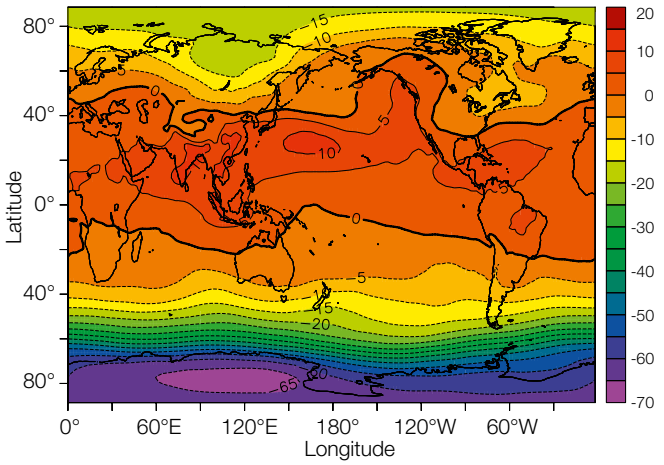

Figure 2. The annual mean total column ozone difference (DU) between the 2008–2018 and 1960–1970 periods.

Stratospheric ozone depletion started in 1970, stabilised between 1996 and 2005, and is now increasing due to Montreal protocol limitations. Judging from the model results, global and annual mean stratospheric ozone should have recovered by 2030–2040. The geographical distribution of the total ozone difference between 2008–2018 and 1960–1970 is illustrated in Figure 2.

The model results demonstrate total ozone depletion over the high latitudes reaching 20 DU in the Northern and 70 DU in the Southern hemispheres. Total ozone increased over the northern low to middle latitude belt, reflecting intensification of the shallow branch meridional circulation caused by greenhouse warming and changes of the extratropical jet configuration (Zubov et al., 2013). The model also simulates well the evolution of other species such as: i) the increase in stratospheric water vapour due to the continuous increase in methane emissions, ii) variability in mesospheric nitrogen oxides related to energetic electron precipitation, and iii) warming and ozone depletion in the lower tropical stratosphere caused by the Mt. El Chichon and Pinatubo eruptions.

The data will be made available to the community next year. We are also preparing a model run, REF-D2, which will cover ozone evolution in the future.

Acknowledgment: The study was funded by the SNSF project, POLE (200020_182239), and supported by CSCS under projects ID S-901 and ID S-1029.

References:

Sukhodolov T., et al.: 2021, Atmosphere-Ocean-Aerosol-Chemistry-Climate model SOCOLv4.0: description and validation, Geophys. Mod. Dev., 2021, submitted.

Zubov V., et al.: 2013, Role of external factors in the evolution of the ozone layer and stratospheric circulation in 21st century, Atmos. Chem. Phys., 13, 4697-4706. doi:10.5194/acp-13-4697-2013

Multi-Model Comparison of the Sulphate Aerosol Microphysical and Optical Properties after the 1815 Eruption of Mt. Tambora

Timofei Sukhodolov and Eugene Rozanov in collaboration with University of Colorado (Boulder, USA) and VolMIP participants

As part of the Model Intercomparison Project on the climatic response to Volcanic forcing (VolMIP), several climate modelling centres performed a coordinated pre-study experiment with interactive stratospheric aerosol models simulating the volcanic aerosol cloud from an eruption resembling the 1815 Mt. Tambora event. We participated in this activity with SOCOL-AER. Analysis of the multi-model ensemble showed large disparities between models in the stratospheric global mean aerosol optical depth, with the SOCOL-AER model being in the middle of the multi-model spread.

Volcanic eruptions inject sulphur dioxide gas (SO_2) into the atmosphere, which is quickly converted to sulphuric acid, and then to sulphate aerosol. The sulphate aerosol scatters sunlight and thus, causes an increase in aerosol optical depth (AOD), which is a key volcanic forcing parameter, defining the related cooling of the Earth's temperature in the troposphere. This final parameter, AOD, is dependent on the lifetime and optical properties of sulphate aerosols, which, in turn, is also a result of many chemical, microphysical, and dynamical processes in the stratosphere. Interactive sulphate aerosol models are specifically designed to address all these processes, but, as it was shown earlier, they can significantly differ from each other in their results. A coordinated VolMIP experiment was created to understand the inter-model differences by using a consistent set of volcanic injection parameters across models focused on the Tambora eruption in 1815, which is one of the strongest known eruptions of the last centuries.

Ensemble means of global mean stratospheric AOD outputs from participating models are plotted in Figure 1. They are wide-ranging

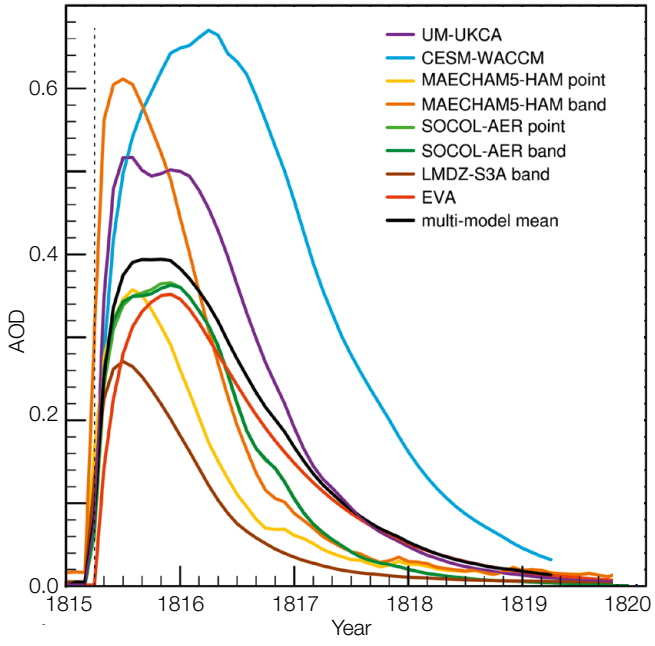

Figure 1. Global mean stratospheric AOD in the visible spectrum of participating models. The black is the multi-model mean. SOCOL-AER and MAECHAM5-HAM band injection experiments are in green and orange respectively. Vertical dotted line marks date of injection of SO_2.

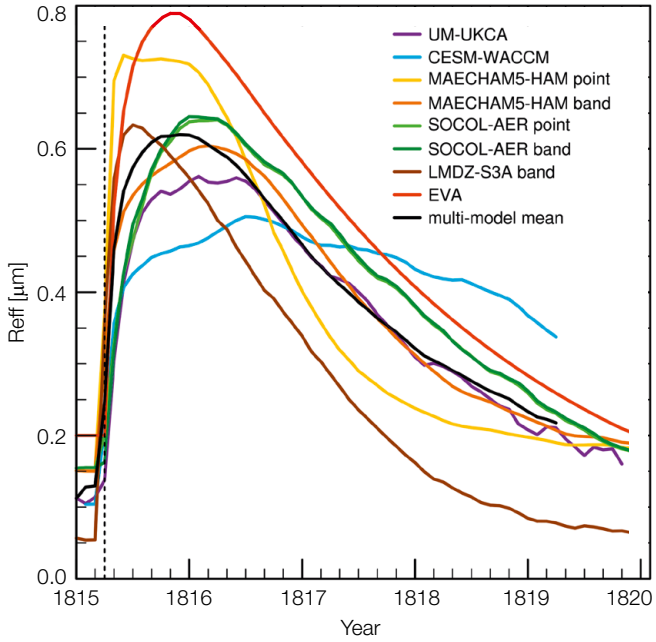

Figure 2. Global stratospheric mean effective radius (R_{eff}) timeseries. Vertical dotted line marks date of injection of SO_2. The calculation of R_{eff} is weighted by surface aerosol density and grid cell volume.

both in magnitude and time. After the analysis of many other model parameters, it was shown that the stratospheric global mean AOD differences among the participating models are primarily due to differences in aerosol size, which can be tracked by the calculated aerosol effective radius shown in Figure 2. The further study identified specific physical and chemical processes that are missing in some models and/or parameterised differently between models, which are together causing the differences in effective radius. In particular, the analysis indicated that interactively tracking hydroxyl radical (OH) chemistry following a large volcanic injection of SO_2 is an important factor in allowing for the timescale for sulphate formation to be properly simulated. In addition, depending on the timescale of sulphate formation, there can be a large difference in effective radius and subsequently AOD that results from whether the SO_2 is injected in a single model grid cell near the location of the volcanic eruption, or whether it is injected as a longitudinally averaged band around the Earth. A paper describing these findings in more detail has recently been published (Clyne et al., 2021).

The SOCOL-AER model showed no large biases compared to other models and is very close to the multi-model mean in many simulated parameters. Further work in the same direction of multi-model intercomparison for models with interactive sulphate aerosol modules will be done in the frame of the ISA-MIP campaign (Timmreck et al., 2018).

References: Clyne M., et al.: 2021, Atmos. Chem. Phys., 21, 3317–3343, doi.org/10.5194/acp-21-3317-202

Timmreck C., et al.: 2018, Geosci. Model Dev., doi:10.5194/gmd-2017-308

Arosa/Davos Total Column Ozone Measurements and their Representativeness for Global Ozone Analysis

Eugene Rozanov, Tatiana Egorova, Luca Egli, Arseniy Karagodin-Doyennel, Timofei Sukhodolov, Herbert Schill, René Stübi, and Julian Gröbner in collaboration with MeteoSwiss

Here we investigate the representativeness of the Total Column Ozone (TCO) measurements from the ground-based instruments located at Arosa/Davos sites to analyse the global ozone layer behaviour in the past and future. Statistical analysis of the multi-sensor re-analysis (MSR) and model data showed a high correlation of the Arosa data with the near-global and Northern Hemisphere annual mean TCO for the 1980–2018 time period. We show that the application of the Arosa data as an additional proxy for multiple linear regression analysis allows TCO behaviour from 1926 up to the present day to be estimated. We demonstrate that the real-time measurements and high homogeneity level of the Arosa TCO time-series can also be used for fast analysis of the future ozone layer recovery.

The longest continuous total column ozone time-series worldwide started in 1926 at the Lichtklimatisches Observatorium Arosa, Switzerland. Since 2010, simultaneous measurements at Arosa and in the nearby valley of Davos have been ongoing, to support the transfer of the instrumentation to PMOD/WRC (Stübi et al., 2020). The evaluation of the Arosa/Davos TCO time-series applicability for the fast analysis of the future global ozone recovery is performed using the results from experiments with the Atmosphere-Ocean-Aerosol-Chemistry-Climate Model (AOACCM) SOCOLv4.0 (hereafter SOCOLv4; Sukhodolov et al., 2021). These model results, which are based on one realistic scenario, are used to address the potential for detecting a future ozone recovery using the dataset obtained at Arosa/Davos with current and potentially new instrumentation (Rozanov et al., 2021). For the evaluation of the TCO behaviour on different time and space scales, we apply multiple linear regression analysis (hereafter MLR).

Figure 1 shows that the evolution of TCO at Arosa almost exactly coincides with the Northern Hemisphere mean showing steady ozone depletion up to 1995 and a rather flat evolution thereafter. However, during 1983–1991, Arosa TCO overestimates the Northern Hemisphere mean and does not fully reproduce interannual variability. From 2011 to 2015 the variability in the

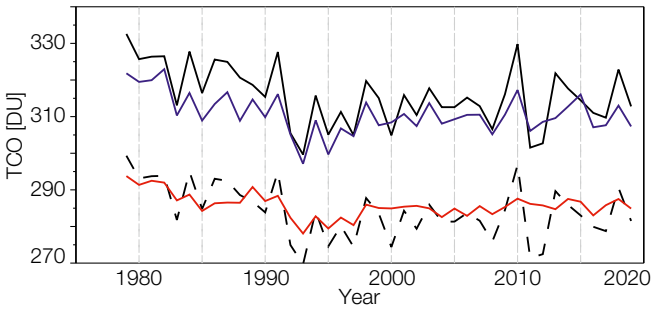

Figure 1. Annual mean TCO evolution from Arosa measurements (black lines), near-global (red line) and Northern Hemisphere (blue line) means from the MSR data (Van der A et al., 2015). Black dashed line shows Arosa TCO scaled by 0.9. The correlation coefficients are 0.74 for the near-global and 0.87 for the Northern Hemisphere means.

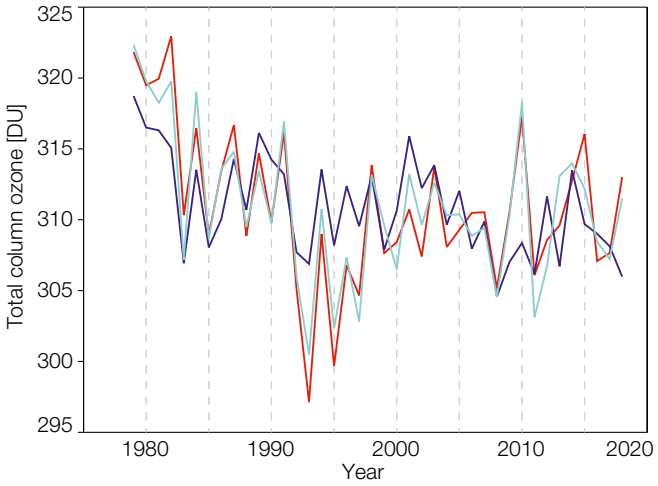

Figure 2. Evolution of near-global TCO obtained from the MSR2 data (red line) and retrieved from proxies without (blue line) and with Arosa TCO as additional proxy (light blue line). The correlation coefficients are 0.68 and 0.89 for the cases without and with Arosa TCO.

Arosa time-series is much higher and shifted in time. As can be expected, Arosa TCO is about 10% higher and much more variable than the near-global mean showing strong spikes in 1993 (after the Mt. Pinatubo eruption) and 2011 (when the northern polar vortex was rather strong and persistent during the cold season). The correlation coefficient between the near-global (Northern Hemisphere) means and Arosa TCO is 0.74 (0.87).

To understand the potential for the improvement of these quantities, we applied MLR analysis to the TCO variability during the recent past (1979–2018) and calculated sensitivity coefficients for all earlier-introduced, independent proxies. Then we compare observed near-global and Northern Hemisphere mean TCO values with the reconstruction based on these proxies. The results are presented in Figure 2 for the near-global means. Our results show that the Arosa/Davos TCO data are representative for annual mean near-global and Northern Hemisphere mean total ozone and can be used to analyse historical and future behaviour of the ozone layer. More details are presented by Rozanov et al. (2021).

References:

Rozanov E., et al.: 2021, Representativeness of the Arosa measurements for the historical analysis of the global total column ozone behaviour, Frontiers in Eraths science, submitted.

Stübi R., et al: 2020, Quality assessment of Dobson spectrophotometers for ozone column measurements before and after automation at Arosa and Davos, Atmos. Meas. Tech. Discuss. [preprint], doi.org/10.5194/amt-2020-441, in review.

Sukhodolov T., et al.: 2021, Atmosphere-Ocean-Aerosol-Chemistry-Climate model SOCOLv4.0: description and validation, Geophys. Mod. Dev., submitted.

Van der A R., Allaart, M., Eskes H.: 2015, Extended and refined multi sensor reanalysis of total ozone for the period, 1970-2012, Atmos. Meas. Tech., 8, 3021-3035, doi:10.5194/amt-8-3021-2015

The Response of Stratospheric Ozone and Dynamics to Changes in Atmospheric Oxygen

Iga Józefiak, Timofei Sukhodolov, Tatiana Egorova, and Eugene Rozanov

Photolysis of molecular oxygen (O_2) maintains the stratospheric ozone layer, protecting living organisms on Earth by absorbing harmful ultraviolet radiation. Over the last ~500 Mio. years, it ranged between 10% and 35% depending on the level of photosynthetic activity of plants and oceans (Berner et al., 2003). Previous estimates, however, showed very different ozone (O_3) responses to atmospheric O_2 changes, differing even in the sign of their correlation. Motivated by these discrepancies, we addressed this topic by means of our state-of-the-art chemistry-climate model SOCOL - AERv2.

In our study, we assess the ozone layer sensitivity to past and potential future concentrations of atmospheric oxygen varying from 5% to 40%. In contrast with previous studies, our findings, illustrated in Figure 1, suggest that the current mixing ratio of O_2 at 21%, maximises the O_3 layer thickness, representing a favourable, possibly even, optimal state for life on Earth. This result contests previous studies performed with 1-D or 2-D models. Figure 1 also shows an interesting asymmetry between the 5% and 40% experiments, meaning that very low oxygen levels decrease the ozone content faster due to some of the ozone-producing ultra-violet radiation starting to reach the ground.

Although slight changes in the oxygen levels do not strongly affect the global mean total ozone, there are significant geographical ozone redistributions, presented in Figure 2. Total ozone column in low-latitude regions is less sensitive to the changes, because of the "self-healing" effect, i.e. more UV entering lower levels, where O_2 photolyses forming O_3, can partly compensate for the reduced O_3 abundances higher up. Mid and high-latitudes, however, are characterised by total column ozone redistributions of ±20 DU even for small (±5%) variations in the O_2 content. Additional regional patterns result from the hemispheric asymmetry of meridional

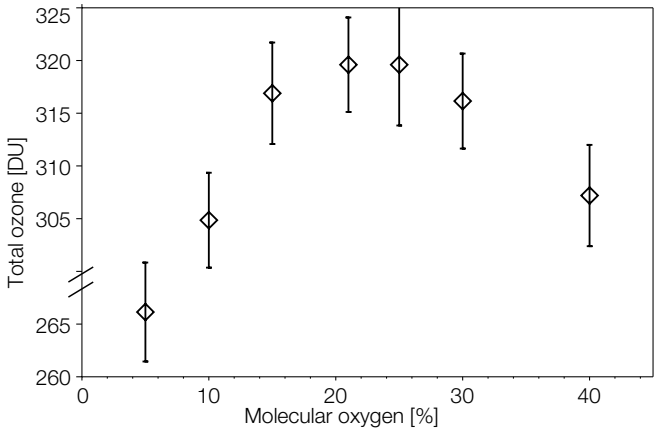

Figure 1. Global mean total ozone averaged over the last five years of model integration for seven experiments with different oxygen levels (5%, 10%, 15%, 21%, 25%, 30%, 40%).

transport pathways via the Brewer-Dobson circulation (BDC). These effects are further modulated by the influence of ozone on stratospheric temperatures and thus on the BDC, indicating a chemistry-radiation-transport feedback. Lower O_2 cases result in a deceleration of the BDC and vice versa for higher O_2 cases. This renders the relation between ozone and molecular oxygen changes non-linear on both global and regional scales.

Overall, our findings show that any alteration in the atmospheric oxygen would result in less ozone and therefore more UV reaching the troposphere, and this non-linearity is mostly caused by the feedbacks in the stratosphere. Currently, we are finalising a paper based on these results.

References: Berner R.A., Beerling D.J., Dudley R., Robinson J.M., Wildman R.A.: 2003, Phanerozoic atmospheric oxygen, Annu. Rev. Earth Planet. Sci., 31, 105-134.

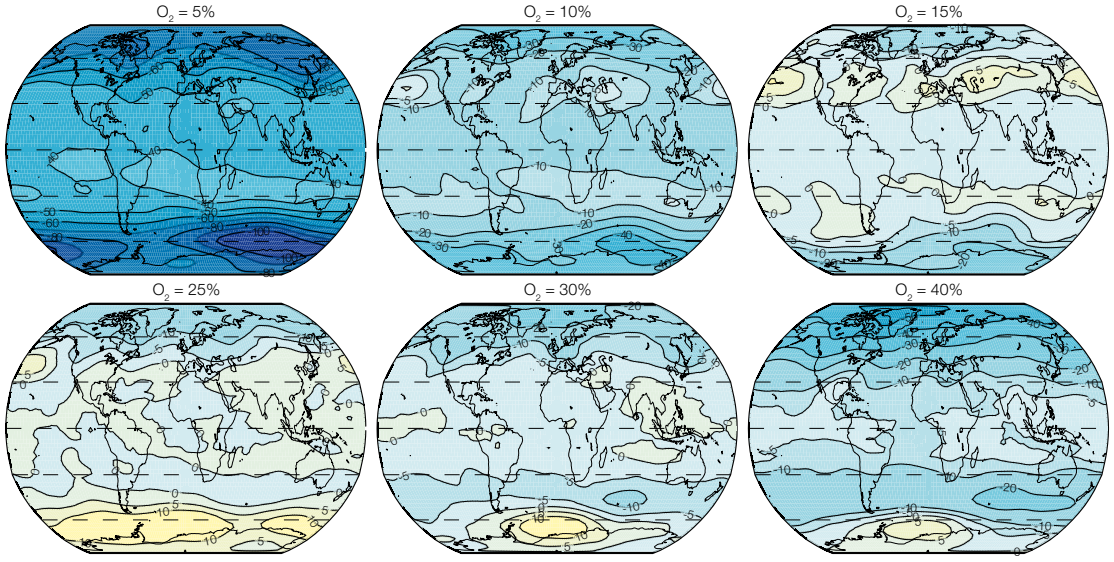

Figure 2. Total ozone column differences (DU) to the reference (O_2 = 21%) experiment averaged over the last five years of integration. Horizontal dashed lines mark the -60, -30, 0, 30, and 60° latitudes.

Modelling Aspects of the Sulphate Aerosol Evolution after Recent Volcanic Activity

Christina Brodowsky, Timofei Sukhodolov, and Eugene Rozanov in collaboration with IAC ETH Zurich

Volcanic activity is one of the main natural climate forcings, and therefore an accurate representation of volcanic aerosols in global climate models is essential. However, direct modelling of sulphur chemistry, sulphate aerosol microphysics and transport is a complex task involving many uncertainties including those related to the volcanic emission magnitude, vertical shape of the plume, and observations of atmospheric sulphur. This study aims to investigate some of these uncertainties and to analyse the performance of the aerosol-chemistry-climate model SOCOL-AERv2 for the medium-sized volcanic activity during the 2008–2013 period.

Since the Pinatubo eruption almost 30 years ago, there have not been any major eruptions. The most notable events have been Kasatochi (2008), Sarychev (2009), Nabro (2011), and Raikoke (2019), each injecting between 1 and 2 Tg of sulphur into the stratosphere. The 1991 Pinatubo eruption released about ten times more SO_2 than Sarychev or Nabro. It led to a surface cooling of about 0.5 K though the exact amount and distribution of SO_2 following this event is still very uncertain, which complicates an understanding of the underlying physics. A major volcanic eruption like this can and most likely will happen again. With the means we have today, it is possible to make projections and prepare in order to mitigate societal or political effects. But before that, it is necessary to validate the models and to address the modelling uncertainties.

As observations have become more accurate in the meantime, it presents an opportunity to study the effects of more recent, though smaller events in much more detail than the larger events of the more distant past. A time span from 2008 to 2013 was chosen, since the three medium-sized eruptions that occurred during this time all produced a large enough signal in stratospheric aerosol to be easily distinguished from the background conditions. We used our aerosol-chemistry-climate model SOCOL-AERv2 (Feinberg et al., 2019) and tried to assess the following main points: i) the differences in datasets for volcanic emissions, ii) the variability of the model in a free-running mode, iii) the influence of nudging on the stratospheric aerosol, and iv) the difference in stratospheric aerosol with a higher vertical model resolution.

Comparing the modelled evolution of the stratospheric aerosol loading and its spread with the Brewer-Dobson circulation to satellite measurements reveals in general very good performance of SOCOL-ERv2 during the period of study. However, the large spread in emission estimates logically leads to significant differences in the modelled aerosol burden, which is illustrated in Figure 1a. This spread results from both the uncertainty in the total emitted mass of sulphur as well as its vertical distribution relative to the tropopause. An additional source of modelled uncertainty is the tropopause height, which varies among the free-running simulations (Figure 1b). Furthermore, the validation is complicated by disagreement between two independent observational datasets SAGE3λ and MIPAS. Nudging effects on the

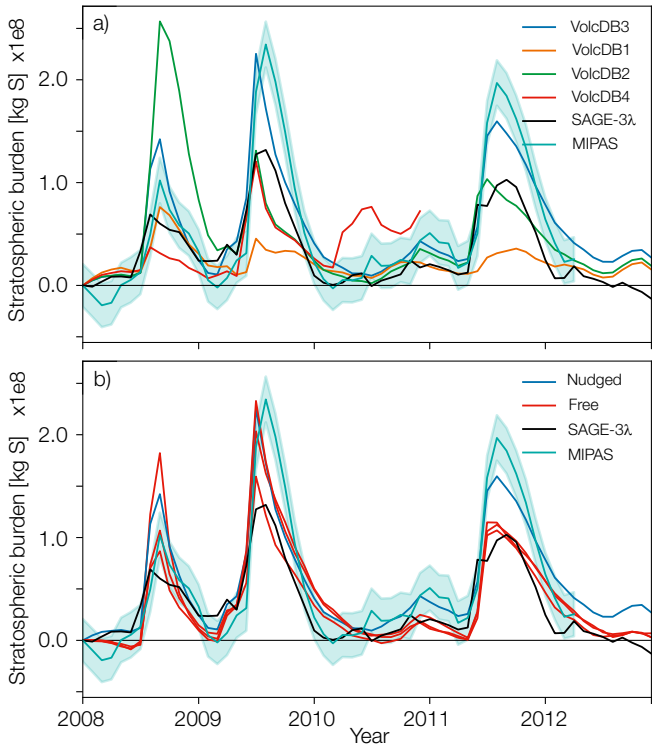

Figure 1. Evolution of the global stratospheric aerosol burden as calculated by the model and compared to observational data retrieved from MIPAS, as well as the SAGE-3λ dataset. All are normalised by subtracting the first month. Panel a) Evolution with emission input from four different databases used in the model, and b) shows three free running simulations and one nudged, all of which were conducted with the emission database, VolcDB3.

tropospheric clouds were found to affect the tropospheric SO_2 oxidation paths and the cross-tropopause transport, leading to increased background burdens both in the troposphere and the stratosphere. This effect can be reduced by nudging only horizontal winds but not temperature. A higher vertical resolution of 90 levels (as opposed to 39 in the standard version) increases the stratospheric residence time of sulphate aerosol after low-latitude eruptions by reducing the diffusion speed out of the tropical reservoir. We conclude that the model's uncertainties can be largely defined by both its set-up as well as by the volcanic emission parameters.

A paper discussing these results in detail is currently in preparation. Further research in this direction will be made in the multi-model mode in frames of the Interactive Stratospheric Aerosol Model Intercomparison (ISA-MIP) project (Timmreck et al., 2018).

References: Feinberg A., Sukhodolov T., et al.: 2019, Improved tropospheric and stratospheric sulfur cycle in the aerosol–chemistry–climate model SOCOL-AERv2, Geosci. Model Dev., 12, 3863–3887, doi: 10.5194/gmd-12-3863-2019

Timmreck C., et al.: 2018, The Interactive Stratospheric Aerosol Model Intercomparison Project (ISA-MIP): Motivation and experimental design, Geosci. Model Dev., doi: 10.5194/gmd-2017-308

Modelling of the Upper Atmosphere Response to Energetic Electron Precipitation

Timofei Sukhodolov and Eugene Rozanov in collaboration with the SPARC SOLARIS/HEPPA3 team

The project is part of the SOLARIS/HEPPA (Solar Influences on Climate / High Energy Particle Precipitation in the Atmosphere) activity within SPARC (Stratosphere-troposphere Processes And their Role in Climate), aimed at analysing the impact of energetic electron precipitation on the atmosphere. We compared simulated and observed nitric oxide (NO) variability during a geomagnetic storm in April 2010 using four chemistry-climate models (CCM) and satellite data sets. We contributed to this study by providing and analysing the results of experiments with CCM HAMMONIA (Hamburg Model of the Neutral and Ionised Atmosphere).

The understanding of the impact of energetic electron precipitation on the atmosphere is far from complete due to large uncertainties in the ionisation rates, satellite observations and model results. The SPARC SOLARIS/HEPPA community approached the problem by studying a geomagnetic storm in April 2010 because this period is well covered by multiple satellite observations of nitric oxide and electron fluxes. For the study, we used the ionisation rates calculated with three independent methods. These data were applied to force the simulation of the atmospheric state with four high-top chemistry-climate models. In 2020, all modelling groups performed 4-month long experiments using several combinations of the forcing to evaluate model performance and sensitivity to different driving mechanisms. Model runs were separately carried out using the changes of auroral electrons, middle range energy electrons (MEE), photoionisation and protons. Nitric oxide production strongly depends on the temperature, therefore the analysis of the results began with a comparison of the simulated temperature profiles with MIPAS observations (Fischer et al., 2008).

The comparison shows that most of the participating models reproduce well the observed temperature profile in the mesosphere and lower thermosphere, which confirms accurate treatment of the radiation, dynamical and chemical processes in the models. The relative contribution of NO formation by auroral electrons etc to the overall simulated NO amount for the main storm phase on 6 April 2010 is illustrated in Figure 2.

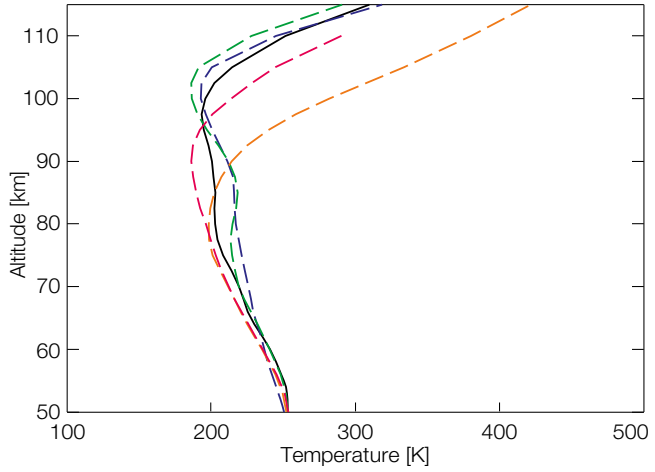

Figure 1. The comparison of zonal mean temperatures from the MIPAS upper atmosphere mode (black solid line) on 30 March 2010 for daytime to model results on the respective satellite footprint (WACCM, blue dashed-dot-dot; HAMMONIA, green dots; EMAC, orange dashed, and KASIMA, red dash-dot) over high southern latitudes.

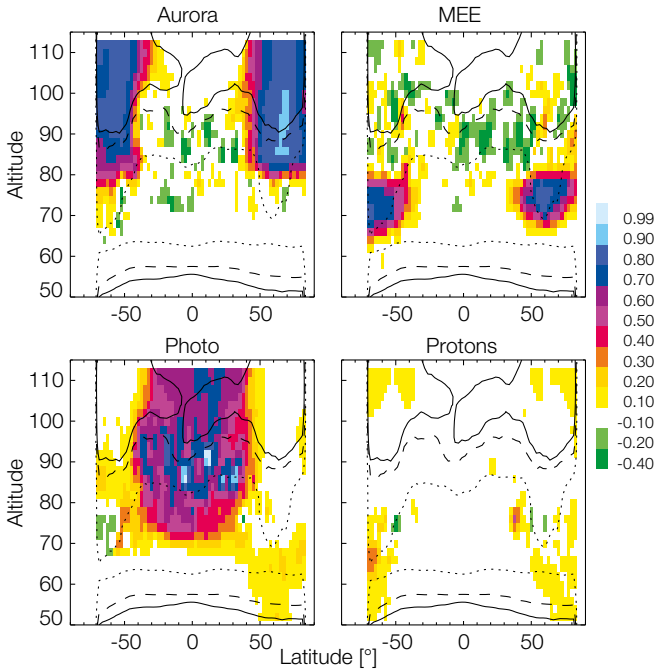

Figure 2. Relative contribution of NO formation by auroral electrons, medium-energy electrons, photoionisation, and solar and soft protons to the overall simulated NO amount for the storm main phase on 6 April 2010.

The auroral or low energy electrons dominate in the thermosphere, where they deposit the energy interfacing with the neutral molecules. Mid-range energy electrons can penetrate deeper, and dominate in the 60–80 km layer. However, the contribution from downward transport of NO produced in the thermosphere can reach 50% in some areas. While this estimate is rather uncertain, because of known problems with downward NO transport in high-top models, it agrees with conclusions by Arsenovic et al. (2019) obtained with non -high-top CCM and parameterised influx of the thermospheric nitrogen oxides. It justifies using the model with the top at the mesopause to study the influence of energetic particles on the ozone layer and climate. The contribution of solar and magnetospheric protons does not exceed 20% and maximises around 70 km. The photoionisation by solar X-rays and EUV dominates over the middle and low latitudes, contributing to the total NO amount by more than 60%. The rest of NO is produced by solar UV at longer wavelengths as well as NO photoionisation by solar irradiance in the Lyman-alpha line.

References: Arsenovic P., et al.: 2019, Reactive nitrogen (NOy) and ozone responses to energetic electron precipitation during Southern Hemisphere winter, Atmos. Chem. Phys., 19, 9485-9494, doi: 10.5194/acp-19-9485-2019

Fischer H., et al.: 2008, MIPAS: an instrument for atmospheric and climate research, Atmos. Chem. Phys., 8, 2151–2188. doi:10.5194/acp-8-2151-2008

Response of the Upper Atmosphere to Irradiance Increase after the Solar Flare on 6 September 2017

Timofei Sukhodolov and Eugene Rozanov in collaboration with SPbSU (St. Petersburg, Russia)

Solar flares induce significant increases in fluxes of high energy particles and short-wave radiation reaching the Earth atmosphere. Unlike the effects of solar particle events following the flares, the atmospheric effects of solar flare radiation have not been widely addressed in the past. This work investigates these effects in the upper atmosphere after the 6 September 2017 solar flare by using the high-top chemistry-climate model HAMMONIA (Hamburg Model of the Neutral and Ionised Atmosphere) and the flare radiation model, FISM.

On 6 September 2017, a giant sunspot on the sun erupted with a colossal solar flare that registered X9.3 on the solar storm scale. This flare produced an increase in irradiance in the extreme ultraviolet and soft X-ray ranges of the solar spectrum that are most important for the sunlit regions of the upper mesosphere and lower thermosphere. To characterise these effects, we used the chemistry-climate model, HAMMONIA (Schmidt et al., 2006), which covers the atmosphere from the surface to the thermosphere (approximately 250 km). However, the typical lifetimes of solar flares are minutes to hours, while the typical irradiance input cadence in global models is daily, which is clearly too coarse to resolve the irradiance variations caused by flares. To address this problem, we used a sophisticated Flare Irradiance Spectral Model (FISM; Chamberlin et al., 2008), which has a very high temporal and spectral resolution. The duration and amplitude of the soft X-ray flare irradiance calculated by FISM for 6 September 2017 is presented in Figure 1.

HAMMONIA was then applied in the nudged mode by using the re-analysis fields from ERA5 from 850 hPa to 1 hPa. The nudging assures that the model captures the tropospheric and stratospheric dynamics, and thus, the wave forcing for the upper atmosphere as observed. Two calculations were carried out for September 2017: i) with the variations in short-wave radiation parameterised as the function of the daily F10.7 index, and ii) with the hourly fluxes calculated by FISM.

Figure 2 shows the time series of the odd nitrogen (species with an odd number of nitrogen atoms) group NO_y ($N+NO+NO_2+NO_3+N_2O_5+HNO_3$) mixing ratio relative differences

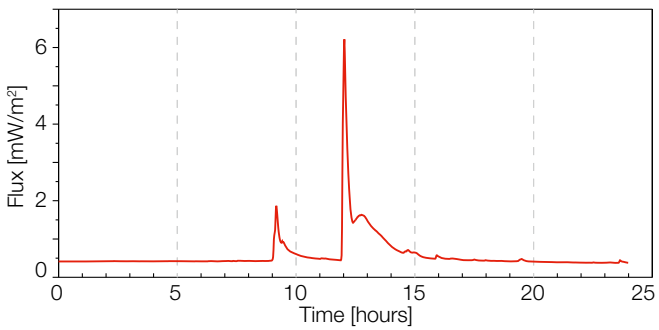

Figure 1. Solar irradiance calculated by FISM for 6 September 2017 and integrated over the 0.5–10 nm range.

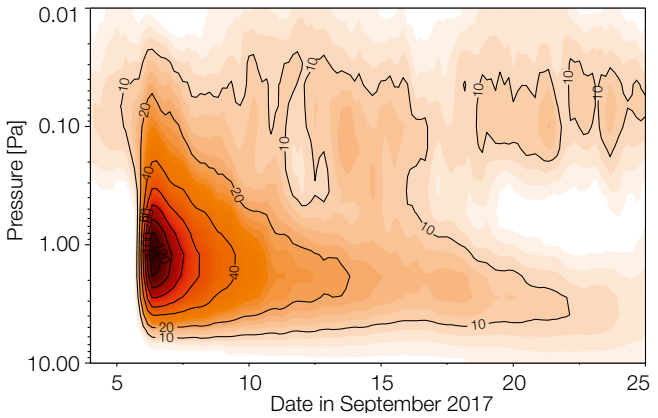

Figure 2. Relative change in NO_y (%) produced by the solar flare on 6 Sep. 2017 calculated by HAMMONIA and averaged over 45°S–45°N.

between the two experiments averaged over 45°S–45°N. Odd nitrogen is produced through a complex set of processes, starting with the direct photodissociation and photoionisation of neutrals and followed by a series of indirect effects of secondary electrons. The flare-induced signal in NO_y is the most pronounced in the mesosphere, around 1 Pa (~80 km), and reaches values of more than 120% in the first days after the event. The elevated values then persist for several weeks, mostly in the lower mesosphere. This increase, however, did not cause significant changes in ozone.

It has to be noted that experiments with HAMMONIA have been performed as a preparatory work for the more detailed study with the model version upgraded into the EAGLE configuration that also includes a full coupling to the ionosphere-thermosphere model (Bessarab et al., 2020). Besides odd nitrogen production, the enhanced photoionisation during a flare causes a dramatic increase in electron concentration in the ionospheric E region and an increased heating in the thermosphere. These changes in the sunlit part of the atmosphere happen in parallel with the energetic particle precipitation in the polar regions, which also lead to local increase in ionization, heating, and modulation of chemistry. As was shown in our previous work (Bessarab et al., 2020), alteration of the thermal regime of the thermosphere would lead to changes in dynamics, transport of neutrals, and finally to the additional changes in the total electron content. As the next stage of this work, we will evaluate in detail the relative contributions of both the particle and radiation fluxes, and the related feedbacks between the ionosphere and the neutral atmosphere.

References:

Bessarab F.S., et al..: 2020, Ionospheric response to solar and magnetospheric protons during January 15-22, 2005: EAGLE whole atmosphere model results, Advances in Space Research, doi.org/10.1016/j.asr.2020.10.026

Chamberlin P.C., et al.: 2008, Flare Irradiance Spectral Model (FISM): Flare component algorithms and results, Space Weather, 6, S05001, doi:10.1029/2007SW000372

Schmidt H., et al.: 2006, The HAMMONIA chemistry climate model: Sensitivity of the mesopause region to the 11-year solar cycle and CO2 doubling, J. Clim., 19, 3903-3931, doi:10.1175/JCLI3829.1

Atmospheric Effects of the Exceptional Middle Latitude Electron Precipitation Detected by Balloon Observations

Timofei Sukhodolov and Eugene Rozanov in collaboration with the H-EPIC community

Energetic particle precipitation leads to ionisation in the Earth's atmosphere, initiating the formation of active chemical components that destroy ozone and have the potential to impact climate. Recently, exceptionally strong high-energy electron precipitation was detected by balloon measurements in middle latitudes. Within the framework of the High-energy Electron Precipitation Into the atmosphere (H-EPIC) community, we have analysed how important such events are for the atmosphere.

Permanent sources of atmospheric ionisation are galactic cosmic rays and solar ultraviolet radiation, but the flux of energetic particles can increase by orders of magnitude due to episodic precipitation of solar or magnetospheric energetic particles. The precipitation of electrons from the outer radiation belt is a consequence of the violation of the adiabatic motion of the trapped electrons, mostly as a result of the wave-particle interaction. Precipitation mainly occurs at high latitudes, in the zone of the auroral oval. An exceptional case of energetic electron precipitation outside of the auroral oval was observed over Moscow (55.96°N, 37.51°E) on 14 December 2009. The derived ionisation rates are much larger than expected for mid-latitude precipitation and resemble in strength and altitude the coverage of large solar proton events.

To estimate the potential of this event to affect atmospheric chemistry we used the 3-D chemistry-climate model, (HAMMONIA Hamburg Model of the Neutral and Ionized Atmosphere; Schmidt et al., 2006). However, HAMMONIA does not include a detailed description of the ionospheric D-layer, and therefore we had to use an additional 1-D ion chemistry model ExoTIC (Herbst et al., 2019) to calculate the formation and loss rates of neutral species caused by the ionisation rates derived from the balloon observations. These time-dependent rates were then provided as input to HAMMONIA, allowing for instance the direct HNO_3 production from ion chemistry. As the information about the spatial and temporal characteristics of the event is basically limited to balloon observations over Moscow, we had to apply the forcing only in the model profile above Moscow and only at the hours covered by the balloon flight.

To illustrate the HAMMONIA modelling results, we used the spatial extreme statistics instead of averaging globally or over a certain region. This is justified by the forcing localisation and the 3-D dynamics of the model that quickly transports away the produced anomalies in chemical species. Produced NO_x is above the unperturbed maximum values by 1–2 orders of magnitude in the middle and upper mesosphere (Figure 1a). The HNO_3 mixing ratio in the lower mesosphere reaches values up to 2 ppmv (Figure 1b), which is 2–2.5 orders of magnitude larger than the unperturbed maximum values at those altitudes. Modelled HNO_3 is also plotted at 68 km as maximum zonal values (Figure 1d) to illustrate the meridional transport of the plume. The start of the plume is located within the polar vortex and it circled the globe in about 3 days. From Figures 1a and 1b, we can also see the

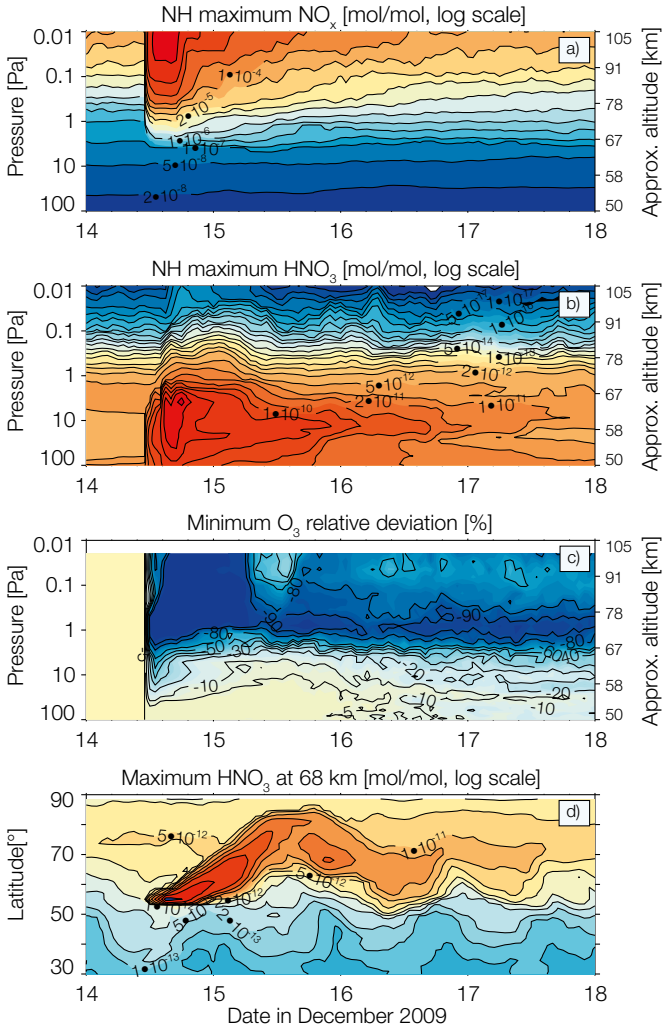

Figure 1. HAMMONIA results for: (a) northern hemispheric (NH) maximum value of NO_x, (b) NH maximum value of HNO_3, (c) NH minimum value of the relative difference between runs with and without the event, and (d) zonal maximum value of HNO_3 at 68 km.

downward propagation of the signal below 1 Pa and upward propagation above 1 Pa following the large-scale residual circulation. The downward propagation of the odd nitrogen produced by energetic particles is an important contributor to the stratospheric high-latitude ozone budget. However, because the event is so localised in the model, this effect is indistinguishable. The modelled ozone response, therefore, almost completely comes from the HO_x enhancement, showing an ozone destruction of up to 95% in the upper mesosphere above Moscow during the event (Figure 1c). A paper, which discusses this and also includes the detailed analysis of the satellite observations in December 2009, is currently in preparation for submission to the Nature journal group.

References: Herbst K., et al.: 2019, A&A, 631, A101, doi: 10.1051/0004-6361/201935888

Schmidt H., et al.: 2006, J. Clim., 19(16), 3903-3931, doi:10.1175/JCLI3829.1

^{7}Be Activity by Cosmic Rays: Modelling with the Chemistry-Climate Model SOCOL-AERv2-BEv1 and Comparison with Direct Measurements

Eugene Rozanov and Timofei Sukhodolov in collaboration with the Cosmic ray group (University of Oulu, Finland)

We simulated the short-lived activity of the cosmogenic isotope ^{7}Be using the chemistry-climate model SOCOL-AERv2-BEv1. ^{7}Be production was calculated using the 3-D time-dependent Cosmic Ray induced Atmospheric Cascade (CRAC) model (Poluianov et al., 2016). The comparison with observations of ^{7}Be in the air and water revealed a good (within 12%) agreement on time scales longer than about a month, for the 2002 – 2008 period. It confirms the model ability to reliably model production, transport, and deposition of the cosmogenic isotopes, which is needed for studies of cosmic-ray variability in the past and solar-terrestrial interactions.

For the model verification, we used data of the measured activity (concentration) of ^{7}Be isotope in near-ground air, with a weekly sampling rate (corrected for decay) performed in different hemispheres, for the 2002 – 2008 period. Traditionally, for short-lived isotopes, the measured quantity is not atomic concentration but activity concentrations, in units of becquerel (number of radioactive decays per second) per cubic meter of air (Bq/m^3), as directly measured by a γ-spectrometer. Correction for decay is performed as standard. The activity and concentration can be easily translated to each other using the known lifetime of the isotope.

Comparison of the modelled and measured ^{7}Be activity for the all-Finland record is shown in Figure 1a. The coherence is highly significant (confidence level above 95%) on all time scales between one month and two years. Although there are discrepancies on the very short time scales, related to the synoptic noise, the model correctly reproduces some strong spikes in the beryllium activity (e.g., early 2003) which are often related to sudden stratospheric warming (SSW) events (Brattish et al., 2020). On the other hand, there is an essential difference between the model and the measurements regarding the magnitude of summer peaks in 2007 and 2008. It could be potentially related to local atmospheric aerosol properties, but the AERONET (AErosol RObotic NETwork) (Emery and Camps, 2017) station in Sodankylä (Northern Finland) did not show any anomalies for that time.

For the Canadian station, the agreement between the modelled and measured activities (Figure 1b) is nearly perfect, including a correct reproduction of the very strong seasonal cycle and sudden short spikes, as for instance, in late 2003. The overall mean level of modelled activity (2.15 mBq/m^3) is close to the measured value (2.4 mBq/m^3), and is within 10% (the difference is 0.24±0.22 mBq/m^3). The most pronounced difference between the model and the measurements was observed in 2008.

The Chilean data (Figure 1c) depicts a reasonable agreement between the model and the measurements. Since the data contains no seasonal pattern, as correctly reproduced by the model, the formal correlation is insignificant r = 0.06. The mean levels of the modelled and measured series agree nearly perfectly, within 2%, namely 1.74 vs. 1.71 mBq/m^3 for the modelled and measured activities, respectively.

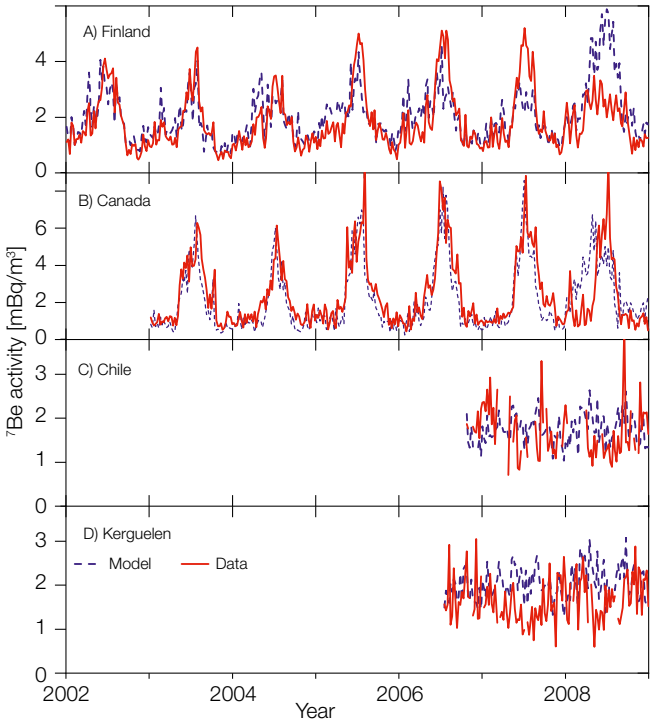

Figure 1. Datasets of ^{7}Be activity concentrations in the near-ground air used in this study, including (panels A through D respectively): Finland (a composite of four stations): Yellowknife (Canada), Punta Arenas (Chile), and Kerguelen island (France). The measured and modelled activities are shown as solid red and dashed blue curves, respectively.

Data from Kerguelen Island (Figure 1d) also depicts a reasonable agreement, including correctly reproduced spikes. Similar to the Chilean data, the formal correlation is insignificant r = 0.06. The mean levels of the modelled and measured series are not well-matched, with a difference of 18%, namely 2.02 vs. 1.65 mBq/m^3 for the modelled and measured activities, respectively. This may be related to the peculiarity of this site which is located on a small island (about 100 km across) in the middle of the ocean, while the model grid (~300 × 300 km) is too rough to catch the orography.

The obtained results demonstrate that CCM AERv2-BEv1 can be applied in the future for the studies of solar influence on production, transport and deposition of different radionuclides.

Acknowledgment: The study was partly funded by the Finnish Academy of Science project ESPERA, No. 321882.

References:

Brattish E., et al.: 2020, Advection pathways at the Mt.Cimone WMO-GAW station: Seasonality, trends, and influence on atmospheric composition, Atmos. Environ., 234, doi: 10.1016/j.atmosenv.2020.117513

Emery W., Camps A., 2017: Introduction to Satellite Remote Sensing, Elsevier, doi: 10.1016/B978-0-12-809254-5.00008-7

Poluianov S., et al.: 2016, Production of cosmogenic isotopes ^{7}Be, ^{10}Be, ^{14}C, ^{22}Na, and ^{36}Cl in the atmosphere: Altitudinal profiles of yield functions, J. Geophys. Res. Atmos., 121, 8125-8136, doi:10.1002/2016JD025034

Traceability of Solar Direct Irradiances Measured with Precision Filter Radiometers

Natalia Kouremeti, Julian Gröbner, and Stelios Kazadzis with the collaboration of PTB (Germany)

One Precision Filter Radiometer (PFR) measuring Solar direct irradiances for the retrieval of aerosol optical depth (AOD), was characterised and calibrated at the Physikalisch-Technische Bundesanstalt (PTB) and PMOD/WRC in 2018, as well as within the framework of the MAPP project at PTB, in Jan. 2021. The measured irradiances are used in the classical Langley extrapolation method to assess the precision of the extra-terrestrial Solar spectrum, as well as the accuracy of AOD measurements that can be currently achieved following this SI-traceable related methodology.

The relative spectral responsivities (RR) of a PFR (N01), have been primarily determined using a pulsed Optical Parametric Oscillator (OPO) system (EKSPLA NT242 model) at PTB and at PMOD/WRC. The RR measurements at PTB were carried out relative to a calibrated silicon photodiode using a monitor photodiode. Similar measurements at PMOD/WRC used a pyroelectric radiometer as a reference detector.

The spectral irradiance responsivity of the PFRs in SI units has been determined twice with the help of the PTB based TULIP setup and with the direct irradiance calibration setup of PMOD/WRC. The measurements with the Tuneable Lasers in Photometry (TULIP) setup were carried out within bandpasses of the channels against a calibrated 3-element silicon trap detector equipped with an aperture. The reference plane of the PFR for the TULIP measurements has been validated against the reference detector by introducing displacements along the beam propagation direction.

The calibration factors in SI units (V/Wm^{-2}) were calculated as an integral of the TULIP responsivity functions (combined with the pulsed OPO data) over the measured spectral bandpasses. For the lamp calibration method, the afore-mentioned responsivities were converted to relative ones and convolved with the spectral irradiance of the reference lamp calculated for the distance of the instrument.

In order to evaluate the calibration accuracy that can been achieved (with both methods mentioned), we have used the publicly available solar extra-terrestrial spectra (ETS), QASUMEFTS and ATLAS. A direct solar irradiance measurement comparison campaign of the calibrated PFR against the PFR-Triad at PMOD/WRC was organised in March 2019. Nine clear days with Langley atmospheric conditions were experienced, and aerosol loads ranging from 0.01 – 0.03 AOD at 500 nm were compared.

Figure 1 illustrates the AOD differences against the PFR reference as median (red dot), 5th and 95th percentiles (colored squares) and extreme values (black lines) of the comparison period, as well as for different calibration procedures. The shaded area shows the maximum AOD difference limits, designated by WMO for Langley calibrated instrument agreement. Following the SI-traceable retrieval of AOD, for wavelengths up to 500 nm, both methods

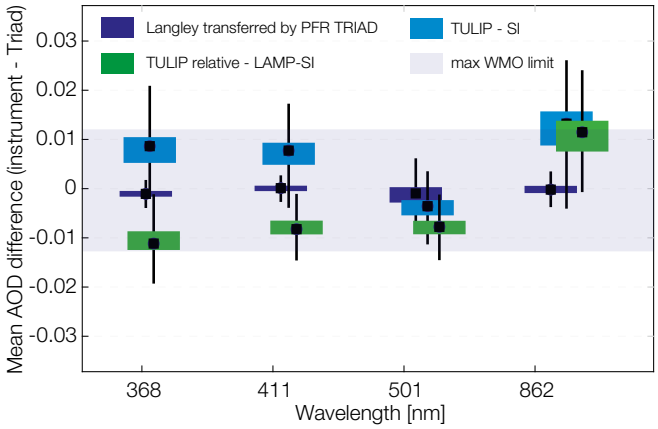

Figure 1. AOD comparison between SI-traceable retrievals and the PFR-TRIAD.

fall within the WMO limits, with a minimum difference for the TULIP method. At 862 nm, despite the best agreement of all SI calibrations constants (standard deviation of 0.45%), an offset of 0.012 in AOD is observed, which can be attributed to underestimation of the ETS by 1% using ATLAS. The second TULIP measurement from 2021 showed an improved agreement with the used ETS of 1.05, 0.51, 0.32 and 0.15% for the 4 channels assuming a constant responsivity.

Acknowledgments: These activities have received funding from the EMPIR program co-financed by the Participating States and from the European Union's Horizon 2020 research and innovation programme through project 19ENV04 MAPP and by the ESA project No. QA4EO/ SER/ SUB /09.

References: Gröbner J., Kröger I., Egli L., Hülsen G., Riechelmann S., Sperfeld P.: 2017, The high-resolution extraterrestrial solar spectrum (QASUMEFTS) determined from ground-based solar irradiance measurements, Atmos. Meas. Tech., 10, 3375-3383, doi.org/10.5194/amt-10-3375-2017

Thuillier G., Hersé M., Labs D., et al.: 2003, The solar spectral irradiance from 200 to 2400 nm as measured by the SOLSPEC spectrometer from the Atlas and Eureca missions, Solar Physics 214, 1-22, doi.org/10.1023/A:1024048429145

Total Ozone Column Measurements and Data Quality Control of Nairobi Data

Herbert Schill

Since 1984, Total Ozone Column Ozone (TOC) measurements have been performed in Nairobi (Kenya) with a Dobson spectrophotometer to monitor the stratospheric ozone layer in the tropics. In 2019, a Brewer spectrophotometer was added to the equipment. The station in Nairobi is supported by MeteoSwiss, which is also responsible for the data quality control and assurance of the measurements. In 2020, this task was handed over to PMOD/WRC to profit from the know-how of the similar procedures done for the Arosa-Davos ozone series.

Looking at a global map reveals, at the first sight that observatories monitoring the stratospheric ozone layer are distributed extremely unevenly over the globe, and are mostly concentrated in Western Europe and North America. This led to the decision, within the GAW framework, to establish additional stations in the tropics, equipped with worldwide standard instruments such as Dobson or Brewer spectrophotometers. In 1984, Dobson D018 was put into operation at the University of Nairobi, Kenya, and provided data up until 1999.

In 2005, D018 was transferred to the Kenya Meteorological Department (KMD) headquarters and revived after substantial revisions in a joint effort by Deutscher Wetterdienst (DWD), Czech Hydrometeorological Institute (CHMI) and MeteoSwiss. In 1996, a first ozone sounding system was also installed at the Nairobi GAW Regional Station based on the Vaisala RS80 radiosonde and the ECC ozone sonde. Since then, MeteoSwiss has supported these operations (Klausen et al., 2014). Moreover, surface ozone observations have started that can be compared with observations at the Mt. Kenya Global GAW Station. In 2007, Herbert Schill, then employed at MeteoSwiss, became responsible for the data quality control of D018.

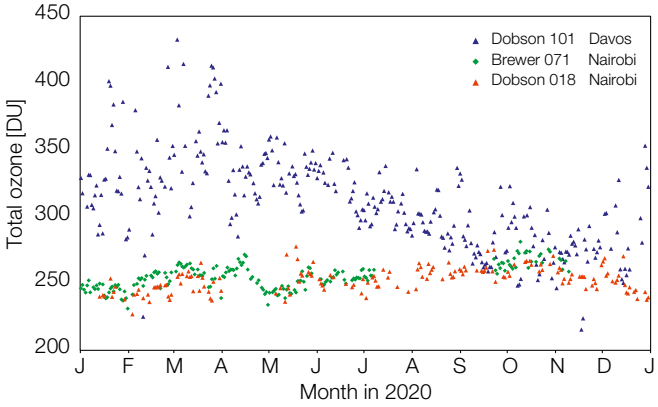

Figure 1. Daily total ozone values in 2020 from direct sun measurements of Dobson 101 (blue) at PMOD/WRC, Davos, and Brewer 071 (green) and Dobson 018 (red) at KMD, Nairobi. The interdiurnal changes and the annual cycle of the ozone column – with the maximum in Spring (433 DU on 3 March) and the minimum in Autumn (216 DU on 18 November) – in middle latitudes (Davos, 47°N) stay in clear contrast to the steady observations with few changes in the tropics (Nairobi, -1.3°S), with the maximum of 278 DU on 18 May and the minimum of 227 DU on 3 February.

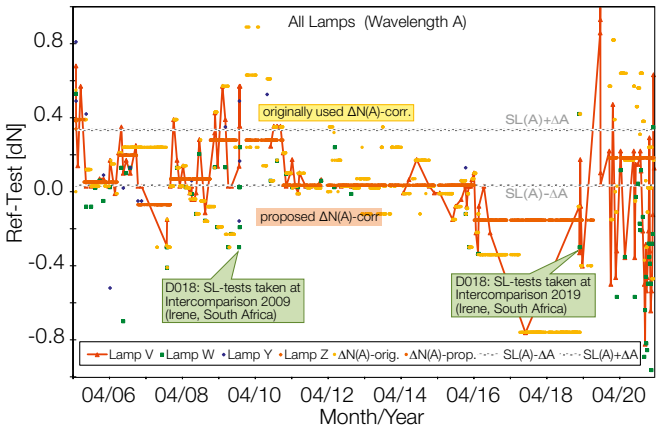

Figure 2. Standard lamp tests of Dobson D018 performed at Nairobi for 2005 – 2021. This test gives information about the performance of the instrument photomultiplier tube, and the deviations towards the reference values (the so-called dN-values) are used to correct TOC in the data post-processing. To guarantee that changes in dN-values come from the photomultiplier tube and not the lamp, at least two lamps are used in parallel.

Figure 3. Measurements of Dobson spectrophotometer D018 captivate the interest of a class visiting the site at Kenya Meteorological Department (Photo: B. Calpini, MeteoSwiss).

In July 2020, following an agreement between Meteo-Swiss, PMOD/WRC and WMO, the data quality control of Dobson D018 and Brewer 071 in Nairobi became part of the QC/QA duties of Herbert Schill. The required specifications consist of: i) control and analysis of the instrument tests (standard-lamp and mercury-lamp tests in the first instance), ii) to analyse and apply the results of intercomparisons towards a standard instrument (Nyaga et al., 2019), iii) the control, analysis and statistical treatment of the ozone measurements, their comparison with satellite overpass data, and iv) documentation and upgrading of the tools used for these tasks, including recommendations to the local staff in Nairobi.

References: Klausen J., et al.: 2014, Thirty Years of ozone Observations in Kenya, Joint 13th Quadrennial iCACGP Symposium and 13th IGAC Science Conference, Natal, Brasil, 22-26 Sep. 2014, poster presentation.

Nyaga Annet, et al.: 2019, GAW Stations in Kenya, Dobson Intercomparison Campaigns meeting at Irene Inst. Pretoria, South Africa, Oct 2019, oral presentation.

The QasumeIR Spectroradiometer within the Project 19ENV04 MAPP

Gregor Hülsen and Julian Gröbner

Within the EMPIR project 19ENV04 MAPP, a new spectroradiometer was built – the QasumeIR. The system will be used for solar direct irradiance measurements in the wavelength range from 500 nm up to 1.7 µm. The construction was finished at the end of 2020. The system is calibrated and will start recording solar irradiance in Spring 2021.

Within MAPP (WP2 Task 2.1.1) a new spectroradiometer system was built at PMOD/WRC. The long experience of the two existing UV spectroradiometers of the WCCUV (Qasume and QasumeII; Hülsen et al., 2016) has been used to setup up a similar system with a complementary wavelength range. The former devices are designed for solar UV irradiance measurements from 250 nm to 550 nm whereas the new QasumeIR system is intended for direct solar irradiance measurements from 500 nm to 1700 nm.

The core part is a Bentham TM300 single monochromator with a 300 mm focal length (see Figure 1). It is equipped with three diffraction gratings: 1200, 830 and 600 lines/mm. For wavelengths below 950 nm, a Bentham silicon diode together with the 1200 lines/mm grating is used whereas in the infrared wavelength range, a Bentham InGaAs-diode and a 830 lines/mm grating was chosen. An order sorting filter wheel is located inside the entrance port of the monochromator, and is fitted with six filters selected for the spectral range of use.

A similar temperature-controlled box as for UV spectroradiometers has been constructed for QasumeIR, which stabilises the temperature of the monochromator and detectors to ±0.1°C. The solar irradiance is collected by a Bentham D8 cosine-corrected integrating sphere coupled to the monochromator using a 7 mm FOP type fibre bundle (250–2500 nm). The system has been calibrated separately for its two wavelength regions both for dispersion, angular responsivity of the input optic and responsivity of the system. For the dispersion wavelength calibration, a set of spectral calibration lamps were selected (Hg, Cd, Zn, Ne, Ar). In addition, a tunable laser system together with a spectral line analyser provides additional reference lines (Figure 2). The system resolution (slit width) is 1.6 nm for the shorter wavelength range and 2.4 nm for the IR range. The absolute calibration is traceable to SI by 1000 W Tungsten Halogen Irradiance Standards calibrated at PTB. The expected response from the signal using the absolute calibration and modelled solar spectra is shown in Figure 3. For most of the wavelength range, the ammeter signal is expected to be in the nA-range for a clear sky day in Davos, using a modelled solar spectrum and a preliminary responsivity measurement of the system. The QasumeIR data acquisition system will be able to record signal levels with statistical uncertainties of ~0.1%.

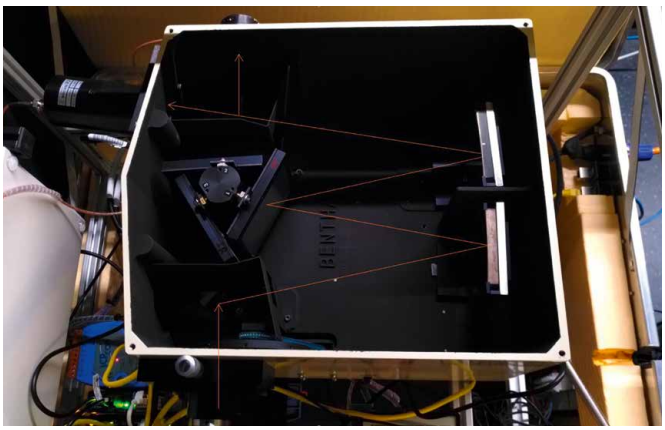

Figure 1. The TM300 Monochromator of QasumeIR with its grating turret in the centre. The Si-Diode is located at the first exit port (top) and the InGaAs-Diode at the second exit port, seen in the top left-hand side of the picture. The entrance port can be seen at the bottom.

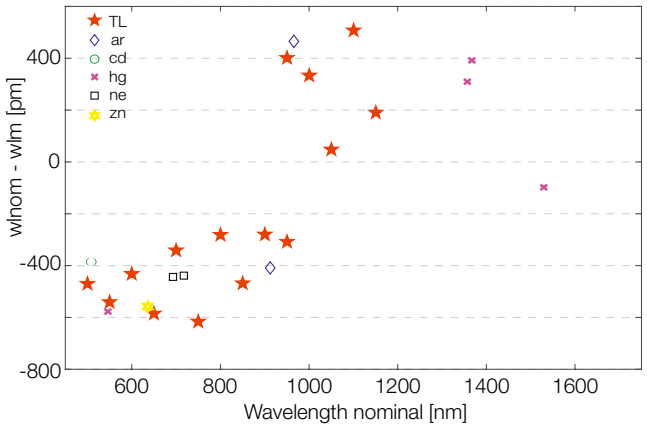

Figure 2. The result of the QasumeIR wavelength dispersion calibration corrects the wavelength offsets in the lower regions to within ±100 pm and ±200 pm in the IR range.

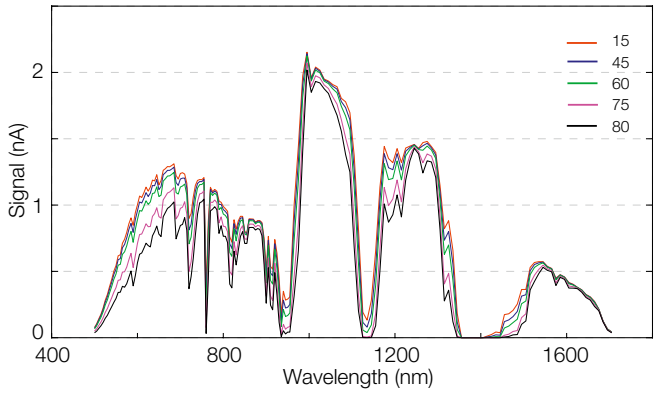

Figure 3. Expected signal from direct solar irradiance measurements using QasumeIR. Line colours correspond to increasing solar zenith angles (15° to 90°).

Acknowledgment: The project 19ENV04 MAPP has received funding from the EMPIR programme co-financed by the Participating States and from the EU Horizon 2020 research and innovation programme.

References: Hülsen G., et al.: 2016, Traceability of solar UV measurements using the QASUME reference spectroradiometer, Appl. Opt. 55, 7265-7275.

Consistency of Total Ozone Column Measurements Between the Brewer and Dobson Spectroradiometers of the LKO Arosa and PMOD/WRC Davos

Julian Gröbner, Herbert Schill, and Luca Egli in collaboration with Meteoswiss

The world's longest total ozone column time series was initiated in 1926 at the Lichtklimatisches Observatorium (LKO), at Arosa, in the Swiss Alps. The main instruments used to report total ozone column are Brewer and Dobson spectrophotometers. The systematic differences observed between these two instrument types can be attributed to the temperature sensitivity of approx. +0.1%/K when the Bass & Paur ozone absorption cross-sections are used to retrieve the total ozone column from the measurements. The consistency between Brewer and Dobson spectrophotometers can be significantly improved when the ozone absorption cross-sections from Serdychenko et al., 2013 together with the measured line-spread functions of the instruments are used.

The operational ozone absorption coefficients used by the Brewer and Dobson networks are based on the ozone cross-sections from Bass & Paur. We have investigated additional datasets of ozone absorption cross-sections available for the wavelength range between 300 nm and 345 nm. The selected cross-sections are also available at several ozone temperatures, in order to calculate the ozone absorption cross-sections for the effective ozone temperature at Davos and Arosa. Furthermore, the line-spread functions measured with the portable tunable source TuPS were used for Dobson D101 instead of the nominal literature values:

- BPOp - The nominal ozone absorption coefficients based on the standard operational procedures of the Brewer and Dobson networks. For Brewer spectroradiometers, these are based on the Bass & Paur cross-sections at a temperature of 228 K, while for the Dobson spectroradiometers, they are equal to those of Dobson D083.
- IGQ - The quadratic polynomial temperature approximation of the Bass&Paur ozone absorption cross sections.
- DBM - The dataset of Daumont, Brion and Malicet.
- IUP - Dataset of ozone absorption cross-sections measured by the University of Bremen, IUP in 2013.
- IUP_ATMOZ - were measured in 2017 during the EMRP ATMOZ project and have improved noise characteristics in the wavelength region 295 nm to 350 nm when compared to the original IUP cross-sections.
- ACS - A recent dataset measured in the frame of the ESA project SEOM-IAS between ~243 nm and ~346 nm.

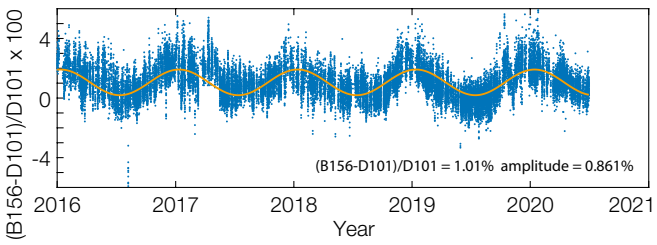

Figure 1. Relative differences in total ozone column between Brewer B156 and Dobson D101 using the operational ozone retrieval procedure with the ozone absorption cross-sections from Bass & Paur. The yellow curve is a periodic fit to the data.

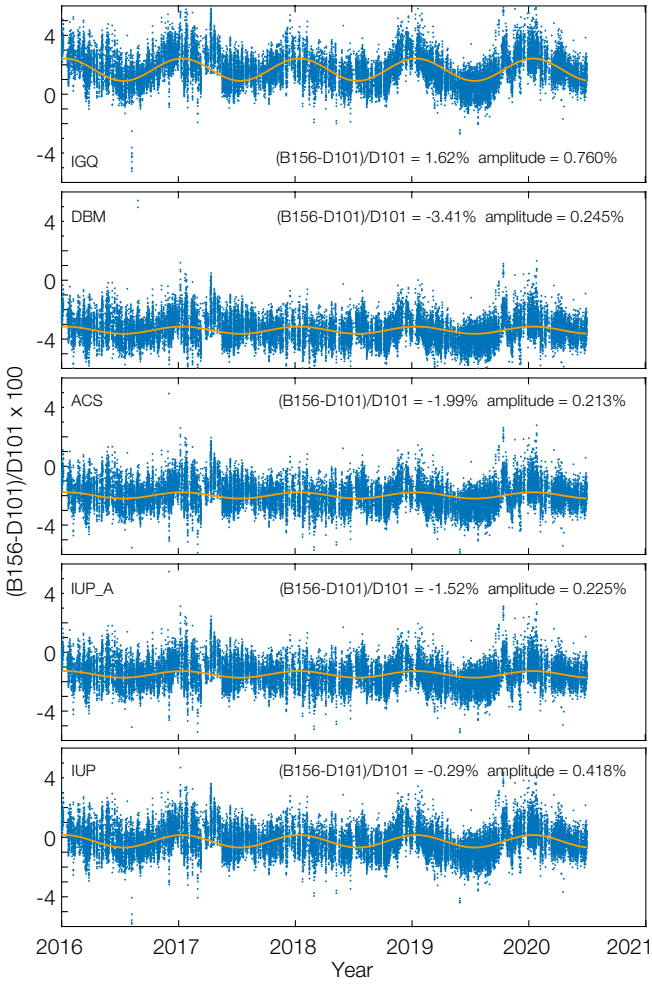

Figure 2. Relative differences in total ozone column calculated with different ozone absorption cross-sections and effective ozone temperature relative to the operational ozone datasets for Brewer B156. The yellow curves are periodic fits to the data.

As can be seen in Figure 1, the relative difference between Brewer B156 and Dobson D101 for the period 2016 to 2020 has an offset of 1% and a seasonal amplitude of 0.86% which correlates very well with the effective ozone temperature retrieved from ozone sonde profiles. In Figure 2 we show the same datasets, calculated with different ozone absorption cross-sections and taking into account the effective ozone temperature. The best agreement between Brewer B156 and Dobson D101 is then obtained with the IUP cross-sections, with an overall offset of only 0.2% and a significantly reduced seasonal variability. This study has been published as a peer-reviewed publication (Gröbner et al., 2021).

Acknowledgment: The study was partly funded by the ESA QA4EO project, No. QA4EO/SER/SUB/09, and by the INFO3RS project, funded by MeteoSwiss, Grant number 123001926.

References: Gröbner J., Schill H., Egli L., Stübi R.: 2021, Atmos. Meas. Tech. Discuss, doi.org/10.5194/amt-2020-497, accepted.

Serdyuchenko A., et al.: 2013, Atmos. Meas. Tech. Discuss., 6, 6613-6643, doi:10.5194/amtd-6-6613-2013

The Global Climate Observing System (GCOS) and the GAW-PFR Network for Aerosol Optical Depth Long-Term Measurements

Stelios Kazadzis, Natalia Kouremeti, and Julian Gröbner

The project "Global Atmosphere Watch Precision Filter Radiometer (GAW-PFR) Network for Aerosol Optical Depth long term measurements" has received funds from the Federal Office of Meteorology and Climatology MeteoSwiss, Swiss Global Climate Observing System (GCOS) Office.

In the early 1990s, PMOD/WRC developed the Precision Filter Radiometer (PFR) that has been used for long-term AOD measurements in a GAW-PFR Network of sun-photometers which started in 1995 at Davos (Switzerland) and from 1999 at other worldwide locations. They provide long-term measurements of AOD.

During this project harmonisation, re-evaluation and improvement of the GAW-PFR AOD time series have been performed. Using these data, we evaluated the long-term trend analysis of the GAW-PFR AOD data with emphasis on the free troposphere (high mountain), polar stations and also stations that coincide with sun-photometers from other existing AOD networks (Cuevas et al., 2019; Nakajima et al., 2020). In addition, an uncertainty analysis of the retrieved AOD data and also an uncertainty of the long-term calculated trends for each GAW-PFR station, based on the GCOS and WMO-GAW related measurement and uncertainty requirements, have been reported.

Out of the 15 GAW-PFR stations seven have 15 or more years and another seven have 10 or more years of AOD measurements. More details about the calibration procedure and the instrument locations and measurement periods can be found in Kazadzis et al. (2018).

Using the Mann Kendall test, only four stations showed positive trends although none were statistically significant. The remaining 11 stations showed generally small but negative trends, all of them lower than 2% per year or 0.02 in AOD units per decade. High mountain stations showed small but negative trends (Izana (IZO), Mauna Loa (MLO), Mount Walliguan (WLG)) while Jungfraujoch (JFJ) showed a small but positive trend mostly associated with the second decade of measurements. In the cases of MLO, IZO and JFJ, the AOD trend is 0.001 – 0.002/decade. Four and six stations showed statistically significant trends at wavelengths of 500 nm and 865 nm, respectively.

The high mountain stations at MLO, JFJ and IZO showed the lowest AOD (0.018, 0.029, 0.049 at 500 nm, respectively) values, with IZO measurements giving higher AOD and lower Ångström exponent (AE) values during Saharan intrusion periods. WLG station exhibited high AOD and low AE values for a +4000 m altitude station. However, WLG is also affected by dust intrusions from middle China. AE values at JFJ, MLO and DAV were found to be in the 1.3 – 1.4 range that suggests the presence of natural aerosols. The station at Alice Springs (ASP) also had low AOD at 500 nm (0.056). The annual variation of AOD shows the standard pattern of low/high values in Austral winter/summer. Minimal daily means are comparable to high altitude stations in the northern hemisphere.

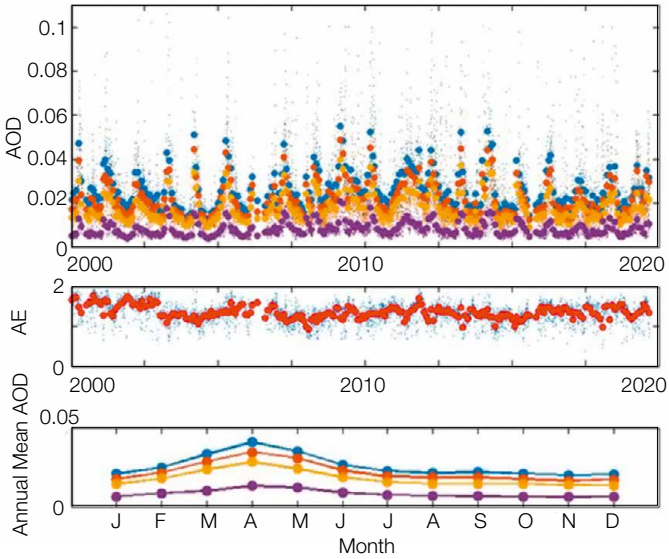

Figure 1. Top panel: Mauna Loa time-series of AOD at the four PFR wavelengths (blue line: 368 nm; red: 412 nm; green: 500 nm; violet: 862 nm), middle panel: the Ångström exponent (AE), and lower panel: intra-annual AOD variability.

Acknowledgment: Research has been funded by the Federal Office of Meteorology and Climatology MeteoSwiss International Affairs Division, Swiss GCOS Office.

References:

Cuevas E., et al.: 2019, Aerosol Optical Depth comparison between GAW-PFR and AERONET-Cimel radiometers from long term (2005–2015) 1-minute synchronous measurements, Atmos. Meas. Tech. Discuss., doi.org/10.5194/amt-2018-438

Kazadzis S., Kouremeti N., Nyeki S., Gröbner J., Wehrli C.: 2018, The World Optical Depth Research and Calibration Center (WORCC) quality assurance and quality control of GAW-PFR AOD measurements, Geosci. Instrum. Method. Data Syst., 7, 39-53, doi.org/10.5194/gi-7-39-2018

Nakajima T., et al.: 2020, An overview and issues of the sky radiometer technology and SKYNET, Atmos. Meas. Tech., doi.org/10.5194/amt-2020-72

Traceability of AERONET-EUROPE to the GAW-PFR WMO Reference for Aerosol Optical Depth

Stelios Kazadzis, Natalia Kouremeti, and Julian Gröbner

The World Optical Depth Research and Calibration Center (WORCC), a section within the World Radiation Center at the Physikalisch-Meteorologisches Observatorium Davos (PMOD/WRC), Davos, Switzerland, is recognised by the WMO as the primary WMO reference centre for Aerosol Optical Depth (AOD) measurements. Within the ESA QA4EO project, a Precision Filter Radiometer (PFR) travelling standard was installed at the European calibration site of AERONET Europe to provide continuous traceability of AOD measurements to the World reference of AOD, maintained at Davos through a PFR Triad. The objective is to homogenise the two global monitoring networks of passive remote sensing of aerosol optical properties, which serve as a fiducial reference for satellite-derived aerosol properties.

The PFR travelling standard was installed on a solar tracker provided by the Laboratory of Atmospheric Optics (LOA) at the Observatoire de Haute Provence (OHP) in southern France (Figure 1). During clear sky periods the measurements of spectral solar irradiance are used to retrieve AOD from the master instrument of ACTRIS/AERONET-Europe and the PFR. A web-page displays the real-time comparison between both instruments and provides continuous quality control of the measurements.

The comparison between both networks over the period of measurements so far (August to January 2021) has been excellent with AOD differences of less than 0.01, while also satisfying the WMO criteria for AOD traceability for 3 out of the 4 channels (see Table 1 and Figure 2).

It is planned to extend the campaign at OHP to the end of 2021, with the expectation to keep a permanent PFR system deployed at OHP to provide a continuous link between AERONET-Europe and the WMO PFR reference maintained at Davos.

Figure 1. Platform at the Observatoire de Haute Provence (OHP), France with four CIMEL sunphotometers and the travelling standard PFR on its own solar tracker (right).

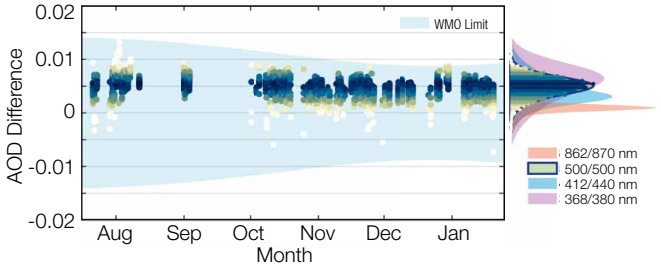

Figure 2. Left panel: The AOD difference, Cimel#1141 - PFR_N014, is shown at 500 nm for the period 21 Jul. 2020 to 19 Jan. 2021. The shaded area represents the WMO limit for AOD agreement between two instruments. The coloured AOD difference (dots) is based on the probability density function shown in the coloured bars in the right panel. Right panel: Normalised probability density functions of the AOD differences for the four wavelengths, approximated by double gaussian distribution functions.

Table 1. Comparison of AOD measurements between the master AERONET-Europe sunphotometer (CIMEL #1141) and the PFR travelling standard 014. The WMO limits are defined as measurements being within 0.01/m±0.005, where m is the path length through the atmosphere (air-mass). Rows marked with an asterisk were extrapolated to a common wavelength using the Ångström law. The data set consists of 2359 coincident data points with a 1-min window from 21 Jul. 2020 to 19 Jan. 2021.

Wavelength (PFR/CIMEL) [nm]	AOD difference			% within WMO limits
	Median	5th percentile	95th percentile	
861/870	0.001	-0.001	0.002	100.0
500/500	0.005	0.001	0.008	99.0
411/440*	0.004	-0.000	0.010	98.3
367/380*	0.005	-0.002	0.011	91.5

In parallel to this activity, the project 19ENV04 MAPP (Metrology for aerosol optical properties), funded jointly by EURAMET and the European Commission through EMPIR (European Metrology for Innovation and Research), aims to extend the traceability of these networks to SI through the characterisation and calibration of sunphotometers from these networks. This collaboration between research institutes and the European metrology community will establish a consistent framework providing calibrations of sunphotometers with traceability to SI as well as comprehensive uncertainty budgets that will be an integral part of the data provided to the users and stakeholders of these networks.

References: Kazadzis S., Kouremeti N., Nyeki S., Gröbner J., Wehrli C.: 2018, The World Optical Depth Research and Calibration Center (WORCC) quality assurance and quality control of GAW-PFR AOD measurements, Geosci. Instrum. Method. Data Syst., 7, 39-53, doi.org/10.5194/gi-7-39-2018

Comparison of the PMOD/WRC Blackbody with the PTB Radiation Temperature Scale

Julian Gröbner and Christian Thomann in collaboration with the PTB (Germany).

The PMOD/WRC reference blackbody provides the traceability of atmospheric longwave irradiance measurements to the International Temperature Scale (ITS-90). A hemispherical blackbody cavity was developed by a joint collaboration between PMOD/WRC and the Physikalisch-Technologische Bundesanstalt (PTB) within the project, EMPIR 16ENV03 METEOC-3, to compare and validate the traceability chain for atmospheric longwave irradiance with target uncertainties of less than 2 Wm^{-2}.

Atmospheric longwave irradiance measurements are ultimately traceable to the radiation emitted by blackbody cavities run at temperatures from about -20°C to +20°C. The PMOD/WRC blackbody has been in operation since 2007 and is used to characterise pyrgeometers and serves as reference for the calibration of the IRIS radiometers (Gröbner 2008, Gröbner, 2012). In the frame of the project EMPIR 16ENV03 METEOC-3, a measurement campaign was organised from 29 September to 9 October 2020 to compare the blackbody operated at PMOD/WRC with the PTB radiation temperature scale – an independent path to the ITS-90.

The comparison at PMOD/WRC was performed using a Temperature Stabilised Radiation Thermometer (TSRT) as a transfer radiometer and the portable Hemispherical Blackbody (HSBB) developed specifically for this purpose serving as a transfer standard. The TSRT was used to measure the radiation temperatures of the PMOD/WRC blackbody and the HSBB, as shown in Figure 1. Before and after the campaign, the HSBB was calibrated at PTB by comparison to the radiation temperature scale of the PTB. Figure 2 shows preliminary results of the nominal radiation temperature of the PMOD/WRC blackbody, and its radiation temperature measured against the HSBB between -18°C and +29°C. The agreement between both curves is excellent in the region of the plateaus with differences well below 0.5 K.

Atmospheric longwave irradiance is measured with instruments having hemispherical acceptance angles, i.e. they measure the incoming longwave radiation over the full hemisphere. For the IRIS radiometer, this is accomplished by using an integrating sphere as a collecting element (Gröbner, 2012). This is fundamentally different

Figure 1. Left panel: TSRT placed below the aperture of the PMOD/WRC blackbody. Right panel: TSRT placed below the aperture of the HSBB. A gold-plated mirror connected to the TSRT reflects the radiation emitted by the cavities to the TSRT.

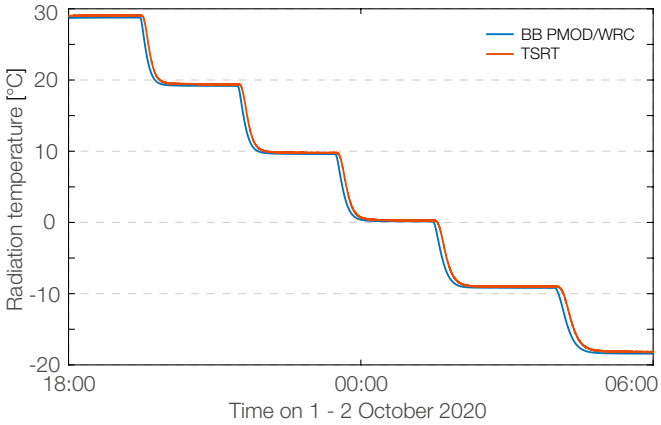

Figure 2. Radiation temperature of the blackbody of PMOD (BB PMOD) and as measured with the PTB radiation thermometer (TSRT PTB).

from most of the blackbody cavities operated with radiometers which have a narrow field-of-view placed at a distance from the cavity aperture. Instead, IRIS and the pyrgeometers need to be mounted directly at the blackbody aperture and sample the hemispherical exitance at the aperture of the blackbody cavity.

The HSBB was explicitly made to accept radiometers with hemispherical acceptance angles. During the campaign, one IRIS and one pyrgeometer were calibrated with the PMOD blackbody using their default calibration procedures. Subsequently, each instrument was placed at the aperture of the HSBB to measure the hemispherical exitance of the HSBB over the temperature range from approx. -20°C to +10°C for the pyrgeometer and from 0°C to +20°C with the IRIS radiometer. The IRIS radiometer was operated continuously at ambient temperature, while the pyrgeometer was instead thermally stabilised to temperatures ranging from -10°C to +20°C. Preliminary results indicate that the radiation measured by IRIS and the CG4 pyrgeometer at the HSBB aperture was within 1 Wm^{-2} of the expected HSBB exitance confirming the excellent agreement between the HSBB and the PMOD/WRC blackbody.

The next steps in the analysis will be to establish the traceability chain from the PMOD/WRC blackbody to the International Temperature Scale (ITS 90) via the PTB radiation temperature scale including a robust uncertainty estimation taking into account all steps in the chain. This work will be continued in the follow-up project, 19ENV07 METEOC-4.

Acknowledgment: The projects 16ENV03 METEOC-3 and 19ENV07 METEOC-4 have received funding from the EMPIR programme co-financed by the Participating States and from the European Union's Horizon 2020 research and innovation programme.

References: Gröbner J.: 2008, Operation and investigation of a tilted bottom cavity for pyrgeometer characterizations, Applied Optics, 47, 4441-4447.

Gröbner J.: 2012, A Transfer Standard Radiometer for atmospheric longwave irradiance measurements, Metrologia, 49, S105-S111.

E-Shape: EuroGEO Showcases: Applications Powered by Europe

Stelios Kazadzis in collaboration with the National Observatory of Athens (Greece), MINES ParisTech (France), Transvalor (France), Centre for Environment and Development for the Arab Region (Egypt)

E-Shape (https://e-shape.eu/) has received funding from the European Union's Horizon 2020 Research and Innovation Programme (April 2019–March 2023) with the aim of bringing together Earth Observation and in-cloud capabilities into services for decision-makers, citizens, industry and researchers. EuroGEO, as Europe's contribution to the Global Earth Observation System of Systems (GEOSS), aims to bring together Earth Observation resources in Europe. In E-Shape, 27 pilot applications under seven thematic areas address societal challenges, foster entrepreneurship and support sustainable development, in alignment to the three main priorities of GEO (SDGs, Paris Agreement and Sendaï Framework).

One of the seven thematic areas in E-Shape is Solar Energy. Three pilot studies were initiated, dealing with: solar radiation and energy forecasting, high photovoltaic penetration in urban scale and wind energy. PMODWRC is leading the “Solar radiation and energy forecasting" pilot that is based on the results of a previous EU funded project: GeoCradle.

The main goal is the development of a short-term forecast (STF) model of solar energy called nextSENSE. This model is based on the use of Cloud Motion Vectors (CMV) and Fast Radiative Transfer Models (FRTM) to forecast Downwelling Surface Solar Irradiation (DSSI). Using near-real-time cloud optical thickness (COT) data derived from multi-spectral images from the Spinning Enhanced Visible and Infrared Imager (SEVIRI) onboard the Meteosat Second Generation (MSG) satellite, we introduce a novel short-term forecasting system (3 hours ahead) which is capable of calculating solar energy in large-scale (1.5 million-pixel areas covering Europe and North Africa) and with a high spatial (5 km over nadir) and temporal resolution (15-minute intervals).

The impact of cloud forecasting uncertainty on DSSI was quantified in terms of the Cloud Modification Factor (CMF), for all sky and clear sky conditions. The forecast accuracy was evaluated against the real cloud images under different cloud motion patterns and the correlation was found to range from 0.9 to 0.5 for 15 minute and 3 hours ahead, respectively. The CMV forecast revealed an overall DSSI uncertainty in the range 18%–34% under consecutive alternations of cloud presence, highlighting the ability of the proposed system to follow the cloud movement in opposition to the baseline persistent (PRS) forecasting. The proposed system aims to support the energy production management of distributed solar plants, as well as electricity handling entities and smart grid operations.

The analysis has revealed that the error from the CMV and PRS models increases with COT, and that the CMV methods are seen to outperform the PRS model for higher COT values. The correlation between the forecasted and the actual data was seen to deteriorate with the increasing forecast horizon (from 15 min to 3 h). A location and temporal-based comparison of the developed CMV model with PRS can determine, in the future, a hybrid approach on using both methods with spatio-temporal based weights, exploiting the advantages of both methods. The comparison of the forecasts with the observed MSG/SEVIRI reference images also showed that the COT-related approach presents a lower error, followed by the CMF-related approach and the PRS, which cannot follow the forecast, especially during cloudy sky conditions. Unfortunately, none of these methods can properly deal with all of the many challenges that exist simultaneously during highly dynamic natural phenomena where the objects have no definitive features (e.g. cloud, water) or many similar features (e.g. orographic cloud streets) (Kosmopoulos et al., 2020).

Acknowledgment: This research was partly funded by the European Commission project EuroGEO e-shape (grant agreement No 820852) and the Excelsior project (grant agreement No 857510).

References: Kosmopoulos P., et al.: 2020, Short-term forecasting of large-scale clouds impact on downwelling surface solar irradiation, Energies 2020, 13, 6555.

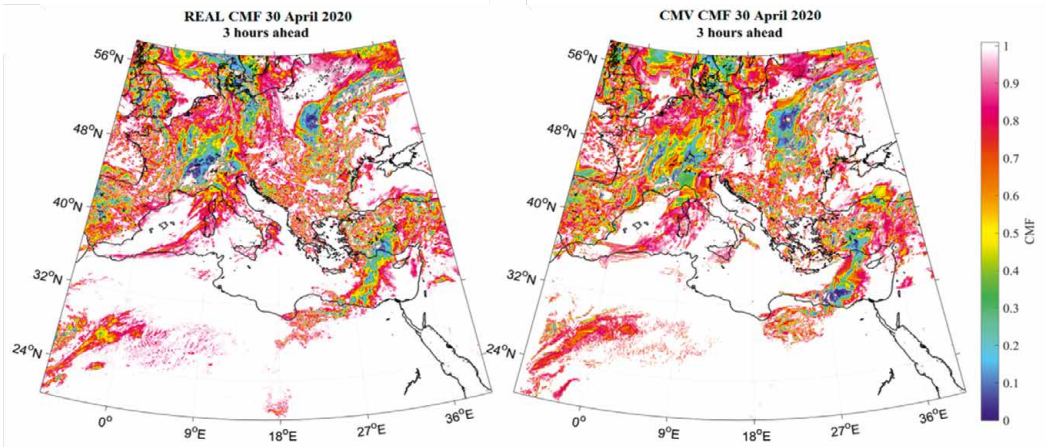

Figure 1. The real (left) and the CMV forecasted (right) CMF map for the 30 April 2020 at 12:15 UTC for 3 hours ahead (12 time-step forecast).

Aerosol Optical Depth Measurements with a Lunar-PFR

Natalia Kouremeti, Stelios Kazadzis, Julian Gröbner, Daniel Pfiffner and Ricco Soder

The growing interest in night-time observations of aerosol optical depth (AOD) led to the development of the Lunar Precision Filter Radiometer (Lunar-PFR) at PMOD/WRC. The instrument has been in operation since 2014, monitoring AOD during the polar winter at Ny-Ålesund, Norway within the framework of the SIOS project, while the rest of the year it is operated at PMOD/WRC. The instrument participated in two intercomparison campaigns in 2020, where the agreement with the CIMEL instruments was re-confirmed during different operational conditions and aerosol loads.

Atmospheric aerosols are known to impact the climate, but they still represent one of the largest uncertainties in climate change studies. Night-time AOD measurements could provide valuable information for the climatology of aerosols at high latitude stations, where direct sun measurements are not possible throughout the year. For example, in the northern hemisphere they can be used for monitoring the arctic (aerosol) haze during polar winter.

The Lunar Precision Filter Radiometer (Lunar-PFR) is a standard PFR instrument that has been developed at PMOD/WRC, and is based on experience from the solar PFR with enhanced sensitivity. It measures at four wavelengths 412 nm, 500 nm, 675 nm and 865 nm, while the sensor is temperature stabilised at 20°C. The instrument has been characterised three times during the last 5 years using the radiometric calibration laboratory facilities at PMOD/WRC, and shows excellent stability within 1%. In addition, a more detailed characterisation of the spectral response of the filters was performed in June 2020.

In the Polar-AOD Retreat (U.S., May 2019), due to the need for more intercomparison campaigns it was decided to investigate the current level of agreement between lunar and star photometers, after experience was gathered during the 1st campaign in 2017 (Barreto et. al., 2019).

The Polar-AOD community, with the support of the SIOS project, organised the 2nd intercomparison campaign for night-time AOD retrievals at Ny-Ålesund, Svalbard, Norway (78.9°N, 11.9°E), from February to March 2020, with the participation of one CIMEL (UVA, AEMET), the Lunar-PFR (PMOD/WRC), a starphotometer and two Lidars (AWI), and the prototype CLIDAR (NOAA) for the first lunar cycle. The Prede-POM (operated by ISAAC) photometer joined the campaign in the second cycle.

The third campaign, SCILLA (Summer Campaign for Intercomparison of Lunar measurements of Lindenberg's Aerosol) was organised by the German Meteorological Service (Deutscher Wetterdienst; DWD), Lindenberg in August to September 2020. Six lunar photometers and one starphotometer participated in total. DWD provided all auxiliary data pressure, ozone, and aerosol profiles from ceilometers and radiosondes.

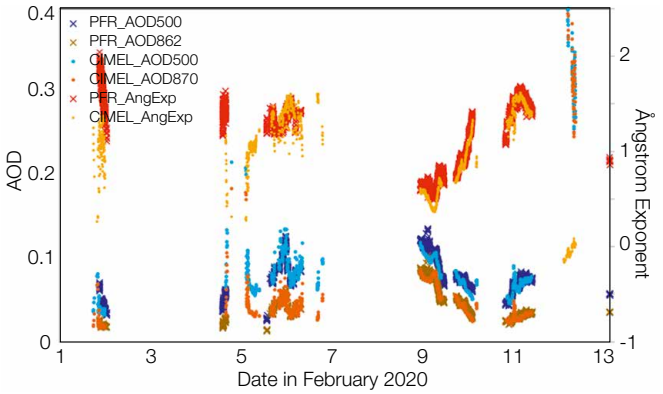

Figure 1. Night-time aerosol measurements at 500 nm, 862 nm and the Ångström exponent from the participating instruments, Cimel and Lunar-PFR, for the February 2020 lunar cycle at Ny-Ålesund.

The agreement of the Lunar-PFR with the CIMEL instruments was within 0.01 for the common wavelengths. The comparison results in both campaigns have been improved since Izaña 2017, due to the dark correction of the CIMEL and the higher aerosol loads in both Ny-Ålesund and Lindenberg.

Both sites were challenging for the cloud screening algorithms of the participating photometers, especially the depiction of polar stratospheric clouds at Ny-Ålesund, which was verified from the Lidar systems. Such results provided valuable information for filtering out these cloud contamination events in the night-time AOD measured by the Lunar-PFR over the 2014–2020 period.

The data sets from both campaigns are being further analysed to include the participating star-photometers and profiling instruments.

Acknowledgments: These activities have received funding from the EMPIR programme co-financed by the Participating States and from the European Union's Horizon 2020 research and innovation programme through project 19ENV04 MAPP.

"Svalbard Integrated Arctic Earth Observing System Infrastructure development of the Norwegian node" (SIOS) (2018-2022) as well as the extended activities of WORCC.

References:

Barreto A., et. al.: 2019, Evaluation of night-time aerosols measurements and lunar irradiance models in the frame of the first multi-instrument nocturnal intercomparison campaign, Atmospheric Environment, 202, p.190-211 , doi.org/10.1016/j.atmosenv.2019.01.006

Kouremeti N., Kazadzis S., Mazzola M., Hansen G., Stebel K., Gröbner J.: 2018, Development and aerosol optical depth measurements with a Lunar photometer at Ny-Ålesund, Polar conference, June 2018, Davos.

Long-Term Measurements of Total Ozone Column with the Koherent System at PMOD/WRC Davos

Luca Egli, Julian Gröbner, and Herbert Schill in collaboration with Meteoswiss

Within the Swiss Global Atmosphere Watch project, INFO3RS, the new system Koherent to monitor total ozone column (TOC) was developed at PMOD/WRC. The aim of the new instrument is to measure TOC with traceable full solar spectrum measurements. Data from more than one year of synchronous measurements with the Brewer 156 double monochromator instrument is compared with Koherent. The comparison shows that TOC from Koherent is in good agreement with Brewer 156 (within 0.23%), however, with a strong seasonal variation of ±1.4% due to changes of the stratospheric temperature. The stratospheric temperature will be considered in a future version of the retrieval algorithm.

The Koherent system consists of the commercially available array spectroradiometer BTS-2048-UV-S-F connected by a fibre to a lens based telescope (Egli and Gröbner, 2018). Measurements from Koherent were acquired with a 1-min resolution over the period from 1 October 2019 to 9 February 2021. Virtually no technical failures occurred and therefore very low operational maintenance was needed. The system was calibrated for absolute irradiance in the PMOD/WRC laboratory facilities.

The raw data was post-processed by: 1) converting the raw data into calibrated absolute irradiance, 2) correcting for the wavelength-shift using the PMOD/WRC Matshic software, and 3) retrieving TOC with a least squares fitting algorithm with the following settings and input parameters:

- Wavelength range: 305 nm to 350 nm
  Extraterrestrial spectrum: QASUMEFTS (Gröbner et al., 2017).
- Ozone absorption cross-section: IUP, measured by the University of Bremen in 2013 (Serdyuchenko et al., 2013).
- Stratospheric temperature: -45°C.
- Linear aerosol optical depth parameterisation.

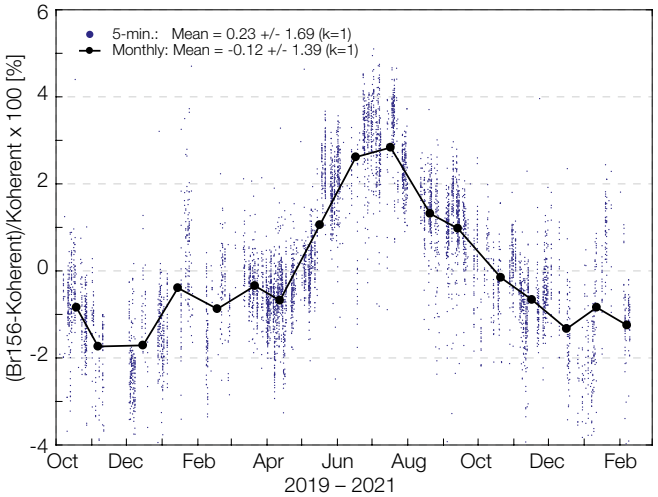

Figure 1. Relative differences of total ozone column between Brewer B156 and Koherent using the full spectrum ozone retrieval with the IUP cross-section for Koherent and the standard Brewer retrieval with the IUP cross-section corrected for stratospheric temperature.

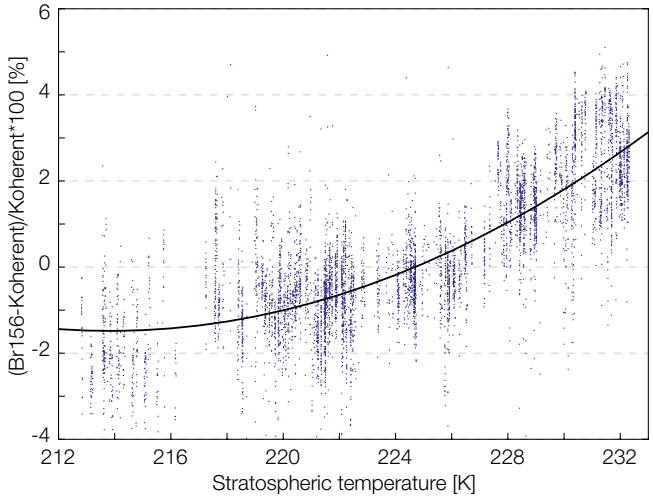

Figure 2. Stratospheric temperature dependency of the relative differences of total ozone column between Brewer B156 and Koherent, revealing a temperature sensitivity of about 0.28%/K.

TOC retrieved by Koherent and Brewer 156 is compared using the IUP ozone absorption cross-section accounting for stratospheric temperature. See: "Consistency of total ozone column measurements between the Brewer and Dobson spectroradiometers of the LKO Arosa and PMOD/WRC Davos" on page 41.

Figure 1 presents the relative difference between Brewer B156 and Koherent for the period of the comparison. The long-term comparison reveals an average offset of only 0.23%, however, with a strong variation of ±1.7% for the individual measurements and ±1.4% for monthly means. The monthly variability indicates the seasonal dependency due to changes in stratospheric temperature. Figure 2 shows the dependency of the seasonal variation on stratospheric temperature of about 0.28%/K, highlighting the sensitivity of Koherent TOC to this parameter. The sensitivity on stratospheric temperature may allow this parameter to be retrieved by a least squares fit algorithm or it needs to be considered as an input parameter, in a future version of the Koherent traceable full spectrum retrieval.

Acknowledgment: The study was partly funded by the ESA project QA4EO, No. QA4EO/SER/SUB/09 and by the project INFO3RS funded by MeteoSwiss, grant number 123001926.

References:

Gröbner J., et al.: 2017, The high-resolution extraterrestrial solar spectrum (QASUMEFTS) determined from ground-based solar irradiance measurements, Atmos. Meas. Tech., 10, 3375-338.

Serdyuchenko A., et al.: 2013, High spectral resolution ozone absorption crosssections – Part 2: Temperature dependence, Atmos. Meas. Tech. Discuss., 6, 6613-6643, doi:10.5194/amtd-6-6613-2013

Egli L., Gröbner, J.: 2018, A novel array-spectrometer system for Total Column Ozone retrieval, Annual Report 2018, PMOD/WRC, Davos.

The International Network to Encourage the Use of Monitoring and Forecasting Dust Products: InDust COST Action

Stelios Kazadzis in collaboration with inDust partners

The "International Network to Encourage the Use of Monitoring and Forecasting Dust Products" (inDust) is the COST Action CA16202 (2017-2021). The overall objective of inDust is to establish a network, involving research institutions, service providers and potential end-users of information, about airborne aerosol dust particles (https://cost-indust.eu/).

Amongst the most significant extreme meteorological phenomena are Sand and Dust Storms (SDS). Due to SDS, significant amounts of airborne mineral dust particles are generated and they have impacts on climate, the environment, human health, and many socio-economic sectors (e.g. aviation, solar energy, agriculture). Several studies and reports have mentioned that society has to understand, manage and mitigate the risks and effects of SDS on life, health, property, the environment and the economy in a more unified way.

Towards this direction, the EU-funded InDust project, has an overall objective to establish a network, involving research institutions, service providers and potential end-users, about airborne dust information. Participants consist of a multidisciplinary group of international experts on aerosol measurements, aerosol modelling, stakeholders and social scientists working together, exchanging ideas to better coordinate and harmonise the process of transferring dust observation and prediction data to users, as well as to assist the diverse socio-economic sectors affected by the presence of high concentrations of airborne mineral dust (Nemuc et al., 2020).

A video produced by InDust describing SDS effects can be found here: https://www.youtube.com/watch?v=SdMLm5Xajv4&list=PLbABsNMD2jhyiShk74M7jDlYWjr874Hwu&index=6

The main InDust objectives are to:

- Establish a network of scientific knowledge and services about airborne dust.
- Identify and exploit dust monitoring observations (from both ground-based and satellite platforms).
- Identify and exploit dust forecast products best suited to be transferred/tailored to the needs of end-users.
- Build capacity through the high-level teaching of end-users in order to promote the use of the delivered dust products.
- Enhance the cooperation with institutions from near-neighbouring and international partner countries in Northern Africa and the Middle East, and to involve them in the European-driven climate change science and mitigation/adaptation strategies.

The InDust COST Action is active through a range of networking tools, such as workshops, conferences, training schools, short-term scientific missions (STSMs), and dissemination activities.

For more information: www.youtube.com/playlist?list=PLbABsNMD2jhyiShk74M7jDlYWjr874Hwu

Acknowledgment: We would like to acknowledge the contribution of the COST (European Cooperation in Science and Technology) Action: InDust (CA16202). COST (European Cooperation in Science and Technology) is a funding agency for research and innovation networks.

References: Nemuc A., Basart S., Tobias A., Nickovic S., Barnaba F., Kazadzis S., Monteiro A.: 2020, International Network to Encourage the Use of Monitoring and Forecasting Dust Products (InDust), European Review, 1-15, doi:10.1017/S1062798720000733

Figure 1. InDust summary. Credit: inDust COST action, CA16202.

Stability of Three Precision Solar Spectroradiometers over the 2019–2021 Period

Natalia Kouremeti, Julian Gröbner, and Stelios Kazadzis

The 24-month performance of the three Precision Spectroradiometers (PSR), PSR008, PSR009, and PSR010, is presented. Absolute direct sun spectral measurements have been used to retrieve spectral Aerosol Optical Depth (AOD) measurements at Davos over the 315–1030 nm wavelength range. The measurements have been compared with the WORCC Precision Filter Radiometer (PFR) reference sunphotometers at seven common spectral channels.

The Precision Solar Spectroradiometer (PSR) is a grating-type array spectroradiometer, designed for high precision and accurate measurements of direct normal spectral solar irradiance in the approximate 315–1030 nm wavelength range. Each PSR is radiometrically characterised and calibrated in the optical laboratory of PMOD/WRC.

A series of three PSR (PSR-Triad) have been operating at PMOD/WRC since the beginning of 2019 with the long-term objective of expanding the World Optical depth Research and Calibration Center (WORCC) services over the PSR wavelength range. The main difference of these three PSR instruments is that the suppression of 2nd and 3rd dispersion orders is no longer realised with the aid of a cut-off filter in front of the detector. Instead, they are removed explicitly with the stray-light correction matrix determined for each instrument using a tunable laser system.

The expanded relative uncertainty for spectral solar irradiance measurements in the 400–1000 nm range is between 1.7% and 2.0%, with larger uncertainties below 400 nm which are mainly caused by the low signal levels (Gröbner and Kouremeti, 2019).

Working towards the traceability of aerosol optical depth (AOD), the spectral AOD is retrieved using the direct solar irradiance in $Wm^{-2}nm^{-1}$ and the extraterrestrial spectrum (ETS) QASUMEFTS (Gröbner et al., 2017) (300–500 nm) and Thuillier et al. (2003) (500–1030 nm) convolved with the PSR line-spread functions. The AOD product of the PSRs is evaluated against the World AOD reference, realised by three Precision Filter Radiometers (PFRs) with centre wavelengths at 368 nm, 412 nm, 500 nm, and 862 nm. Additional wavelengths are available at 675 nm, 778 nm, and 1024 nm in supplementary PFRs.

The AOD comparison under the pristine environment of Davos is sensitive to small instrumental changes, and therefore provides additional information about the stability of the PSR over the full spectral range for the operational period. In Figure 1, the AOD comparison between the PSRs and the PFR-TRIAD at 500 nm is illustrated.

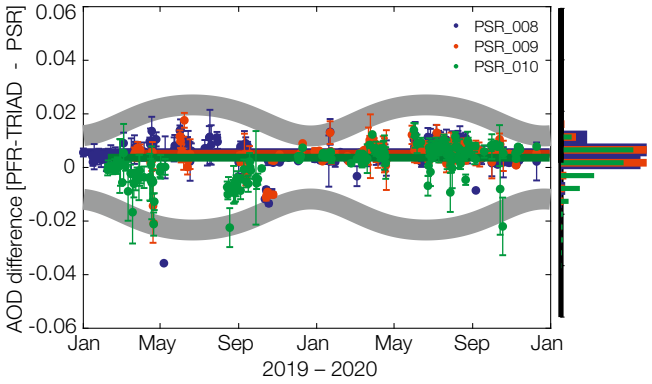

Figure 1. AOD comparison between the PSRs #008 (blue), #009 (red), #010 (green) and the PFR-TRIAD at 500 nm, shown as daily mean differences. The median differences of more than 30500 points are 0.006, 0.005, 0.004, respectively, with a spread (2σ) of 0.013.

The AOD differences between the SI-traceable and Langley-based retrievals at this wavelength, are within the WMO limits for instrument agreement and is better than 92% for all PSRs. The spread of the distributions is less than 0.015 which is better than 1.5% (2σ) when translated in spectral stability, for a period of 24-months where more than 30,500 common measurements were compared.

Acknowledgments: These activities have received funding from the EMPIR programme co-financed by the Participating States and from the European Union's Horizon 2020 research and innovation programme through project 19ENV04 MAPP and by the ESA project QA4EO, No. QA4EO/ SER/ SUB /09.

References:

Gröbner J., Kouremeti N.: 2019, The Precision solar Spectroradiometer (PSR) for direct solar irradiance measurements, Solar Energy 185, 199-210.

Gröbner J., et al.: 2017, The high-resolution extraterrestrial solar spectrum (QASUMEFTS) determined from ground-based solar irradiance measurements, Atmos. Meas. Tech., 10, 3375-3383.

Thuillier G., et al.: 2003, The Solar Spectral Irradiance from 200 to 2400 nm as Measured by the SOLSPEC Spectrometer from the Atlas and Eureca Missions, Sol. Phys., 214, 1-22.

Extending the Calibration Traceability of Longwave Radiation Time-Series (ExTrac)

Stephan Nyeki and Julian Gröbner in collaboration with MeteoSwiss (Switzerland), European Commission Joint Research Centre (Ispra, Italy), Alfred Wegener Institute (Bremerhaven and Potsdam, Germany)

The Earth's surface radiation budget plays a crucial role in the climate system, and accurately characterising components of the radiation budget is therefore an important task. The Baseline Surface Radiation Network (BSRN) is an archive of high quality traceable data going back to the early 1990s. The main objective of ExTrac is to develop methodologies to provide traceability of BSRN longwave measurements to the World Infrared Reference (WISG) hosted by the Infrared Radiometry Section of the World Radiation Center.

The Baseline Surface Radiation Network (BSRN; bsrn.awi.de; Ohmura et al., 1998) is one of several international networks to coordinate the measurement and archiving of surface radiation data. Amongst other parameters, longwave surface radiation time-series using pyrgeometers from BSRN stations are also archived. Many of these time-series are traceable to the World Infrared Standard Group of pyrgeometers (WISG), established in 2004 and maintained by PMOD/WRC. Although this has led to better global homogenisation of longwave time-series and has increased their reliability and accuracy, a number of traceability and instrumental issues still remain to be resolved by the research community.

The first aspect concerns the submission of longwave radiation data to the BSRN archive that may not be traceable to the WISG. In addition, BSRN has not archived a comprehensive set of raw pyrgeometer data, necessary to reprocess measurements with updated calibration coefficients. The second aspect concerns the WISG reference scale whose traceability to SI is under investigation (e.g. Gröbner et al., 2014; Nyeki et al., 2017). The ExTrac project is focused on developing a methodology that can be applied to archived BSRN longwave radiation data to reprocess longwave data from the BSRN archive without access to the original raw measurements. The aim is to prevent the loss of legacy data and ensure their availability for future use when traceability and instrumental issues (e.g. CIMO, 2018) in this field have been resolved.

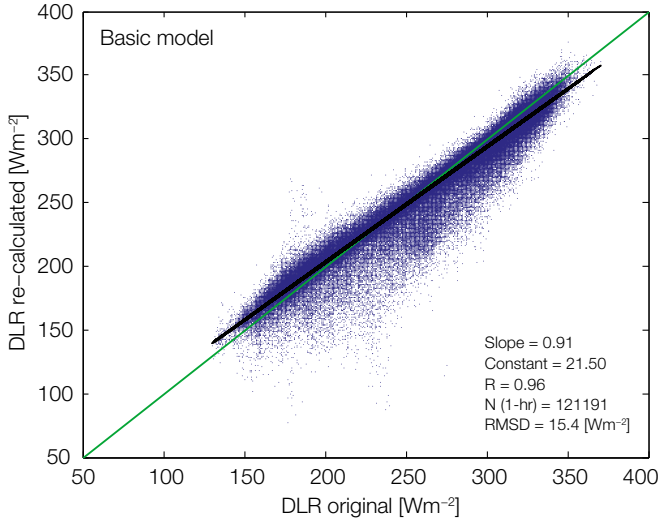

Figure 1. Basic model: Downward longwave radiation (DLR) data from the Ny-Ålesund (Svalbard) BSRN station for the 2006 – 2019 period. Original DLR data from Eppley PIR pyrgeometers is compared with re-calculated DLR. The root-mean-square-deviation (RMSD) is calculated with respect to DLR original.

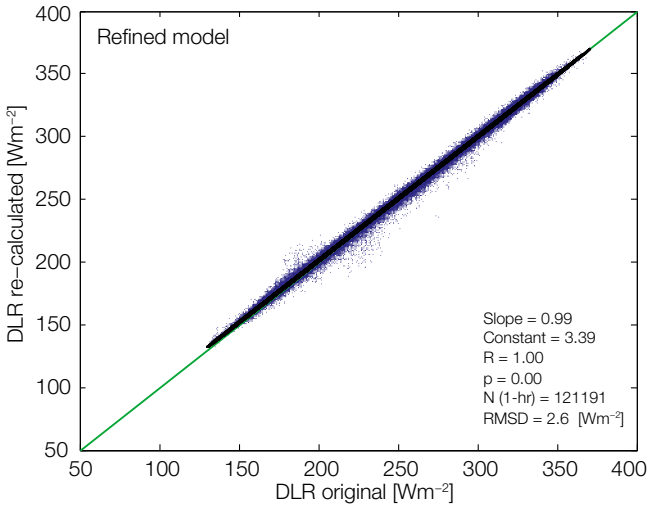

Figure 2. Refined model: Similar to the basic model but further refined by correcting T_{2m} using 1-hr values of: i) downward shortwave radiation, ii) wind speed at 2 m height, and iii) cloud fraction.

In principle, part or all of the raw data (pyrgeometer voltage, and body (T_b) and dome (T_d) temperatures) can be recovered. However, this is not a trivial task as the equation to determine longwave radiation is non-linear. Raw data from a number of BSRN stations has been acquired to develop a methodology. Figure 1 illustrates how downward longwave radiation (DLR) from Ny-Ålesund (Svalbard) can be recovered when using ambient temperature at 2 m above ground (T_{2m}) as a proxy for T_b and T_d. When compared to original DLR data for 2006–2019, the root-mean-square-deviation (RMSD) is ~15.4 Wm^{-2}. This value is higher than the expanded uncertainty (coverage k=2) of DLR measurements (~±4.0 Wm^{-2}). An updated model (Figure 2) has decreased RMSD to ~2.6 Wm^{-2} which is ~5.2 Wm^{-2} for k=2, and is a good basis for further development.

ExTrac has prioritised the analysis of long time-series (e.g. Payerne, Switzerland), as well as data from polar regions (Ny-Ålesund, Svalbard; Neumayer station, Antarctica). As a next step, data from Payerne will be analysed.

Acknowledgment: We thank GCOS Switzerland for financially supporting this project.

References:

CIMO: (2018), Commission for Instruments and Methods of Observation, CIMO-17, WMO, Amsterdam, 12-16 Oct. 2018.

Gröbner J., et al: 2014, J. Geophys. Res. Atmos., 119, doi:10.1002/2014JD021630

Nyeki S., et al.: 2017, Atmos. Meas. Tech., 10, 3057-3071, doi.org/10.5194/amt-10-3057-2017

Ohmura A., et al.: 1998, BAMS, 79, 2115-2136, www.jstor.org/stable/26214877

Publications and Media

Refereed Publications

Aebi C., Gröbner J., Kazadzis S., Vuilleumier L., Gkikas A., Kämpfer N.: 2020, Estimation of cloud optical thickness, single scattering albedo and effective droplet radius using a shortwave radiative closure study in Payerne, Atmos. Meas. Tech., 13, 907-923, doi.org/10.5194/amt-13-907-2020

Antonucci E., Harra L., Susino R., et al.: 2020, Observations of the Solar Corona from Space, Space Science Reviews, 216, 117, doi:10.1007/s11214-020-00743-1

Auchère F., Andretta V., Antonucci E., et al.: 2020, Coordination within the remote sensing payload on the Solar Orbiter mission, Astron. Astrophys., 642, A6. doi:10.1051/0004-6361/201937032

Barczynski K., Aulanier G., Janvier M., Schmieder B., Masson S.: 2020, Electric Current Evolution at the Footpoints of Solar Eruptions, Astrophys. J., 895, id.18, 21 pp., doi:10.3847/1538-4357/ab893d

Barras E., Haefele A., Nguyen L., Tummon F., Ball W., Rozanov E., Rüfenacht R., Hocke K., Bernet L., Kämpfer N., Nedoluha G., Boyd I.: 2020, Study of the dependence of long-term stratospheric ozone trends on local solar time, Atmos. Chem. Phys., 20, 8453-8471, doi:10.5194/acp-20-8453-2020

Bessarab F.S., Sukhodolov T.V., ... Rozanov E.V.: 2020, Ionospheric response to solar and magnetospheric protons during January 15-22, 2005: EAGLE whole atmosphere model results, Adv. Space Res., doi.org/10.1016/j.asr.2020.10.026

Carlesso F., ... Remesal Oliva A., Finsterle W., et al.: 2020, Physical and optical properties of ultra-black nickel-phosphorus for a total solar irradiance measurement, Astrophys. J. Supp. Series, 248, id.4, 10 pp., doi:10.3847/1538-4365/ab7af8

Clyne M., ... Ball W., Rozanov E., Sukhodolov T.: 2020, Model physics and chemistry causing intermodel disagreement within the VolMIP-Tambora Interactive Stratospheric Aerosol ensemble, Atmos. Chem. Phys. Discuss., doi: 10.5194/acp-2020-883

Criscuoli S., Rempel M., Haberreiter M., et al.: 2020, Comparing radiative transfer codes and opacity samplings for solar irradiance reconstructions, Sol. Phys. 295, 50, doi.org/10.1007/s11207-020-01614-2

Egorova T., Rozanov E., Arsenovic P., Sukhodolov T.: 2020, Ozone layer evolution in the early 20th century, Atmosphere, 11, 169, doi: 10.3390/atmos11020169

Fountoulakis I., Diémoz H., Siani A.M., Hülsen G., Gröbner J.: 2020, Monitoring of solar spectral ultraviolet irradiance in Aosta, Italy, Earth Syst. Sci. Data, 12, 2787–2810, doi.org/10.5194/essd-12-2787-2020

Gkikas A., Proestakis E., Amiridis V., Kazadzis S., Di Tomaso E., Tsekeri A., Marinou E., Hatzianastassiou N., Pérez García-Pando C.: 2020, ModIs Dust AeroSol (MIDAS): A global fine resolution dust optical depth dataset, Atmos. Meas. Tech. Discuss., doi.org/10.5194/amt-2020-222

Golubenko K., Rozanov E., Mironova I., Karagodin A., Usoskin I.: 2020, Natural sources of ionization and their impact on atmospheric electricity, Geophysical Research Letters, 47, doi:10.1029/2020GL088619

Harra L., Matthews S., Long D., et al.: 2020, Locating hot plasma in small flares using spectroscopic overlappogram data from the Hinode EUV imaging spectrometer, Solar Physics, 295, 34, doi:10.1007/s11207-020-01602-6

Hülsen G., ... Gröbner J.: 2020, Second Solar Ultraviolet Radiometer Comparison Campaign UVC-II, Metrologia, 57035501, doi.org/10.1088/1681-7575/ab74e5

Karagodin-Doyennel, A., Rozanov E., ... Ball W.: 2020, The response of mesospheric H_2O and CO to solar irradiance variability in models and observations, Atmos. Chem. Phys. Discuss., doi: 10.5194/acp-2020-793

Koenigsberger G., Schmutz W.: 2020, The nature of the companion in the Wolf-Rayet system EZ Canis Majoris, Astron. Astrophys., 639, A18 (16 pp), doi: 10.1051/0004-6361/201937305

Kuai L., ... Rozanov E.: 2020, Attribution of Chemistry-Climate Model Initiative (CCMI) ozone radiative flux bias from satellites, Atmos. Chem. Phys., 20, 281-301, doi: 10.5194/acp-20-281-301

Lakkala, K., et al.: 2020, Validation of the TROPOspheric Monitoring Instrument (TROPOMI) surface UV radiation product, amt.copernicus.org/articles/13/6999/2020

Lakkala K., ... Hülsen G.: 2020, Datasets of UV irradiance, visible and photosynthetically active radiation in Marambio, Antarctica from March 2017 to May 2019, Earth Syst. Sci. Data, doi.org/10.5281/zenodo.3688700

Martinez Pillet V., Tritschler A., Harra L., et al.: 2020, Solar physics in the 2020s: DKIST, parker solar probe, and solar orbiter as a multi-messenger constellation, arXiv:2004.08632

Masoom A., ... Kazadzis, S.: 2020, Solar energy estimations in India using remote sensing technologies and validation with sun photometers in urban areas, Remote Sens., 12, 254.

Mierla M., D'Huys E., West M.J., Seaton A., Berghmans D., Podladchikova E.: 2020, Long-term evolution of the solar corona using PROBA2 data, Solar Physics, 295, 5, 10.1007/s11207-020-01635-x

Müller D., … Harra L.K., et al.: 2020, The Solar Orbiter mission, Science overview, 2020, Astron.Astrophys., 642, A1. doi:10.1051/0004-6361/202038467

Nakajima T., ... Kazadzis S., Kouremeti N., et al.: 2020, An overview of and issues with sky radiometer technology and SKYNET, Atmos. Meas. Tech., 13, 4195-4218, doi.org/10.5194/amt-13-4195-2020

Nemuc A., Basart S., Tobias A., Nickovic S., Barnaba F., Kazadzis S., Monteiro A.: 2020, International network to encourage the use of monitoring and forecasting dust products (InDust), European Review, 1-15. doi:10.1017/S1062798720000733

Nicely J., ... Rozanov E., et al.: 2020, A machine learning examination of hydroxyl radical differences among model simulations for CCMI-1, Atmos. Chem. Phys., 20, 1341-1361, doi: 10.5194/acp-20-1341-2020

Pavanello D., ... Kouremeti N., Gröbner J., et al.: 2020, Results of the IX International Spectroradiometer Intercomparison and impact on precise measurements of new photovoltaic technologies, Prog. Photovol., doi.org/10.1002/pip.3347

Podladchikova O., Harra L., Barczynski K., et al.: 2020, Stereoscopic measurements of corona doppler velocities with SPICE, arXiv:2008.08704

Raptis I.-P., Kazadzis S., Amiridis V., Gkikas A., Gerasopoulos E., Mihalopoulos N.: 2020, A decade of aerosol optical properties measurements over Athens, Greece, Atmosphere, 11, 154.

Rast M.~P., Bello González N., Bellot Rubio L., ...Harra L.K.…., et al.: 2020, Critical science plan for the Daniel K. Inouye Solar Telescope (DKIST), arXiv:2008.08203

Rochus P., Auchère F., Berghmans D., Harra L.K., et al.: 2020, The Solar Orbiter EUI instrument: The Extreme Ultraviolet Imager, Astron. Astrophys., 642, A8, doi:10.1051/0004-6361/201936663

Rouillard A.P., … Haberreiter M., et al.: 2020, Models and data analysis tools for the Solar Orbiter mission, Astron. Astrophys., 642, A2, doi.org/10.1051/0004-6361/201935305

Rozanov E.: 2020, Preface: Ozone evolution in the past and future, Atmosphere, 11(7), 709, doi:10.3390/atmos11070709

Savoska S., ... Rozanov E., et al.: 2020, Toward the creation of an ontology for the coupling of atmospheric electricity with biological systems, Int. J. Biometeorol., doi: 10.1007/s00484-020-02051-3

SPICE Consortium, Anderson M., …Gyo M., Haberreiter M., et al.: 2020, The Solar Orbiter SPICE instrument – An extreme UV imaging spectrometer, Astron. Astrophys., 642, A14, doi.org/10.1051/0004-6361/201935574

Usoskin I.G., Koldobskiy S.A., Kovaltsov G.A., Rozanov, E.V., Sukhodolov T.V., Mishev A.L., Mironova I.A.: 2020, Revisited reference solar proton event of 23 February 1956: Assessment of the cosmogenic-isotope method sensitivity to extreme solar events. J. Geophys. Res., Space Physics, 125, doi: 10.1029/2020JA027921

Velli M., Harra L.K., Vourlidas A., et al.: 2020, Understanding the origins of the heliosphere: integrating observations and measurements from Parker Solar Probe, Solar Orbiter, and other space- and ground-based observatories, Astron. Astrophys., 642, A4, doi:10.1051/0004-6361/202038245

Visioni D., ... Rozanov E., et al.: 2020, Seventeen years of ozone sounding at L'Aquila, Italy: evidence of mid-latitude stratospheric ozone recovery and tropospheric profile changes, Atmos. Chem. Phys. Discuss, doi: 10.5194/acp-2020-525

West M.J., Kintziger C., Haberreiter M., Gyo M., Berghmans D., Gissot S., Büchel V., Golub L., Shestov S., Davies J.A.: 2020, LUCI onboard Lagrange, the next generation of EUV space weather monitoring, J. Space Weather Space Clim., 10, 49, doi.org/10.1051/swsc/2020052

Woods M.M., Inoue S., Harra L.K., et al.: 2020, Serial flaring in an active region: Exploring why only one flare is eruptive, ApJ, 890, 84. doi:10.3847/1538-4357/ab6bc8

Zouganelis I., …. Harra L.K., et al.: 2020, The Solar Orbiter Science Activity Plan. Translating solar and heliospheric physics questions into action, 2020, Astron. Astrophys., 642, A3, doi:10.1051/0004-6361/202038445

Non-Refereed Publications (only with doi number)

Mironova I., Sinnhuber M., Rozanov E.: 2020, Energetic electron precipitation and their atmospheric effect, E3S Web Conf. 196 01005, doi: 10.1051/e3sconf/202019601005

Shimizu T., ... Harra, L., The Solar-C (EUVST) mission: the latest status, 2020, SPIE, 114444, dx.doi.org/10.1117/12.2560887

Walter B., Andersen B. Beattie A., Finsterle W., Kopp G., Pfiffner D., Schmutz W.: 2020, First TSI results and status report of the CLARA/NorSat-1 solar absolute radiometer, Astronomy in Focus, presented at IAU General Assembly, Vienna, Austria, IAU Proc., pp. 358-360, doi:10.1017/S1743921319004617

Media - Selection of Highlights

21 Jan. 2020. “Solar Orbiter - Der Countdown hat begonnen“, newspaper item in the Davoser Zeitung, Switzerland.
https://www.pmodwrc.ch/wp-content/uploads/2020/02/PressArticle_20200121_DZ.pdf

29 Jan. 2020. “Sonnen-Mission bringt Davos ins Weltall“, newspaper item in the Südostschweiz Zeitung, Switzerland.
https://www.pmodwrc.ch/wp-content/uploads/2020/02/PressArticle_20200129_SO.pdf

31 Jan. 2020. “Solar Orbiter - noch acht Tage bis zum Start“, newspaper item in the Davoser Zeitung, Switzerland.
https://www.pmodwrc.ch/wp-content/uploads/2020/02/PressArticle_20200131_DZ.pdf

7 Feb. 2020. “Was uns das Sonnenwetter angeht“, newspaper item in the Tagesanzeiger, Switzerland.
https://www.pmodwrc.ch/wp-content/uploads/2020/02/PressArticle_20200207_TA.pdf

7 Feb. 2020. “Ein bisschen Davos fliegt zur Sonne“, SRF TV, Switzerland.
https://www.srf.ch/play/tv/schweiz-aktuell/video/ein-bisschen-davos-fliegt-zur-sonne?id=d91dcbb8-eea0-47bd-9125-180be80e4f29

9 Feb. 2020. “What is Solar Orbiter and what’s it going to do?”, BBC TV, United Kingdom, interview with Louise Harra.
https://www.bbc.com/news/av/science-environment-51407501/solar-orbiter-launch-what-is-it-and-what-s-it-going-to-do

Feb. 2020. “Solar Orbiter”, newspaper item in the Belfast Telegraph, Northern Ireland.

Apr. 2020. “Here comes the Sun”, Sky at Night TV programme with Louise Harra, BBC TV, United Kingdom.
https://www.bbc.co.uk/programmes/m000hb4p

11 Apr. 2020. “Hinter den Kulissen des PMOD/WRC: Teil 1, Solar Orbiter“, newspaper item, Davoser Zeitung, Switzerland.
https://www.pmodwrc.ch/wp-content/uploads/2020/04/PressArticle_20200411_DZ.pdf

24 Apr. 2020. “Hinter den Kulissen des PMOD/WRC: Teil 2, Forschen in der Polarnacht“, newspaper item in the Davoser Zeitung, Switzerland.
https://www.pmodwrc.ch/wp-content/uploads/2020/04/PressArticle_20200424_DZ.pdf

22 May 2020. “Erste Bilder der Sonne“, newspaper item in the Davoser Zeitung, Switzerland.
https://www.pmodwrc.ch/wp-content/uploads/2020/05/PressArticle_20200522_DZ.pdf

29 May 2020. “Hinter den Kulissen des PMOD/WRC: Teil 3, Auf unserem Dach messen wir die UV-Strahlung“, newspaper item in the Davoser Zeitung, Switzerland.
https://www.pmodwrc.ch/wp-content/uploads/2020/06/PressArticle_20200529_DZ.pdf

Jun. 2020. SWR, TV programme on “Graubunden”, Germany, Louise Harra and Natalia Kouremeti.
https://www.youtube.com/watch?v=kQJtjZu6lP8

5 Jun. 2020. “Hinter den Kulissen des PMOD/WRC: Teil 4, Genauere Klimaprognosen dank Ozonforschung“, newspaper item in the Davoser Zeitung, Switzerland.
https://www.pmodwrc.ch/wp-content/uploads/2020/06/PressArticle_20200605_DZ.pdf

17 Jun. 2020. Public zoom lecture for Kiev state TV, Ukraine, “Culture and Science”, "Influence of Solar Physics on Everyday Life and the Future" with Olena Podladchikova.

19 Jun. 2020. “Hinter den Kulissen des PMOD/WRC: Teil 5, Warum kümmert uns das Wetter im Weltraum?“, newspaper item in the Davoser Zeitung, Switzerland.
https://www.pmodwrc.ch/wp-content/uploads/2020/06/PressArticle_20200619_DZ.pdf

16 Jul. 2020. “Noch nie wurde die Sonne von so nah fotografiert“, newspaper item in the Tages Anzeiger, Switzerland.
https://www.pmodwrc.ch/wp-content/uploads/2020/07/PressArticle_20200716_Tages_Anzeiger.pdf

16 Jul. 2020, “Raumsonde Solar Orbiter schickt erste Bilder der Sonne“, SRF Tageschau, Switzerland, TV news item.
https://www.srf.ch/play/tv/tagesschau/video/raumsonde-solar-orbiter-schickt-erste-bilder-der-sonne?urn=urn:srf:video:58d7404e-bac5-47cc-aafc-d35299b48a86

16 Jul. 2020. “Closest ever photographs of the Sun reveal super-hot flares near the star's surface”, newspaper item in the Evening Standard, UK.
https://www.pmodwrc.ch/wp-content/uploads/2020/07/PressArticle_20200716_Evening_Standard.pdf

17 Jul. 2020. “Die ersten Bilder sind da“, newspaper item in the Davoser Zeitung, Switzerland.
https://www.pmodwrc.ch/wp-content/uploads/2020/07/PressArticle_20200717_DZ.pdf

22 Jul. 2020. EU research interview with Stelios Kazadzis about E-Shape.
https://www.youtube.com/watch?v=E2EigPN7iAw&t=30s

29 Jul. 2020. “SOHO”, newspaper item in The Register, UK.
https://www.pmodwrc.ch/wp-content/uploads/2020/08/PressArticle_2020729_TheRegister_SOHO.pdf

Administration

Personnel Department

Barbara Bücheler

Difficulties were caused by the corona pandemic for staff, but nonetheless our work carried on. The number of staff at PMOD/WRC increased from 42 to 55 employees. The extra staff are hired to work on new projects such as space projects in the operations and build phases, and new science projects.

One of the biggest events in 2020 was the start of the Solar Orbiter mission, which was classified as one of the 50 most influential engineering projects worldwide. The rocket with Solar Orbiter onboard was launched on 10 February 2020 at 05:03 a.m. (GMT + 1). On 5 February 2020, local people from Davos and the surroundings were invited to the PMOD/WRC for the Solar Orbiter Aperó. We hosted over 160 people. The public in Davos were informed about the event several weeks in advance through advertising in the local press and by means of a projector light-show which illuminated the PMOD/WRC building. We were grateful for the external support of Ms. Christine Huovinen and Ms. Sara Niedermann. The lectures were given by Dr. Julian Gröbner and Dr. Wolfgang Finsterle from the science section and Silvio Koller from the technology department. The culmination of the evening was a live broadcast from Cape Canaveral, Florida, involving Prof. Dr. Harra, Dr. Margit Haberreiter and Manfred Gyo. Our hard-working administration team took care of the food and drinks. The first light data from Solar Orbiter was received by 1,300 media in ESA member states in the summer! The first results of Solar Orbiter were presented in international meetings, for example in December 2020, at the American Geophysical Union (AGU) conference (held virtually).

We continued work on the Lagrange Extreme UV Coronal Imager (LUCI) instrument which is onboard the ESA Space Safety Mission, LAGRANGE, one of our space projects. The aim of this mission is to ensure better space weather forecasting from the Lagrange point, L5. The LUCI instrument will send Extreme UV (EUV) images of the Sun.

With the kick-off meeting on 9 June 2020, the science project EMPIR 19ENV04 MAPP began. Our team included Dr. Julian Gröbner, head of science, Dr. Natalia Kouremeti, Dr. Gregor Hülsen and Dr. Stelios Kazantzis. The goal of the project is to improve methods and instruments towards a better understanding of the contribution of atmospheric aerosols to climate change.

On 25 June 2020, the Swiss Polar Physics Day took place online. This year's meeting of the Board of Trustees was on 3 July 2020 in a modern online format.

The PMOD/WRC Science Day was held on 7 July with 15 presentations from science and technology departments, as well as presentations from students and staff. We repeated this format in December as it was so successful.

In September 2020, Dr. Julian Gröbner, Dr. Stylianos Kazantzis and Dr. Wolfgang Finsterle took part in the 4-day virtual WMO meeting in the Team of Experts for Quality Measurement of Atmospheric Composition (ET-ACQM) and QA Central Facilities (QA-CF).

On 29 September 2020, the measurement campaign with Max Reiniger and Moritz Feierabend from the Physikalisch-Technische Bundesanstalt (PTB, Berlin) took place under the leadership of Dr. Julian Gröbner as part of the EMPIR METEOC 3 project.

We submitted a joint proposal with the Fachhochschule Nordwestschweiz (FHNW) to the Swiss Space Office for our participation in NASA's Solaris mission. On 2 October, the SSO endorsed our participation in the Solar-C mission, which involves building a solar spectral irradiance monitor.

The Joint Total Solar Irradiance Monitor (JTSIM) is going through final testing to prepare for launch in Summer 2021 and will be mounted on the Chinese FY-3E satellite. The main objectives of the FY-3E satellite are to collect atmospheric data for medium and long-term weather forecasting and climate research.

In April, we had to accept that IPC-XIII could not be held in 2020 due to the pandemic restrictions. We also had to cancel the holiday pass that is popular every year for our youngest at the Davos school. However, education did continue online, with Dr. Margit Haberreiter giving a talk at the Swiss Alpine Middle School Davos (SAMD).

We are particularly proud of Christine Aebi, who successfully finished her PhD and now works at the Royal Meteorological Institute of Belgium. On 3 December, 2020, she gave a lecture entitled “On the influence of clouds on the surface radiation budget”.

With the increase in the number of hardware projects, we were able to hire additional staff at PMOD/WRC, and are starting to host ETH MSc project students. We needed additional space and have now obtained this in the former Swiss Institute of Allergy and Asthma Research (SIAF) building, now called ICD (Innovation Center Davos).

Two new instrument scientists were hired to work on spacecraft operations and calibration: Dr. Elena Podladchikova as of February 2020 and Dr. Jean-Philippe Montillet from March 2020.

Dr. Natalia Engler joined in October 2020 to work on the further development of the Cryogenic Solar Absolute Radiometer (CSAR) instrument.

A new ETH PhD student Angelos Karanikolas, joined the WRC-WORCC section in December 2020.

We hosted four MSc and BSc students: Andrea Battaglia completed his MSc at ETH and IRSOL, and is now a PhD student since September 2020 under the supervision of Dr. Sam Krucker (FHNW) and Prof. Dr. Louise Harra. Between May and September 2020, Iga Jôzefiak from the University of Geneva completed a thesis on “Is today's oxygen content optimal for the ozone layer?”. Jakob Föller, an ETH MSc student, successfully completed his master's degree on the subject of "The investigation / improvement of the electrical power measurement by DARA". He now works as a technician. Christina Brodowsky successfully completed her Bachelor's topic: "Modelling volcanic events of the recent past" from February to August 2020.

Daniel Tye, an experienced system engineer, joined us on 1 June 2020 to work on space projects.

We are happy to congratulate Christine Aebi on her successful doctoral examination on 14 December 2020 in Bern. We wish her all the best for successfully completing her doctorate. Bravo!

Congratulations also to our two successful apprentices: Andri Schneider and Yanick Schoch. Andri Schneider completed the commercial secondary school at SAMD and the PMOD/WRC as a businessman "EFZ", and gained his professional diploma with flying colours. Yanick Schoch also completed his electronics technician apprenticeship with a professional Matura and a PMOD/WRC record grade of 5.8. Yanick was nominated to participate in the Swiss Skills competition, where he came 7th in the electronics apprentice category. We wish you both continued success in your private and professional careers.

Unfortunately, Alexandra Sretovic, who had actively supported our administration team during her apprenticeship and business IT studies, left on 31 October 2020 in order to further her career in a new company. We will miss her and wish her good luck for the future.

As of 1 July 2020, Fabrizio Vignali joined as a system administrator in the IT department. Through his support, we were able to technically cover the challenges of the pandemic and expand IT systems. Liviu Zambila joined us in June 2020 as a mechanical engineer, and we are pleased that he will be working in the L5 team.

At this point, we give a big thank you to our civil service workers: Lukas Kessler, Basil Maret, Julian Moosmann, Max Kerschbaumer, Stephan Ernst, Fabian Müller, Tishant Sinnathamby and Florian Zurfluh, whose hard work contributed to our success.

Scientific Personnel

Prof. Dr. Louise Harra	Director, affiliated Prof. at ETH-Zürich, Solar Physics researcher
Prof. Dr. Werner Schmutz	PI DARA/Proba-3 Scientist, physicist
Dr. William Ball	Postdoc, Climate Group, physicist (until 31.01.2020)
Dr. Krzysztof Barczynski	Postdoc, Solar Physics Group, physicist
Dr. Luca Egli	Scientist, WCC-UV and Ozone Sections, physicist
Dr. Tatiana Egorova	Scientist, Climate Group, climate scientist
Dr. Natalia Engler	Instrument Scientist, group WRC-SRS (since 01.10.2020)
Dr. Wolfgang Finsterle	Co-Head WRC, Head WRC-SRS, physicist
Dr. Julian Gröbner	Co-Head WRC, Head WRC-Sections IR radiometry, WORCC, WCC-UV and Ozone Section, physicist
Dr. Margit Haberreiter	Project manager/scientist, L5-LUCI, instrument scientist WRC-SRS.
Dr. Gregor Hülsen	Scientist, WCC-UV Section, physicist
Dr. Stylianos Kazantzis	Scientist, WORCC Section, physicist
Dr. Natalia Kouremeti	Scientist, WORCC Section, physicist
Dr. Jean-Philippe Montillet	TSI instrument scientist, geoscientist (since 01.03.2020)
Dr. Stephan Nyeki	Scientist, IR Radiometry Section, physicist
Dr. Elena Podladchikova	Instrument scientist, Solar Orbiter SPICE and EUI (since 01.02.2020)
Dr. Eugene Rozanov	Scientist, Head of Climate Group, physicist
Herbert Schill	Scientist, Ozone Section, environmental scientist
Dr. Timofei Sukhodolov	Scientist, Climate Group, climate scientist
Arseni Doyennel	PhD student, 2nd year, ETH Zurich
Angelos Karanikolas	PhD student, WRC-WORCC Section (since 01.12.2020)
Alberto Remesal Oliva	PhD student, 5th year, University of Zurich (until 31.08.2020)
Conrad Schwanitz	PhD student, 2nd year, ETH Zurich
Andrea Battaglia	MSc student, FHNW (since 09.2020)
Christina Brodowsky	BSc student, ETH Zurich (02.2020 – 08.2020)
Jakob Föller	MSc student, ETH Zurich (06.2020 – 01.2021)
Iga Józefiak	MSc student, University of Geneva (05.2020 – 09.2020)

Technical Personnel

Silvio Koller	Co-Head Technical Department, Project Manager Space
Daniel Pfiffner	Co-Head Technical Department, Project Manager Space
Lloyd Beeler	Electronics Engineer MSc
Valeria Büchel	Project Manager L5-LUCI
Christian Fringer	Electronics Apprentice, 3rd year
Matthias Gander	Electronics Engineer BSc
Manfred Gyo	Electronics Engineer MSc
Patrik Langer	Mechanical Engineer MSc
Nic Matthes	Polymechanic Apprentice 2nd year
Pascal Schlatter	Mechanic, Head of Workshop, Safety Officer
Yanick Schoch	Electronics Apprentice, 4th year (until 31.07.2020) Electronics Technician (01.08. until 31.12.2020)
Marco Senft	IT System Administrator
Marcel Spescha	Technician Mechanics
Dan Tye	System Engineer Space Projects (since 01.06.2020)
Fabrizio Vignali	IT System Administrator (since 01.07.2020)
Liviu Zambila	Structural Engineer MSc

Technical Personnel within the Science Department

Mark Baker	Technical Employee (since 01.12.2020 until 15.01.2021)
Ricco Soder	Calibration Scientist, Quality Systems Manager
Christian Thomann	Technician
Franz Zeilinger	Technician

Administration

Barbara Bücheler	Head Human Resources / Finances / Administration
Sotirios Filios	Administration, apprentice, 2nd year
Irene Keller	Administration, import/export
Angela Lehner	Administration, book-keeping
Andri Schneider	Administration, intern (until 31.07.2020)
	Administration, book-keeping (01.08.–31.12.2020)
Alexandra Sretovic	Administration, book-keeping (until 31.10.2020)
Christian Stiffler	Accountant
Dario Tannò	Administration, apprentice, 2nd year

Personnel in Arosa

Verena Danuser	Observer and maintenance ozone measurement station (since 01.01.2019)

Caretaker(s)

Maria Sofia Ferreira Pinto	General caretaker, cleaning
Fatima Da Conceicao Alves D.C.	General caretaker, cleaning (back-up)

Civilian Service Conscripts

Lukas Kessler	01.08.2019 – until 31.01.2020
Basil Maret	11.11.2019 – until 05.02.2020
Julian Moosmann	02.09.2019 – 28.02.2020
Max Kerschbaumer	10.02.2020 – 30.04.2020
Stephan Ernst	02.03.2020 – 30.05.2020
Fabian Müller	25.05.2020 – 31.07.2020
Tishant Sinnathamby	13.07.2020 – 14.08.2020
Florian Zurfluh	17.08.2020 – 13.01.2021

Lecture Courses, Participation in Commissions

Louise Harra	Chair of ESA Heliophysics User Archive Committee Member of Board of Reviewing Editors for Science Journal Subject editor for Proceedings of the Royal Society A: Mathematical, Physical & Engineering Sciences Chair of ISSI Science Board Ministerial position on management committee of Armagh Observatory and Planetarium Risk and Audit committee of Armagh Observatory and Planetarium Co-chair of the Scientific Advisory Board of the MPS Member of the ESA Space Science Advisory Council Co-PI of EUV Imager, co-I on SPICE on Solar Orbiter Co-I on the NASA IRIS mission COSPAR 2021, Solar Probe and Solo session co-organiser Convener for AGU 2020, Solar and heliospheric science out of the ecliptic PI of the JAXA Solar-C Spectral Irradiance Monitor Lecture Course in "Astronomical instrumentation", Autumn Semester, ETH Zurich
Werner Schmutz	Honorary Member of the International Radiation Commission (IRC, IAMAS) PI of DARA on Proba-3 Co-I of EUV and SPICE instruments on Solar Orbiter
Wolfgang Finsterle	Chair of ISO-TC180/SC1 (until October 2020) Member of WMO ET-RR
Julian Gröbner	Member of the Expert Team on Atmospheric Composition Measurement Quality and QA-Central facilities (ET-ACMQ) of the WMO, since 2020 Member of the Scientific Advisory Group for Ozone and UV (SAG O3UV) in the Global Atmosphere Watch programme of the WMO (as of 2016) Chair of the Scientific Committee of the Conference "New Developments and Applications in Optical Radiometry" (NEWRAD), since 2014 Member of the Swiss Global Atmosphere Watch (GAW) Programme managed by Meteoswiss, since 2005 Member of the Expert Team on Radiation References (ET-RR) the Standing Committee on Measurements, Instrumentation and Traceability (SC-MINT) of the WMO, since 2014 Member of the Baseline Surface Radiation Network (BSRN) and Chair of the Infrared Working Group, since 2006 Member of the Regional Brewer Scientific Group - Europe (RBCC-E, 2005- ongoing). Chair of WG4, UV Calibration of Brewer spectrophotometers, since 1999 Elected member of the International Radiation Commission (IRS), and Chair of the Working Group on solar UV radiation, IAMAS, since 2009 Member International Ozone Commission (IO3C), IAMAS, since 2016 Lecture course in "Solar Ultraviolet Radiation", WS 2020, ETH Zurich
Eugene Rozanov	Co-chair of SCOSTEP PRESTO Member of SWISS SCOSTEP Committee Member of MDPI “Atmosphere” Journal Editorial board Member of RAS “Physics of the Atmosphere and ocean” Editorial board Swiss representative in European COST CA15211, WG3 leader

Margit Haberreiter	President Swiss Society for Astronomy and Astrophysics Vice President European Geophysical Union Member Swiss National SCOSTEP Committee, Treasurer Topical Editor Annales Geophysicae Member of ESA SWE Network Review Board, 13 November 2020 Member of the UN COPUOS Expert Team on Space Weather Swiss Delegate to WMO's IPT-SWeISS
Stylianos Kazantzis	Member IAMAS International Radiation Commission (since 2020) Member of the WMO Expert Team on Measurement Quality (since 2020) Member Scientific Advisory Group Aerosol (WMO/GAW) (since 2015) GAW-CH Working Group (MeteoSwiss) Editor of Atmospheric Chemistry and Physics Guest Editor Atmospheric Measurement and Techniques (two special issues) Associate Researcher; National Observatory of Athens, Greece – Institute of Environmental Research and Sustainable Development Swiss delegate to the Management Group of Cost 16202 International Network to Encourage the Use of Monitoring and Forecasting Dust Products Working Group, Leader of WG3 Swiss delegate to the Management Group of Cost CA18235 "PROfiling the atmospheric Boundary layer at European scale"
Olena Podladchikova	Evaluator of HORIZON Space and Space Weather programme Evaluator of individual Maria Curie grants Evaluator of NASA NSF scientific programme
Timofei Sukhodolov	Guest editor of the research topic "The evolution of the stratospheric ozone" in Frontiers in Earth Science journal Member of WG3 of SPARC SOLARIS/HEPPA project Member of ISSI group "Relativistic electron precipitation and its atmospheric effect" Member of the SPARC activity "Interactive stratospheric aerosol model intercomparison" (ISA-MIP)
Luca Egli	Member IAMAS International Radiation Commission (since 2016) GAW-CH Working Group (MeteoSwiss)

Public Seminars given at PMOD/WRC (most talks were given online)

09.01.2020 Diego de Pablos Aguero, UCL-MSSL, UK
Linking in-situ measurements to on-disk observations of the Solar atmosphere: Do signatures of dynamical activity in the solar corona remain visible in the Solar Wind?

20.02.2020 Krzysztof Barczynski, PMOD/WRC
Electric current evolution at the footpoints of solar eruptions

19.03.2020 Olena Podlachikova, PMOD/WRC
On the EUV diagnostics of the solar corona from space

09.04.2020 Hugh Hudson, University of Glasgow, UK
The topic of coronal dimming, past and future

23.04.2020 Andrea Francesco Battaglia, ETH Zurich
Origin and evolution of the magnetic swirls in numerical simulations of the solar atmosphere, Swiss Solar Physics seminar series

28.04.2020 David Orozco Suárez, Instituto de Astrofisica de Andalucia, Spain
Photospheric magnetic fields driving solar activity

06.05.2020 Conrad Schwanitz, PMOD/WRC and ETH Zurich
Coronal jets, Swiss Solar Physics seminar series

08.05.2020 Aryeh Feinberg, IAC ETH Zurich
The atmospheric sulphur and selenium cycles: a global model of transport and deposition

14.05.2020 Alphonse Sterling, MSFC, USA
Jets on the Sun

26.05.2020 Thomas Rimmele, NSO, USA
New Results from DKIST

11.06.2020 Scott McIntosh, UCAS, USA
Solar Cycle

24.06.2020 Guillame Aulanier, OBS Paris, France
Building 3-D extensions to the standard solar-flare model

25.06.2020 Swiss Solar Physics Day, 15 talks in 3 hours

07.07.2020 1st PMOD Science Day 1, 17 talks in 3 hours

15.07.2020 Astrid Veronig, University of Graz, Austria
Coronal Dimmings: What they tell us about coronal mass ejections

29.07.2020 Angelos Vourlidas, APL, USA
The mysteries of the inner corona: why do we care?

05.10.2020 Moritz Feierabend, PTB, Germany
A new Blackbody for Improved Traceability of Infrared Radiation Measurements of the Atmosphere

20.10.2020 Robert Wimmer-Schweingruber, University of Kiel, Germany
First Results from the Energetic Particle Detector (EPD) on Solar Orbiter

23.10.2020 Arseniy Karagodin, PMOD/WRC
What is the nature of the ozone hole formation?

03.12.2020 Christine Aebi, Royal Meteorological Institute of Belgium, Belgium
On the Influence of Clouds on the surface radiation budget

04.12.2020 Mike Lockwood, University of Reading, UK
Graphical depictions and descriptions of the solar corona seen in eclipses during the Maunder minimum: what do they tell us about solar magnetic activity?

17.12.2020 2nd PMOD Science Day, 14 talks in 2 hours

Meetings/Event Organisation by PMOD/WRC staff

Jan. 2020	ISSI team,"Exploring the Solar Wind in Regions closer than ever observed before"
25.06.2020	Swiss Solar Physics Day
03.07.2020	Board of Trustees (Stiftungsrat) meeting
07.07.2020	1st PMOD/WRC Science Day
05.09.2020	The World Calibration Center for UV (WCC-UV), at the Expert team Atmospheric Composition Measurement Quality (ET-ACMQ) and QA-Central Facilities meeting, Julian Gröbner
05.09.2020	The World Optical Depth Research and Calibration Center (WORCC) at the Expert team Atmospheric Composition Measurement Quality (ET-ACMQ) and QA-Central Facilities meeting
28.09.2020	Karbacher Foundation meeting at PMOD/WRC
29.09.2020	Measurement campaign with Max Reiniger and Moritz Feierabend by PTB (Berlin) within the framework of the EMPIR METEOC-3 project
26.10.2020	Earth Observations with CLARA, online Kick-Off meeting of the ISSI International Team “Towards the determination of the EARTH Energy Imbalance from Space”, Margit Haberreiter
Oct. 2020	First Solar-C SoSPIM meeting
Nov. 2020	SOCOL modelling community annual meeting “Davos SOCOL Day 2020”
13.11.2020	The Advisory Commission (AK) meeting
Dec. 2020	American Geophysical Union session entitled "Solar and Heliospheric science out of the ecliptic", Louise Harra (co-organiser),
17.12.2020	2nd PMOD/WRC Science Day

Bilanz per 2020 (inklusive Drittmittel) mit Vorjahresvergleich

Aktiven	31.12.2020 CHF	31.12.2019 CHF
Flüssige Mittel	2’299’714.29	1'170'707.10
Forderungen	554’591.15	125'049.60
Delkredere	-20’450.00	-20'450.00
Aktive Rechnungsabgrenzungen	321’545.64	549'051.95
Total Aktiven	3’155’401.08	1'824'358.65

Passiven		
Verbindlichkeiten	172’514.85	78'049.25
Kontokorrent Stiftung	157.20	202.50
Passive Rechnungsabgrenzung	1’619’194.15	761'090.38
Rückstellungen	1’205’000.00	885'000.00
Eigenkapital	158’534.88	100'016.52
Total Passiven	3’155’401.08	1'824'358.65

Erfolgsrechnung 2020 (inklusive Drittmittel) mit Vorjahresvergleich

Ertrag	CHF	CHF
Beitrag Bund Betrieb WRC	1’489’200.00	1'460'000.00
Beitrag Bund (BBL), Unterhalt Gebäude	134’861.52	141'784.35
Beitrag Kanton Graubünden WRC	509’268.00	499'282.00
Beitrag Kanton Graubünden für ETH Prof.	240’000.00	140'000.00
Beitrag Gemeinde Davos	664’191.00	651'168.00
Beitrag Gemeinde Davos, Mieterlass	160’000.00	160'000.00
Dienstleistungsauftrag MeteoSchweiz OZON	270’799.25	265'136.70
Dienstleistungsauftrag WMO Genève	10’940.50	0.00
Overhead SNF	55’820.60	30'980.50
Instrumentenverkäufe	5’578.00	225'722.50
Reparaturen und Kalibrationen	168’816.12	217'940.43
Ertrag Dienstleistungen	94’769.68	18'109.75
Übriger Ertrag	1’771.85	18'170.05
Erlösminderungen	0.00	-23'188.00
Finanzertrag	162.40	399.60
Ausserordentlicher Ertrag	19’069.58	1'106.30
Drittmittel	1’991’252.700	1'619'332.03
Total Ertrag	5’816’501.20	5'425'944.21

Aufwand		
Personalaufwand	4’249’169.06	3'876'687.05
Investitionen Observatorium	161’618.63	208'612.91
Investitionen Drittmittel	43’093.50	25'637.70
Unterhalt Gebäude (Beitrag Bund)	134’861.52	141'784.35
Unterhalt	80’379.40	65'030.50
Verbrauchsmaterial Observatorium	39’740.30	31'061.35
Verbrauchsmaterial Drittmittel	172’571.75	172'920.97
Verbrauch Commercial	100’218.50	107'338.95
Reisen, Kurse	33’082.10	110'178.79
Raumaufwand/Energieaufwand	212’764.50	210'153.40
Versicherungen, Verwaltungsaufwand	112’538.00	103'792.99
Finanzaufwand	1’508.45	2'208.14
Übriger Betriebsaufwand	95’056.10	72'499.75
Ausserordentlicher Aufwand	1’381.03	15'699.51
Total Aufwand	5’437’982.84	5'143'606.36
Jahresergebnis vor Auflösung Rückstellungen	**378’518.36**	**282'337.85**
Auflösung Rückstellungen Neubau PFR	80’000.00	0.00
Bildung Rückstellungen	400’000.00	185'000.00
Jahresergebnis	**58’518.36**	**97'337.85**
	5’816’501.20	5'425'944.21

Abbreviations

AERONET	Aerosol Robotic Network, GSFC, USA
AOACCM	Atmosphere-Ocean-Aerosol-Chemistry-Climate Model
AOD	Aerosol Optical Depth
BIPM	Bureau International des Poids et Mesures, Paris, France
BSRN	Baseline Surface Radiation Network of the WCRP
CCM	Chemistry-Climate Model
CIMO	Commission for Instruments and Methods of Observation of WMO, Geneva, Switzerland
CIOMP	Changchun Institute of Optics, Fine Mechanics and Physics
CIPM	Comité International des Poids et Mesures
CLARA	Compact Light-weight Absolute Radiometer (PMOD/WRC experiment onboard the NorSat-1 micro-satellite mission)
CMA	Chinese Meteorological Administration
CMC	Calibration and Measurement Capabilities
CME	Coronal Mass Ejections
COSI	Code for Solar Irradiance (solar atmosphere radiation transport code developed at PMOD/WRC)
COST	European Cooperation in Science and Technology
CSAR	Cyrogenic Solar Absolute Radiometer (PMOD/WRC research instrument)
DARA	Digital Absolute Radiometer (PMOD/WRC experiment onboard the ESA Proba-3 formation flying mission)
EAGLE	Entire Atmosphere Global Model
ECV	Essential Climate Variable
EMRP	European Metrology Research Programme
ESA	European Space Agency
EUI	Extreme Ultraviolet Imager (PMOD/WRC participation in EUI, onboard the Solar Orbiter mission)
EUV	Extreme Ultraviolet region of the light spectrum
FM	Flight Model
FRC	Filter Radiometer Comparisons, held at PMOD/WRC every 5 years
FS	Flight Spare
FY-3E	Chinese weather satellite, Fengyun-3, to be launched in the near future
GAW	Global Atmosphere Watch, a WMO Research Programme
GCM	General Circulation Model
GCR	Galactic Cosmic Rays
HAMMONIA	Hamburg Model of the Neutral and Ionized Atmosphere
HEPPA	High Energy Particle Precipitation in the Atmosphere (SPARC activity)
IACETH Zurich	Institute for Climate Research, ETH Zurich, Switzerland
IPC	International Pyrheliometer Comparisons, held at PMOD/WRC every 5 years
IPgC	International Pyrgeometer Comparisons, held at PMOD/WRC every 5 years
IRCCAM	Infrared Cloud Camera (PMOD/WRC research instrument)
IRIS	Infrared Integrating Sphere Radiometer (PMOD/WRC research instrument)
IRS	Infrared Section of the WRC at PMOD/WRC
ISO/IEC	International Organisation for Standardisation/International Electrotechnical Commission
ISO 17025	General requirements for the competence of testing and calibration laboratories
JTSIM-DARA	Joint Total Solar Irradiance Monitor – DARA (experiment onboard the Chinese FY-3E mission)
LUCI	Lagrange EUV Coronal Imager (experiment onboard the ESA LAGRANGE mission)
METAS	Federal Office of Metrology, (Eidgenössisches Institut für Metrologie), Bern-Wabern, Switzerland
MITRA	Monitor to Determine the Integrated Transmittance (PMOD/WRC research instrument)

→

MRA	Mutual Recognition Arrangement
NASA	National Aeronautics and Space Administration, Washington DC, USA
NIST	National Institute of Standards and Technology, Gaithersburg, MD, USA
NorSat-1	Norwegian Satellite-1
NPL	National Physical Laboratory, Teddington, UK
NREL	National Renewable Energy Laboratory, Golden, CO, USA
PFR	Precision Filter Radiometer (manufactured by PMOD/WRC)
PMO6-cc	Type of absolute cavity radiometer (previously manufactured by PMOD/WRC)
POLE	Past and Future of the Ozone Layer Evolution
Proba	ESA Satellite Missions (Proba-1 to 3)
PRODEX	PROgramme de Développement d'Expériences scientifiques, ESA
PSR	Precision Spectroradiometer (manufactured by PMOD/WRC)
PTB	Physikalisch-Technische Bundesanstalt, Braunschweig and Berlin, Germany
QASUME	Quality Assurance of Spectral Ultraviolet Measurements in Europe
QMS	Quality Management System
SCNAT	Swiss Academy of Sciences
SFI	Schweiz. Forschungsinstitut für Hochgebirgsklima und Medizin, Davos, Switzerland
SIAF	Schweiz. Institut für Allergie- und Asthma-Forschung, Davos, Switzerland
SNSF	Swiss National Science Foundation
SOCOL	Combined GCM and CTM Computer Model developed at PMOD/WRC→
SoHO	Solar and Heliospheric Observatory (ESA/NASA space mission)
SOLARIS	Solar Influences on Climate (SPARC activity, joined with HEPPA as SOLARIS-HEPPA)
Solar Orbiter	SolO; An ESA mission to conduct solar research (PMOD/WRC are participating with the EUI and SPICE instruments)
SPARC	Stratosphere-troposphere Processes And their Role in Climate (A core project of the World Climate Research Programme)
SPE	Solar Proton Events
SPICE	Spectral Imaging of the Coronal Environment (PMOD/WRC participation in SPICE, onboard the Solar Orbiter mission)
SRS	Solar Radiometry Section of the WRC at PMOD/WRC
SSI	Solar Spectral Irradiance
TEC	Total Electron Content
TSI	Total Solar Irradiance
VHS	Ventilation Heating System (manufactured at PMOD/WRC)
VIRGO	Variability of Solar Irradiance and Gravity Oscillations (PMOD/WRC experiment onboard the SOHO mission)
WCC-UV	World Calibration Center for UV in the WRC of the PMOD/WRC
WDCA	World Data Centre for Aerosols, NILU, Norway
WISG	World Infrared Standard Group of pyrgeometers (maintained by WRC-IRS at PMOD/WRC)
WMO	World Meteorological Organisation, a United Nations Specialised Agency, Geneva, Switzerland
WORCC	World Optical depth Research and Calibration Center of the WRC at PMOD/WRC
WRC	World Radiation Center at PMOD/WRC, composed of the Sections: IRS, SRS, WCC-UV, and WORCC
WRR	World Radiometric Reference
WSG	World Standard Group of pyrheliometers (realises the WRR; maintained by WRC at PMOD/WRC)

Annual Report 2020

Editors: Louise Harra and Stephan Nyeki
Layout by Stephan Nyeki
Copy-editing by Stephan Nyeki and Monica Freeman

Publication by PMOD/WRC, Davos, Switzerland
Edition: 600, printed June 2021

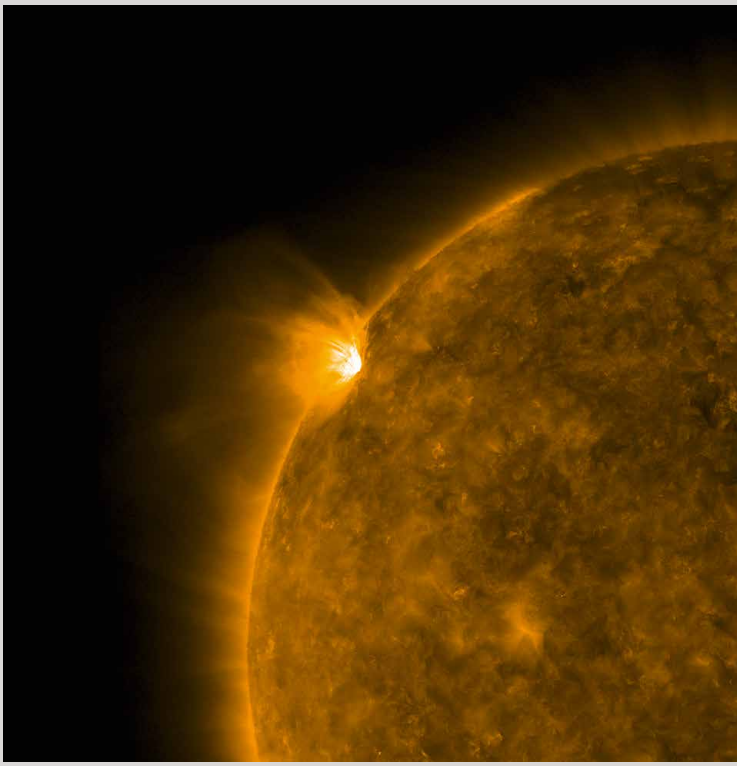

Dorfstrasse 33, 7260 Davos Dorf, Switzerland
Phone +41 81 417 51 11
www.pmodwrc.ch